National Library
of Canada

Bibliothèque nationale
du Canada

CANADIAN THESES
ON MICROFICHE

THÈSES CANADIENNES
SUR MICROFICHE

NAME OF AUTHOR/*NOM DE L'AUTEUR* _Sum Lok Wong_

TITLE OF THESIS/*TITRE DE LA THÈSE* _Liquid Solidification in Parallel-Plate_

Channels with Convective Boundary Conditions

UNIVERSITY/*UNIVERSITÉ* _University of Alberta_

DEGREE FOR WHICH THESIS WAS PRESENTED/
GRADE POUR LEQUEL CETTE THÈSE FUT PRÉSENTÉE _M. Sc_

YEAR THIS DEGREE CONFERRED/*ANNÉE D'OBTENTION DE CE GRADE* _Fall, 1976_

NAME OF SUPERVISOR/*NOM DU DIRECTEUR DE THÈSE* _Prof K C Cheng_

DATED/*DATÉ* _Oct., 12, 1976_ SIGNED/*SIGNÉ* _Wong Sum Lok_

PERMANENT ADDRESS/*RÉSIDENCE FIXE* _12405 - 111 Ave._

Edmonton, Alberta

INFORMATION TO USERS

THIS DISSERTATION HAS BEEN
MICROFILMED EXACTLY AS RECEIVED

This copy was produced from a micro-
fiche copy of the original document.
The quality of the copy is heavily
dependent upon the quality of the
original thesis submitted for
microfilming. Every effort has
been made to ensure the highest
quality of reproduction possible.

PLEASE NOTE: Some pages may have
indistinct print. Filmed as
received.

Canadian Theses Division
Cataloguing Branch
National Library of Canada
Ottawa, Canada   K1A 0N4

AVIS AUX USAGERS

LA THESE A ETE MICROFILMEE
TELLE QUE NOUS L'AVONS RECUE

Cette copie a été faite à partir
d'une microfiche du document
original. La qualité de la copie
dépend grandement de la qualité
de la thèse soumise pour le
microfilmage. Nous avons tout
fait pour assurer une qualité
supérieure de reproduction.

NOTA BENE: La qualité d'impression
de certaines pages peut laisser à
désirer. Microfilmee telle que
nous l'avons reçue.

Division des thèses canadiennes
Direction du catalogage
Bibliothèque nationale du Canada
Ottawa, Canada   K1A 0N4

THE UNIVERSITY OF ALBERTA

LIQUID SOLIDIFICATION IN PARALLEL-PLATE

CHANNELS WITH CONVECTIVE BOUNDARY CONDITIONS

by

Ⓒ   SUM-LOK WONG

A THESIS

SUBMITTED TO THE FACULTY OF GRADUATE STUDIES AND RESEARCH

IN PARTIAL FULFILMENT OF THE REQUIREMENTS FOR THE DEGREE

OF MASTER OF SCIENCE

DEPARTMENT OF MECHANICAL ENGINEERING

EDMONTON, ALBERTA

FALL, 1976

THE UNIVERSITY OF ALBERTA

FACULTY OF GRADUATE STUDIES AND RESEARCH

The undersigned certify that they have read, and recommend to the Faculty of Graduate Studies and Research, for acceptance, a thesis entitled "LIQUID SOLIDIFICATION IN PARALLEL-PLATE CHANNELS WITH CONVECTIVE BOUNDARY CONDITIONS" submitted by SUM-LOK WONG in partial fulfilment of the requirements for the degree of Master of Science.

..... K.C. Cheng .....
Supervisor

.....

.....

Date .. Oct., 8, 1976 .....

ABSTRACT

Analytical solutions are obtained for steady-state symmetric and unsymmetric solidifications of forced laminar liquid flows in parallel-plate channels with convective boundary conditions. The classical Graetz type analysis based on the physical model of Zerkle and Sunderland is made by using the confluent hypergeometric function for the case with uniform convective coolings at upper and lower plates and the case with perfect insulation at lower plate and uniform convective cooling at upper plate. Numerical results are obtained for liquid solidification-free length, ice layer thickness, pressure drop, bulk temperature, heat transfer rate and local Nusselt number for a range of values of Biot number and superheat ratio. The configuration and thermal conditions under consideration may be encountered in heat exchangers using cryogenics and freezing of ice sheets on northern rivers and lakes.

The Graetz problem with axial heat conduction effects in parallel-plate channels considering both the upstream and downstream regions is extended to the case of convective boundary condition. It is found that analytical solution in freezing zone cannot be obtained for low Peclet number flow regime and numerical solution must be sought.

ACKNOWLEDGEMENT

TABLE OF CONTENTS

LIST OF TABLES

LIST OF FIGURES

CHAPTER I

INTRODUCTION

1.1 Liquid Solidification in Parallel-Plate Channels

In recent years, the problem of liquid solidification in circular tubes with fully developed laminar flow at the thermal entrance has been studied by several investigators for the thermal boundary conditions of uniform wall temperature and convective cooling. The solidification of liquids flowing through tubes or channels is of technical importance and may occur in water mains, process equipment and other various hydraulic systems subjected to extreme ambient temperatures.

The solidification of flowing liquid in parallel-plate channels with convective boundary conditions is encountered in natural phenomena such as the freezing of northern rivers and lakes and in various industrial processes such as the solidifying of metal castings in molds, freezing of foods and solidification within liquid flow heat exchanges using a cryogen as the coolant. For the specific configuration of the parallel-plate channel, one notes that the liquid solidification problem has been studied so far for the case of uniform wall temperature condition only.

The purpose of this investigation is to study a class of liquid solidification problems in parallel-plate channels with convective boundary conditions.

1.2 Statement of the Problem

The problem is concerned with plane Poiseuille liquid flow in

parallel-plate channels with surface solidification. At the thermal entrance (X = 0), the liquid has a fully developed velocity profile and a uniform temperature distribution. In the downstream region (X ≥ 0), heat is transfered by convection from the channel surface to the surrounding medium with an ambient temperature below the freezing temperature of a warm flowing liquid.

With a step decrease in wall temperature, ice will cover the entire wall starting from the thermal entrance X = 0. In constrast, with a uniform external convective cooling, ice will not form until a sufficient amount of sensible heat has been removed. Thus, the thermal entrance region consists of a solidification-free zone and a freezing zone where a growing solid layer appears along the channel wall. In this investigation, the liquid flow rate into the cooled section is assumed to be maintained constant and only the steady-state condition is under consideration.

Apparently, the flow field in the freezing zone is characterized by a boundary layer flow due to the interface between the solid and the liquid phases moving inward. A fully developed flow is reached further downstream. The present investigation utilizes the physical model employed by Zerkle and Sunderland [1] which assumes that the axial velocity profile of the liquid remains parabolic even as the liquid accelerates due to a constriction of the flow area by the solid phase. This basic assumption together with the assumption that the axial variation of the solid layer thickness is gradual leads to a considerable simplification in theoretical analysis and enables one to employ a Graetz type analysis in the freezing zone.

For parallel-plate channels, various combinations of thermal

boundary conditions at the upper and lower plates are possible. However, the following two cases are under consideration in this study:

1. Uniform external convective cooling at upper and lower plates (Chapter 2).

2. Different but uniform external convective coolings at upper and lower plates (Chapter 3).

The first case represents a symmetrical solidification problem and the second case deals with an unsymmetrical one. For the second case, numerical results are obtained only for a specific case with perfect insulation at the lower plate and a uniform convective cooling at the upper plate. The analytical solutions for the foregoing two cases are obained by the eigenfunction expansion method using the confluent hypergeometric function.

For low Peclet number flow regime, axial heat conduction effects are known to be important in thermal entrance region problem. Thus, it is of practical interest to consider the axial conduction effects on liquid solidification in parallel-plate channels with convective boundary conditions (Chapter 4). It is found that analytical solution in the freezing zone cannot be obtained when one considers the axial heat conduction effects. Consequently, numerical results are obtained only for the solidification-free zone and are presented in Chapter 4.

1.3 Format of Presentation

A remark regarding the structure and the method of presentation for the present thesis is now in order. In view of the analytical solutions obtained for three different cases, it is decided that each

case will be treated independently in each Chapter. Thus, the litera-
ture review can be made separately for each case and the scope of re-
sults, conclusions and significance for each case can be examined
separately.

REFERENCE

1. Zerkle, R.D. and Sunderland, J.E., "The effect of liquid solidifi-
   cation in a tube upon laminar-flow heat transfer and pressure drop",
   J. Heat Transfer 90C, 1968, pp. 183-190.

CHAPTER II

LIQUID SOLIDIFICATION IN A
CONVECTIVELY-COOLED PARALLEL-PLATE CHANNEL

A theoretical analysis of liquid solidification in the thermal entrance region of a parallel-plate channel with a uniform external convection is carried out by using the confluent hypergeometric function in the solution for laminar flow and steady-state conditions. Theoretical results are obtained for liquid solidification-free length, liquid-solid interface profile, pressure drop, bulk temperature, heat transfer rate and local Nusselt number for the cases of Biot numbers $Bi = 0.25, 0.5, 1, 2, 10, \infty$, superheat ratios $\epsilon = 1, 2, 4, 8$, $Pr = 13.2$ and $k_\ell/k_s = 0.25$ using 20 eigenvalues. The results can be used in assessing the effect of thermal insulation and predicting the thermal insulation required to protect a channel flow from a severe cold environment.

NOMENCLATURE

a, b = parameters in Kummer's equation

Bi, Bi_s = Biot numbers, $h_0 L/k$ and $(k_\ell/k_s)Bi$

B_{1j}, B_{2j} = constants in Eq. (8)

c_p = specific heat at constant pressure

E_j, K_j = eigenconstants, Eqs. (3) and (29)

G = function of $\bar{x}$, Eq. (25)

h = local heat transfer coefficient, Eqs. (55) and (56)

h_0 = overall heat transfer coefficient between inner wall and ambient defined by $-k(\partial T/\partial Y)_{Y=L} = h_0(T_{y=L} - T_\infty)$

k = thermal conductivity of liquid

L = half-distance between parallel plates

$M(a, b, z)$ = confluent hypergeometric function

N_j, Y_j = eigenfunctions, Eqs. (26) and (4)

Nu = Nusselt number

P, P_0 = pressure and pressure at $X=0$

Pe = Peclet number, $4 U_m L/\alpha$

Pr = Prandtl number, ν/α

p = dimensionless pressure drop, $2(P_0 - P)/\rho U_m^2$

$Q, \bar{Q}$ = total heat transfer rate and dimensionless Q, Eq. (50)

q = local heat transfer rate, Eqs. (55) and (56)

T, T_b, T_f = liquid temperature, bulk temperature and freezing temperature.

T_0, T_∞ = uniform entrance temperature and ambient temperature

U, V = axial and transverse velocities

U_m = average axial velocity

w	= solution of Kummer's equation
X, Y	= rectangular coordinates
X'	= axial coordinate with origin at solid-phase entrance
x, y	= (X/LPe), (Y/L)
$\bar{x}$, $\bar{y}$	= (X'/LPe), (Y/L) in freezing zone
x_f	= dimensionless solidification-free length
z	= transformed variable

Greek Letters

α	= thermal diffusivity
α_j, β_j	= eigenvalues in Eqs. (3) and (29)
δ, $\bar{\delta}$	= transverse coordinate of liquid-solid interface and δ/L
ϵ	= superheat ratio, $(T_0 - T_f)/(T_f - T_\infty)$
η	= dimensionless transverse coordinate, $\bar{y}/\bar{\delta} = Y/\delta$
θ	= dimensionless temperature difference, $(T - T_\infty)/(T_0 - T_\infty)$
θ_b	= dimensionless bulk temperature, Eqs. (47) and (48)
θ_f	= $(T_f - T_\infty)/(T_0 - T_\infty)$
μ, ν	= dynamic viscosity and kinematic viscosity
ρ	= density
ϕ	= dimensionless temperature difference, $(T - T_f)/(T_0 - T_f)$

Subscripts

ℓ, s	= liquid and solid-phase
1, 2	= solidification-free and freezing zone

2.1 Introduction

The problem of liquid solidification and pressure drop in a circular tube with laminar flow has been studied by Zerkle and Sunderland [1], DesRuisseaux and Zerkle [2], Bilenas and Jiji [3,4] and Hwang and Sheu [5] for the case of a uniform wall temperature below the freezing point. When a pipe is exposed to a meteorological environment or is buried underground in the permafrost region with thermal insulation, then the convective boundary condition (thermal boundary condition of a third kind) outside the pipe is more realistic. The case of convective boundary condition was studied by Zerkle [6] and Lock, Freeborn and Nyren [7]. One notes that the uniform wall temperature represents a limiting case of the convective boundary condition with Biot number equal to infinity.

The solidification problem of liquids flowing through ducts or channels is of considerable practical importance in various engineering processes or devices ranging from casting of metals in metallurgical processes to freezing of water pipes under northern climatic conditions. Lee and Zerkle [8] presented theoretical results for liquid solidification in a parallel-plate channel with laminar flow using the physical model of Zerkle and Sunderland [1].

The present problem is concerned with the solidification and pressure drop of the superheated laminar liquid flow in a parallel-plate channel subjected to a uniform convective cooling condition with the surrounding sink temperature below the freezing point. The freezing in parallel-plate channels occurs, for example, in various plate coolers. The analysis assumes steady-state conditions [1,2,6] and a constant finite thermal resistance between the channel inner wall and

the external cold environment. With a convective boundary condition, liquid soldification will not occur over an initial thermal entrance length due to insufficient cooling. Thus, the thermal entrance region consists of a solidification-free zone and a zone with solid-phase where soldification grows inwards with the distance along the channel. The purpose of this investigation is to study the effects of superheating and thermal insulation on heat transfer, solidification-free zone, liquid-solid interface profile and pressure drop in parallel-plate channels. The solution for thermal entry problem is obtained by the eigenfunction expansion method using the confluent hypergeometric function [9-12].

2.2 Problem Formulation and Physical Model

Consider the steady-state freezing of a liquid with constant physical properties flowing between two parallel plates from the upstream adiabatic section to the downstream section with a uniform convective cooling (see Fig. 1). It is assumed that the flow is a steady plane Poiseuille flow with a uniform entrance temperature T_0 at $X = 0$ which is greater than the freezing temperature T_f. The basic assumption [1,6,8] that the axial velocity profile of the liquid in the region with surface solidification remains parabolic even as the liquid accelerates due to a continuously increasing constriction of the flow area along the channel axis proves to be a good approximation [3,5] and leads to a considerable simplification enabling one to employ a Graetz type analysis. This assumption together with the assumptions of negligible viscous energy dissipation and free convection will be used in the present analysis. An order of magnitude analysis given in appendix 1 reveals

that axial heat conduction may be neglected if $1/Pe \ll 1$.

2.3 The Liquid Solidification-Free Zone

2.3.1 Analysis

The energy equation and its boundary conditions describing the temperature field in the liquid are,

$$U\frac{\partial T}{\partial X} = \alpha\frac{\partial^2 T}{\partial Y^2}$$

$$T(0,Y) = T_0$$

$$\partial T(X,0)/\partial Y = 0$$

$$-k\partial T(X,L)/\partial Y = h_0[T(X,L) - T_\infty]$$

The Poiseuille velocity profile which satisfies the constant mass flow rate criteria $\int_0^L UdY = LU_m$ is given by

$$U = \frac{3}{2} U_m [1 - (\frac{Y}{L})^2]$$

Thus, the energy equation in dimensionless form and the thermal boundary condition can be written as

$$\frac{3}{8} (1-y^2)\frac{\partial \theta}{\partial x} = \frac{\partial^2 \theta}{\partial y^2} \tag{1}$$

$$\theta(0,y) = 1, \quad \partial\theta(x,0)/\partial y = 0, \quad \partial\theta(x,1)/\partial y = -Bi\theta(x,1) \tag{2}$$

where $x = X/LPe$, $y = Y/L$, $\theta = (T-T_\infty)/(T_0-T_\infty)$ and $Bi = h_0L/k$ and all other symbols are defined in Nomenclature. By separation of variables, the solution to Eq. (1) is found as

$$\theta = \sum_{j=1}^{\infty} E_j Y_j(y)\exp(-\frac{8}{3}\alpha_j^2 x) \tag{3}$$

where the eigenvalues α_j and eigenfunction Y_j satisfy the following Sturm-Liouville system of equations:

$$\frac{d^2 Y_j}{dy^2} + (1-y^2)\alpha_j^2 Y_j = 0 \tag{4}$$

$$dY_j(0)/dy = 0, \; dY_j(1)/dy = -BiY_j(1) \tag{5}$$

In order to overcome the difficulty in obtaining the higher eigenvalues, the series solution is replaced by a solution involving the confluent hypergeometric function [9-12]. By introducing the transformations, $z = \alpha_j y^2$ and $w(z) = \exp(z/2) \cdot Y_j(y)$, Eq. (5) becomes

$$z\frac{d^2 w}{dz^2} + (\frac{1}{2} - z)\frac{dw}{dz} - (\frac{1}{4} - \frac{\alpha_j}{4})w = 0 \tag{6}$$

which is seen to be Kummer's equation,

$$z\frac{d^2 w}{dz^2} + (b - z)\frac{dw}{dz} - aw = 0 \tag{7}$$

with $a = (1-\alpha_j)/4$, $b = 1/2$. The general solution of Eq. (7) can be expressed in terms of the confluent hypergeometric function [11] $M(a,b,z)$ and the eigenfunction $Y_j(y)$ becomes

$$Y_j(y) = \exp(-\alpha_j y^2/2)[B_{1j}M(a_j,1/2,\alpha_j y^2)$$

$$+ B_{2j}\alpha_j^{1/2}yM(a_j+1/2,3/2,\alpha_j y^2)] \tag{8}$$

where B_{1j} and B_{2j} are the constants.

2.3.2 Eigenvalues and Eigenfunctions

From Eq. (8), one obtains

$$dY_j(y)/dy = \exp(-\alpha_j y^2/2)[-B_{1j}\alpha_j yM(a_j,1/2,\alpha_j y^2)$$

$$+ B_{2j}\alpha_j^{1/2}(1-\alpha_j y^2)M(a_j+1/2,3/2,\alpha_j y^2)$$

$$+ 4B_{1j}a_j\alpha_j yM(a_j+1,3/2,\alpha_j y^2)$$

$$+ (4/3)B_{2j}\alpha_j^{3/2}y^2(a_j+1/2)M(a_j+3/2,5/2,\alpha_j y^2)] \tag{9}$$

Applying the symmetry condition $dY_j(0)/dy = 0$, one obtains $B_{2j} = 0$ indicating that all odd terms vanish. With $B_{2j} = 0$, the constants B_{1j} can be absorbed by the eigenconstants E_j in Eq. (3). Thus, Eqs. (8) and (9) become

$$Y_j(y) = \exp(-\alpha_j y^2/2)M(a_j,1/2,\alpha_j y^2) \tag{10}$$

$$dY_j(y)/dy = \exp(-\alpha_j y^2/2)[-\alpha_j yM(a_j,1/2,\alpha_j y^2)$$

$$+ 4a_j\alpha_j yM(a_j+1, 3/2, \alpha_j y^2)] \tag{11}$$

The confluent hypergeometric function $M(a,b,z)$ is

$$M(a,b,z) = 1 + \frac{a}{b} z + \frac{a(a+1)}{b(b+1)} \frac{z^2}{2!} + \cdots + \frac{a(a+1)\ldots(a+n-1)}{b(b+1)\cdots(b+n-1)} \frac{z^n}{n!} + \cdots$$

With $b = 1/2$ and $a_j = (1-\alpha_j)/4$, one obtains

$$M(a_j,1/2,\alpha_j) = 1 + \sum_{n=1}^{\infty} \frac{(1-\alpha_j)\ldots(4n-3-\alpha_j)}{(2n)!} \alpha_j^n$$

Substituting Eqs. (10) and (11) into the convective boundary condition in Eq. (5), one obtains

$$(Bi - \alpha_j - 2a_j)M(a_j, 1/2, \alpha_j) + 2a_j M(a_j+1, 1/2, \alpha_j) = 0 \tag{12}$$

after applying the following recurrence formula.

$$zM(a, b+1, z) = bM(a, b, z) - bM(a-1, b, z) \tag{13}$$

It is convenient to express Eq. (12) in series form as

$$(Bi-\alpha_j) + \sum_{n=1}^{\infty} \frac{(1-\alpha_j)\cdots(4n-3-\alpha_j)}{(2n)!} \alpha_j^n (Bi + 2n - \alpha_j) = 0 \tag{14}$$

The eigenvalues α_j are the roots of Eq. (14) and can be found by tabulating the value of the left-hand side of Eq. (14) versus a sequence of closely spaced values of α_j. One may thus inspect the whole spectrum of the eigenvalues before they are improved by the variable secant method.

2.3.3 Eigenconstants

Utilizing the orthogonality relationship, the eigenconstants E_j can be determined from

$$E_j = \int_{-1}^{1} (1-y^2) Y_j dy / \int_{-1}^{1} (1-y^2) Y_j^2 dy = -2/\alpha_j \left[\frac{\partial Y_j}{\partial \alpha_j} + \frac{1}{Bi} \frac{\partial}{\partial \alpha_j} \left(\frac{dY_j}{dy} \right) \right]_{y=1} \tag{15}$$

$$Y_j(y) = \exp(-\alpha_j y^2/2)\left[1 + \sum_{n=1}^{\infty} \frac{(1-\alpha_j)\cdots(4n-3-\alpha_j)}{(2n)!} \alpha_j^n y^{2n}\right] \tag{16}$$

where

$$\left[\frac{\partial Y_j}{\partial \alpha_j}\right]_{y=1} = \exp(-\alpha_j/2)\left[-\frac{1}{2} + \sum_{n=1}^{\infty} \frac{(1-\alpha_j)\cdots(4n-3-\alpha_j)}{(2n)!} \alpha_j^n \right.$$

$$\cdot(-\frac{1}{2} + \frac{n}{\alpha_j} - \sum_{p=1}^{n} \frac{1}{(4p-3-\alpha_j)})]$$

$$[\frac{\partial}{\partial\alpha_j}(\frac{dY_j}{dy})]_{y=1} = \exp(-\alpha_j/2)[-1 + \frac{\alpha j}{2} + \sum_{n=1}^{\infty} \frac{(1-\alpha_j)\cdots(4n-3-\alpha_j)}{(2n)!}\alpha_j^n$$

$$\cdot(-1 + \frac{\alpha_j}{2} - 2n + \frac{2n^2}{\alpha_j} - \sum_{p=1}^{n} \frac{1}{(4p-3-\alpha_j)}(2n-\alpha_j))]]$$

The first twenty eigenvalues, derivatives and constants are computed for n = 150 and are given in Table 1 for Bi = 0.25, 0.5, 1, 2, 10.

2.3.4 Liquid Solidification-Free Length

The solidification starts at the point where the wall temperature reaches the freezing temperature. Using Eq. (3), the liquid solidification-free length x_f can be evaluated from

$$\theta(x_f,1) = \theta_f = \sum_{j=1}^{20} E_j Y_j(1)\exp(-8\alpha_j^2 x_f/3) \tag{17}$$

where $\theta_f = (T_f - T_\infty)/(T_0 - T_\infty)$. For the determination of x_f, it is convenient to define a superheat ratio ϵ as

$$\epsilon = (T_0 - T_f)/(T_f - T_\infty) = \theta_f^{-1} - 1 \tag{18}$$

It is readily seen that $x_f = f(\epsilon, Bi)$.

2.4 The Freezing Zone

2.4.1 Analysis

Assuming that the axial velocity profile remains parabolic [1,8] in the freezing zone (see Fig. 1 for coordinate system), the ve-

locity components which satisfy continuity relations and boundary condition can be shown to be

$$U(X',Y) = (3LU_m/2\delta)[1 - (Y/\delta)^2]$$ (19)

$$V(X',Y) = (3/2)(LU_m Y/\delta^2)(d\delta/dX')[1 - (Y/\delta)^2]$$

Substituting Eq. (19) into energy equation, $U(\partial T/\partial X') + V(\partial T/\partial Y) = \alpha(\partial^2 T/\partial Y^2)$, one obtains

$$\frac{3}{2}\frac{LU_m}{\delta}[1 - (\frac{Y}{\delta})^2]\frac{\partial T}{\partial X'} + \frac{3}{2}\frac{LU_m}{\delta^2}Y\frac{d\delta}{dX'}[1 - (\frac{Y}{\delta})^2]\frac{\partial T}{\partial Y} = \alpha\frac{\partial^2 T}{\partial Y^2}$$ (20)

Defining the dimensionless variables,

$\bar{x} = (X'/LPe)$, $\bar{y} = Y/L$, $\bar{\delta} = \delta/L$, $\phi = (T-T_f)/(T_0-T_f)$, Eq. (20) becomes

$$\frac{3}{8}\frac{1}{\bar{\delta}}[1 - (\frac{\bar{y}}{\bar{\delta}})^2][\frac{\partial\phi}{\partial\bar{x}} + \frac{\bar{y}}{\bar{\delta}}\frac{d\bar{\delta}}{d\bar{x}}\frac{\partial\phi}{\partial\bar{y}}] = \frac{\partial^2\phi}{\partial\bar{y}^2}$$ (21)

The boundary conditions are

$$\phi(\bar{x},\bar{\delta}) = 0 \text{ (interface)}, \quad \partial\phi(\bar{x},0)/\partial\bar{y} = 0 \text{ (symmetry)},$$

(22)

$$\phi(0,\bar{y}) = [(1 + \epsilon)/\epsilon]\theta(x_f,y) - (1/\epsilon) \text{ (entrance condition)}$$

where the temperature distribution at the solid-phase entrance $\theta(x_f,y)$ can be determined from Eq. (17). Introducing the variable transformation [1,8] from $\phi(\bar{x},\bar{y})$ to $\phi(\bar{x},\eta)$ with $\eta = \bar{y}/\bar{\delta} = Y/\delta$, one obtains the following system of equations which is of the same form as the classical Graetz problem.

$$\frac{3}{8}\frac{\partial\phi}{\partial\bar{x}} = \frac{1}{\delta}\frac{1}{(1-n^2)}\frac{\partial^2\phi}{\partial n^2} \qquad (23)$$

$$\phi(\bar{x},1) = 0, \ \partial\phi(\bar{x},0)/\partial n = 0, \ \phi(0,n) = [(1+\epsilon)/\epsilon]\theta(x_f,y)-(1/\epsilon) \qquad (24)$$

Separating the variables by putting $\phi = G(\bar{x})N(n)$, one obtains:

$$\frac{3}{8}\delta\frac{dG}{d\bar{x}} + \beta_j^2 G = 0, \ G(0) = \frac{1+\epsilon}{\epsilon}\theta(x_f,n) - \frac{1}{\epsilon} \qquad (25)$$

$$\frac{d^2 N_j}{dn^2} + \beta_j^2(1 - n^2)N_j = 0, \ dN_j(0)/dn = 0, \ N_j(1) = 0 \qquad (26)$$

Integrating Eq. (25), one obtains

$$G(\bar{x}) = \exp\ [-(8/3)\beta_j^2\int_0^{\bar{x}}\frac{d\bar{x}}{\delta}] \qquad (27)$$

Since Eq. (26) can be transformed into Kummer's equation, the solution is found to be

$$N_j(n) = \exp(-\beta_j n^2/2)M(\frac{1}{4} - \frac{\beta_j}{4}, 1/2, \beta_j n^2) \qquad (28)$$

Thus, the series solution for $\phi(\bar{x},n)$ is

$$\phi(\bar{x},n) = \sum_{j=1}^{\infty} K_j N_j(n)\exp[(-8/3)\beta_j^2\int_0^{\bar{x}}\frac{d\bar{x}}{\delta}] \qquad (29)$$

where K_j are the eigenconstants.

2.4.2 Eigenvalues and Eigenconstants

The eigenvalues β_j can be determined by using the boundary

condition $N_j(1) = 0$. This leads to

$$M(\frac{1}{4} - \frac{\beta_j}{4}, 1/2, \beta_j) = 0 \tag{30}$$

The roots representing the eigenvalues can be determined by the procedure using variable secant method discussed earlier.

Applying the entrance condition for $\phi(0,\eta)$ and using the orthogonality relationship, the eigenconstants can be evaluated from

$$K_j = \int_{-1}^{1} (1-\eta^2)N_j(\eta)\phi(0,\eta)d\eta / \int_{-1}^{1} (1-\eta^2)N_j^2(\eta)d\eta \tag{31}$$

where $\phi(0,\eta) = \frac{1+\epsilon}{\epsilon} \sum_{i=1}^{20} E_i Y_i(\eta)\exp[(-8/3)\alpha_i^2 x_f] - \frac{1}{\epsilon}$

It can be shown (see Appendix 2) that the expression for K_j reduces to

$$K_j = (\frac{1+\epsilon}{\epsilon})2\beta_j \sum_{i=1}^{20} E_i Y_i(1)\exp[(-8/3)\alpha_i^2 x_f]/[(\alpha_i^2-\beta_j^2) \frac{\partial N_j(1)}{\partial \beta_j}]$$

$$+ (2/\epsilon)/(\beta_j \partial N_j(1)/\partial \beta_j) \tag{32}$$

The expressions for the derivatives $\partial N_j(1)/\partial \beta_j$ and $dN_j(1)/d\eta$ are

$$(\frac{\partial N_j}{\partial \beta_j})_{n=1} = \exp(-\beta_j/2)[-\frac{1}{2} + \sum_{n=1}^{\infty} \frac{(1-\beta_j)\cdots(4n-3-\beta_j)}{(2n)!} \beta_j^n$$

$$\cdot(-\frac{1}{2} + \frac{n}{\beta_j} - \sum_{p=1}^{n} \frac{1}{(4p-3-\beta_j)})] \tag{33}$$

$$\left(\frac{dN_j}{d\eta}\right)_{n=1} = \exp(-\beta_j/2)[-\beta_j + \sum_{n=1}^{\infty} \frac{(1-\beta_j)\cdots(4n-3-\beta_j)}{(2n)!} \beta_j^n (2n-\beta_j)] \tag{34}$$

The first twenty eigenvalues and the corresponding eigenconstants together with $dN_1(1)/d\eta \sim dN_{20}(1)/d\eta$ are listed in Table 2.

2.4.3 Solid-Phase Layer Profile

Considering an energy balance for steady state at the liquid-solid interface, one obtains the following interface equation which is a characteristic feature of the solidification problem.

$$k_\ell \partial T_\ell(X',\delta)/\partial Y = k_s \partial T_s(X',\delta)/\partial Y \tag{35}$$

where $\partial T_\ell(X',\delta)/\partial Y = [(T_0 - T_f)/(L\delta)]\partial\phi(\bar{x},1)/\partial\eta \tag{36}$

The temperature in the solid-phase layer is described by the following system of equations.

$$\frac{d^2 T_s}{dY^2} = 0, \quad T_s(X',\delta) = T_f, \quad k_s \frac{dT_s(X',L)}{dY} = -h_0[T_s(X',L) - T_\infty] \tag{37}$$

The temperature solution is

$$T_s = T_f - \frac{Bi_s(T_f-T_\infty)}{L+Bi_s(L-\delta)} (Y - \delta) \tag{38}$$

where $Bi_s = h_0 L/k_s = (\bar{k}_\ell/k_s)Bi$.

The linear temperature gradient for solid layer is

$$\frac{dT_s}{dY} = -\frac{Bi_s(T_f-T_\infty)}{L+Bi_s(L-\delta)} \tag{39}$$

From Eq. (35), one then obtains

$$\bar{\delta}(\bar{x}) = \frac{(1+Bi_s)\partial\phi(\bar{x},1)/\partial\eta}{Bi_s[\partial\phi(\bar{x},1)/\partial\eta-(k_s/k_\ell\epsilon)]} \tag{40}$$

where $\partial\phi(\bar{x},1)/\partial\eta = \sum_{j=1}^{20} K_j \frac{dN_j(1)}{d\eta} \exp[(-8/3)\beta_j^2\int_0^{\bar{x}} \frac{d\bar{x}}{\delta}]$ (41)

Solutions for $\bar{\delta}$ $(\bar{x})$ can be found numerically by a method of successive substitution[8].

2.5 Pressure Drop and Heat Transfer Characteristics

2.5.1 Pressure Distribution

The pressure drops linearly with X in the solidification-free zone with a pressure gradient $dP/dX = (-3\mu U_m)/L^2$. Introducing the dimensionless pressure difference $p = (P_0 - P)/(\rho U_m^2/2)$ and upon integrating, one obtains

$$p = 24\ Prx, \quad 0 \leq x \leq x_f \tag{42}$$

To determine the pressure drop in the freezing zone, one integrates the axial momentum equation, $U\partial U/\partial X' + V\partial U/\partial Y = -\partial P/\rho\partial X' + \nu\ (\partial^2 U/\partial X'^2 + \partial^2 U/\partial Y^2)$, from $Y = 0$ to $Y = \delta$ and obtains

$$\frac{d}{dX'} \int_0^\delta U^2 dY = -\frac{\delta}{\rho} \frac{dP}{dX'} + \nu\int_0^\delta \frac{\partial^2 U}{\partial X'^2} dY + \nu \frac{\partial U(X',\delta)}{\partial Y} \tag{43}$$

Substituting U from Eq. (19) and assuming [1] $(d\delta/dX')^2$, $(d^2\delta/dX'^2)\ll 1$, Eq. (43) in dimensionless form becomes

$$\frac{dp}{d\bar{x}} = -\frac{12}{5}\frac{1}{\bar{\delta}^3}\frac{d\bar{\delta}}{d\bar{x}} + 24\frac{Pr}{\bar{\delta}^3} \tag{44}$$

After integrating from $\bar{x} = 0$ to $\bar{x} = \bar{x}$ and noting that $p = 24\ Pr\ x_f$ at $\bar{x} = 0$, one obtains

$$p(\bar{x}) = \frac{6}{5}(\frac{1}{\bar{\delta}^2} - 1) + 24\ Pr(x_f + \int_0^{\bar{x}}\frac{d\bar{x}}{\bar{\delta}^3}) \tag{45}$$

One notes that the first term represents the momentum effect and the second term is due to the viscous effect.

2.5.2 Bulk Temperature

The dimensionless bulk temperature in the solidification-free zone is

$$\theta_b = \frac{\int_0^1 U\theta dy}{\int_0^1 U dy} = \frac{\int_0^1 \sum_{j=1}^{20} E_j(1-y^2)Y_j(y)\exp[(-8/3)\alpha_j^2 x]dy}{\int_0^1 (1-y^2)\ dy} \tag{46}$$

Using Eq. (4), one obtains

$$\int_0^1 (1-y^2)Y_j(y)dy = [-\frac{1}{\alpha_j^2}\frac{dY_j}{dy}]^1_{y=0}$$

Thus, Eq. (46) reduces to

$$\theta_b = -\frac{3}{2}\sum_{j=1}^{20} E_j\frac{dY_j(1)}{dy}\exp[(-8/3)\alpha_j^2 x]/\alpha_j^2, \quad 0 \leq x \leq x_f \tag{47}$$

Following the same procedure, the dimensionless bulk temperature in the freezing zone can be shown to be

$$\theta_b = \frac{1}{1+\epsilon} - \frac{3}{2}\frac{\epsilon}{1+\epsilon} \int_0^1 \sum_{j=1}^{20} (1-\eta^2)K_j N_j(\eta) \exp[(-8/3)\beta_j^2 \int_0^{\bar{x}} \frac{d\bar{x}}{\bar{\delta}}]d\eta \qquad (48)$$

After making use of Eq. (26), one obtains

$$\theta_b = \frac{\epsilon}{1+\epsilon} [\frac{1}{\epsilon} - \frac{3}{2} \sum_{j=1}^{20} K_j \frac{dN_j(1)}{d\eta} \exp[(-8/3)\beta_j^2 \int_0^{\bar{x}} \frac{d\bar{x}}{\bar{\delta}}]/\beta_j^2] \qquad (49)$$

2.5.3 Heat Transfer

The dimensionless total rate of heat transfer from the liquid per unit depth of the channel in the solidification-free zone from $x = 0$ to $x = x$ can be found from

$$\bar{Q}_1 = Q/2LU_m \rho c_p (T_0 - T_f) \qquad (50)$$

where $Q = 2\int_0^X -k_\ell \partial T(X,L)/\partial Y \cdot dX, \quad 0 \leq x \leq x_f.$

One notes that $\bar{Q}$ assumes a value of 1 when the liquid is cooled to its freezing temperature. Using Eq. (3), one obtains

$$\bar{Q}_1 = (\frac{1+\epsilon}{\epsilon})(\frac{3}{2})[\sum_{j=1}^{20} E_j \frac{dY_j(1)}{dy}(\exp[(-8/3)\alpha_j^2 x]-1)/\alpha_j^2], \quad 0 \leq x \leq x_f \qquad (51)$$

Similarly, the dimensionless heat transfer rate in the freezing zone from $\bar{x} = 0$ to $\bar{x} = \bar{x}$ is found as

$$\bar{Q}_2 = -4\int_0^{\bar{x}} \frac{1}{\bar{\delta}} \frac{\partial\phi(\bar{x},1)}{\partial\eta} d\bar{x} \qquad (52)$$

Thus, the total heat transfer rate between the thermal entrance (x=0) and any axial location ($\bar{x}=\bar{x}$) in the freezing zone is simply given by

$(\dot{Q}_1 + \dot{Q}_2).$

2.5.4 Local Nusselt Number

The local Nusselt number provides further insight in understanding the heat transfer mechanism for the present liquid solidification problem and is defined by

$$Nu = \frac{h(2L)}{k_\ell} = -2\frac{\partial\theta(x,1)}{\partial y}/\theta_b, \quad 0 \leq x \leq x_f \qquad (53)$$

$$Nu = \frac{h(2L)}{k_\ell} = -\frac{2}{\delta}\frac{\partial\theta(\bar{x},1)}{\partial\eta}/[\theta_b(\frac{1+\epsilon}{\epsilon})], \quad x > x_f \qquad (54)$$

In deriving the above equations, one notes that

$$q = -k_\ell\frac{\partial T(X,L)}{\partial Y} = h(T_b-T_\infty), \quad 0 \leq x \leq x_f \qquad (55)$$

$$q = -k_\ell\frac{\partial T(X',\delta)}{\partial Y} = h(T_b-T_\infty), \quad x > x_f \qquad (56)$$

2.6   Results and Discussion

The theoretical results for the solidification-free length x_f versus superheat ratio ϵ are shown graphically in Fig. 2 with Bi = 0.25, 0.5, 1, 2, 10. As expected, for a given value of ϵ, x_f increases with the decrease of Biot number. The limiting case Bi = ∞ corresponds to a uniform wall temperature with $x_f = 0$. The superheat ratio $\epsilon = 0 \sim 10$ is considered to be the practical range in engineering applications [7].

Plots of the solid-phase layer thickness δ versus the entrance distance x are given in Fig. 3 for $\epsilon = 1, 2, 4, 8$ and Bi = 1,

2, 10, 100, ∞. The location where the departure of the curve from δ = 1 occurs represents the solidification-free length x_f. The solid-phase increases its thickness with x but stops short of reaching δ = 0 since a constant mass flow rate is assumed in the analysis. This precludes the "freezing-shut" of the channel. The effects of Biot number or superheat ratio on the solid-phase layer profile can be seen clearly in Fig. 3. The limiting case Bi = ∞ corresponds to a constant wall temperature studied by Lee and Zerkle [8]. An examination of Eq. (40) reveals that as Bi → ∞, the expression given by Lee and Zerkle [8] is recovered.

The pressure drop results are presented in Fig. 4 for Pr = 13.2 (water). The straight line part of the pressure distribution curve represents a pressure drop in the solidification-free zone which is independent of Bi and ε. When ice is being formed, the flow accelerates due to the reduction of the flow area and the pressure drop increases rapidly in the freezing zone. Thus, a large pressure difference is required to maintain a constant flow rate when the ice growth nearly fills up the channel. Eqs. (42) and (45) show that the pressure drop increases with Prandtl number.

The dimensionless bulk temperature distributions for Bi = 1, 2, 10, ∞ are shown in Fig. 5 with ε = 1 and 4. Noting that θ_f = 1/(1+ε) in Eq. (48), one sees that the asymptotic value for θ_b is θ_f. When θ_b = θ_f, the bulk temperature approaches the freezing temperature. For a given value of ε, the thermal entrance length for approaching θ_b = θ_f decreases with the increase of Biot number.

The amount of sensible heat to be removed before the bulk temperature approaches the freezing temperature is of considerable

practical interest. The dimensionless heat transfer rate $\bar{Q}$ as a function of χ is shown in Fig. 6 for $Bi = 1, 2, 10, \infty$ with $\varepsilon = 1$ and 4. It is noted that $\bar{Q} \to 1$ as $\theta_b \to \theta_f$ (see Fig. 5) and the effect of superheat ratio is considerable.

The local Nusselt number results are shown in Fig. 7 and the results may be contrasted to the axial variations of θ_b and $\bar{Q}$. It is of interest to note that a local minimum value for Nu exists. The effect of the Biot number and superheat ratio is evident. In this study, the solution is terminated when $\delta < 10^{-3}$ is reached since the physical model may not be valid with further reduction of the flow area. One may wish to define a local Nusselt number in the freezing zone by using the freezing temperature T_f instead of the surrounding fluid temperature T_∞ in Eq. (56). Then the discontinuity in local Nusselt number occurs at the end of the solidification-free zone and the results are presented in Fig. 8. Figs. 7 and 8 show that the local Nusselt number decreases and increases monotonically in the solidification-free and freezing zones, respectively. The behavior of Nu in the solidification-free zone is well understood and is due to the entrance effect caused by the growing thermal boundary layer. For $Bi = 1$ and 2, the end of the solidification-free zone corresponds to the fully-developed condition. The increase in Nusselt number in the freezing zone is caused by the increased axial velocity due to the presence of the increasing solid phase layer. Further insight regarding the local Nusselt number behavior can be gained by noting the following relationship and considering the relative magnitudes of the numerator and denominator.

$$h \sim \frac{\partial T(X,L)/\partial Y}{T_b - T_\infty} = \frac{h_0(T(X,L)-T_\infty)}{T_b - T_\infty}$$

The local Nusselt number behavior for the freezing problem in a circular tube or channel does not seem to have been elucidated in earlier studies. The increase of the pressure drop in the freezing zone (see Fig. 4) is clearly related to the corresponding increase in local Nusselt number.

2.7   Concluding Remarks

The solution of the steady-state liquid solidification problem in a parallel-plate channel flow with uniform external convection is obtained by using the confluent hypergeometric function. The first six eigenvalues in the solidification-free zone for Bi = 1, 2 agree with the available results [12] in the literature. The use of the confluent hypergeometric function in finding the eigenvalues from Eqs. (14) and (30) proves to be very efficient computationally and requires considerably less computing time than the Runge-Kutta method, for example.

Recent theoretical and experimental results of Hwang and Sheu [5] for the liquid solidification in combined hydrodynamic and thermal entrance region of a circular tube with a uniform wall temperature show that the physical model used by Zerkle and Sunderland [1] is a reasonable one. Thus, one may reason that the present analysis for liquid solidification in a parallel-plate channel using the same physical model represents a good approximate solution. The limiting case of the present analysis with Bi = ∞ corresponds to an

isothermal wall studied by Lee and Zerkle [8].

For liquid flow between horizontal parallel plates, the free convection effects will appear only after the onset of a secondary flow in the form of longitudinal vortex rools [13,14]. The thermal instability problem in the solidification-free zone represents a separate problem. However, the free convection effects in the freezing zone are not expected to be important since the temperature difference across the potentially unstable layer between the midplane and the upper liquid-solid interface is very small. This is in contrast to the case of tube flow where the free convection effects always [1] exist and are represented by Grashof number.

The pressure drop results shown in Fig. 4 together with the other results are useful in estimating the conditions [2] under which a parallel-plate channel may freeze shut by noting that the solution is terminated in this study when $\delta = 10^{-3}$ is reached. One notes that solution using the confluent hypergeometric function can also be applied to the internal axisymmetric free-boundary problem involving freezing in a cooled circular tube [1-7]. More eigenvalues and eigenfunctions are required to obtain an accurate solution near the thermal entrance at $x = 0$ or x_f.

REFERENCES

1. Zerkle, R.D. and Sunderland, J.E., "The effect of liquid solidi-
    fication in a tube upon laminar-flow heat transfer and pressure
    drop", J. Heat Transfer 90C, 1968, pp. 183-190.

2. 𝛾 DesRuisseaux, N. and Zerkle, R.D., "Freezing of hydraulic systems",
    Can. J. Chem. Eng. 47, 1969, pp. 233-237.

3. Bilenas, J.A. and Jiji, L.M., "Numerical solution of a nonlinear
    free boundary problem of axisymmetric fluid flow in tubes with
    surface solidification", Heat Transfer 1970, Vol. 1, Elsevier,
    Amsterdam, Cu 2.1.

4. Bilenas, J.A. and Jiji, L.M.,"Variational solution of axisymmetric
    fluid flow in tubes with surface solidification", J. Franklin
    Inst. 289, 1970, pp. 265-279.

5. Hwang, G.J. and Sheu, J.P., "Liquid solidification in combined
    hydrodynamic and thermal entrance region of a circular tube",
    Can. J. Chem. Eng. 54, 1976, pp. 66-71.

6. Zerkle, R.D., "The effect of external thermal insulation on liquid
    solidification in a tube", Proc. 6th Southeastern Seminar on Ther-
    mal Sciences, 1970, pp. 1-19.

7. Lock, G.S.H. Freeborn, R.D.J. and Nyren, R.H., "Analysis of ice
    formation in a convectively-cooled pipe", Heat Transfer 1970,
    Vol. 1, Elsevier, Armsterdam, Cu 2.9.

8. Lee, D.G. and Zerkle, R.D., "The effect of liquid solidification
    in a parallel plate channel upon laminar-flow heat transfer and
    pressure drop", J. Heat Transfer 91C, 1969, pp. 583-585.

9. Lauwerier, H.A., "The use of confluent hypergeometric function in

mathematical physics and the solution of an eigenvalues problem",
Appl. Sci. Res. 2A, 1950, pp. 184-204.

10. Pirkle, J.C. and Sigillito, V.G., "A variational approach to low
Peclet number heat transfer in laminar flow", J. Comp. Phys. 9,
1972, pp. 207-221.

11. Davis, E.J., "Exact solutions for a class of heat and mass trans-
fer problems", Can. J. Chem. Eng. 51, 1973, pp. 562-572.

12. Walker, G. and Davies, T., "Mass transfer in laminar flow between
parallel permeable plates", AIChE Journal 20, 1974, pp. 881-889.

13. Hwang, G.J. and Cheng, K.C., "Convective instability in the ther-
mal entrance region of a horizontal parallel-plate channel heated
from below", J. Heat Transfer 95C, 1973, pp. 72-77.

14. Kamotani, Y. and Ostrach, S., "Effect of thermal instability on
thermally developing laminar channel flow", J. Heat Transfer 98C,
1976, pp. 62-66.

Table 1. Eigenvalues, Eigenconstants and Related Derivatives for Solidification-Free Zone with Bi = 0.25, 0.5, 1, 2, 10

Bi = 0.25

j	α_j	$\dfrac{dY_j(1)}{dy}$	$\dfrac{\partial}{\partial \alpha_j}\left(\dfrac{dY_j(1)}{dy}\right)$	E_j
1	0.577972E+00	-0.463532E+00	-0.723511E+00	0.103062E+01
2	0.439857E+01	0.568570E+00	0.277094E+01	-0.390217E-01
3	0.837617E+01	-0.636071E+00	-0.471687E+01	0.122425E-01
4	0.123665E+02	0.679274E+00	0.652784E+01	-0.603670E-02
5	0.163609E+02	-0.711551E+00	-0.824826E+01	0.362688E-02
6	0.203572E+02	0.737577E+00	0.990208E+01	-0.243507E-02
7	0.243546E+02	-0.759527E+00	-0.115038E+02	0.175565E-02
8	0.283525E+02	0.778591E+00	0.130630E+02	-0.133018E-02
9	0.323509E+02	-0.795496E+00	-0.145865E+02	0.104532E-02
10	0.363496E+02	0.810718E+00	0.160793E+02	-0.844820E-03
11	0.403485E+02	-0.824589E+00	-0.175452E+02	0.698090E-03
12	0.443476E+02	0.837350E+00	0.189873E+02	-0.587320E-03
13	0.483468E+02	-0.849181E+00	-0.204080E+02	0.501541E-03
14	0.523461E+02	0.860218E+00	0.218095E+02	-0.433689E-03
15	0.563455E+02	-0.870573E+00	-0.231933E+02	0.379046E-03
16	0.603450E+02	0.880330E+00	0.245609E+02	-0.334357E-03
17	0.643445E+02	-0.889563E+00	-0.259136E+02	0.297317E-03
18	0.683441E+02	0.898329E+00	0.272524E+02	-0.266256E-03
19	0.723437E+02	-0.906678E+00	-0.285783E+02	0.239940E-03
20	0.763433E+02	0.914651E+00	0.298921E+02	-0.217437E-03

Bi = 0.5

j	α_j	$\dfrac{dY_j(1)}{dy}$	$\dfrac{\partial}{\partial \alpha_j}\left(\dfrac{dY_j(1)}{dy}\right)$	E_j
1	0.775508E+00	-0.602888E+00	-0.921506E+00	0.105440E+01
2	0.449586E+01	0.644911E+00	0.284490E+01	-0.702248E-01
3	0.844313E+01	-0.693286E+00	-0.475908E+01	0.231974E-01
4	0.124193E+02	0.727128E+00	0.655691E+01	-0.116351E-01
5	0.164052E+02	-0.753568E+00	-0.827015E+01	0.704946E-02
6	0.203958E+02	0.775502E+00	0.991946E+01	-0.475684E-02
7	0.243890E+02	-0.794374E+00	-0.115181E+02	0.344114E-02
8	0.283837E+02	0.811014E+00	0.130750E+02	-0.261350E-02
9	0.323796E+02	-0.825943E+00	-0.145968E+02	0.205757E-02
10	0.363762E+02	0.839515E+00	0.160882E+02	-0.166529E-02
11	0.403734E+02	-0.851981E+00	-0.175530E+02	0.137765E-02
12	0.443710E+02	0.863526E+00	0.189943E+02	-0.116046E-02
13	0.483689E+02	-0.874291E+00	-0.204143E+02	0.991512E-03
14	0.523671E+02	0.884384E+00	0.218151E+02	-0.857965E-03
15	0.563655E+02	-0.893893E+00	-0.231983E+02	0.750312E-03
16	0.603641E+02	0.902890E+00	0.245655E+02	-0.662196E-03
17	0.643628E+02	-0.911432E+00	-0.259178E+02	0.589111E-03
18	0.683617E+02	0.919568E+00	0.272562E+02	-0.527784E-03
19	0.723606E+02	-0.927338E+00	-0.285818E+02	0.475794E-03
20	0.763597E+02	0.934778E+00	0.298953E+02	-0.431316E-03

Table 1 continued

$Bi = 1$

j	α_j	$\dfrac{dY_j(1)}{dy}$	$\dfrac{\partial}{\partial\alpha_j}\left(\dfrac{dY_j(1)}{dy}\right)$	E_j
1	0.100000E+01	-0.741558E+00	-0.109628E+01	0.108824E+01
2	0.465614E+01	0.762946E+00	0.292682E+01	-0.116414E+00
3	0.856202E+01	-0.790336E+00	-0.480039E+01	0.417816E-01
4	0.125158E+02	0.811580E+00	0.658039E+01	-0.216177E-01
5	0.164876E+02	-0.829404E+00	-0.828395E+01	0.133105E-01
6	0.204684E+02	0.844862E+00	0.992730E+01	-0.907069E-02
7	0.244542E+02	-0.858867E+00	-0.115219E+02	0.660584E-02
8	0.284432E+02	0.871491E+00	0.130761E+02	-0.504141E-02
9	0.324345E+02	-0.883086E+00	-0.145958E+02	0.398367E-02
10	0.364273E+02	0.893831E+00	0.160857E+02	-0.323354E-02
11	0.404213E+02	-0.903859E+00	-0.175493E+02	0.268132E-02
12	0.444161E+02	0.913273E+00	0.189896E+02	-0.226242E-02
13	0.484117E+02	-0.922153E+00	-0.204088E+02	0.193673E-02
14	0.524078E+02	0.930565E+00	0.218090E+02	-0.167823E-02
15	0.564044E+02	-0.938561E+00	-0.231918E+02	0.146945E-02
16	0.604013E+02	0.946186E+00	0.245586E+02	-0.129826E-02
17	0.643985E+02	-0.953478E+00	-0.259105E+02	0.115607E-02
18	0.683960E+02	0.960467E+00	0.272487E+02	-0.103660E-02
19	0.723938E+02	-0.967181E+00	-0.285740E+02	0.935193E-03
20	0.763917E+02	0.973644E+00	0.298872E+02	-0.848350E-03

$Bi = 2$

j	α_j	$\dfrac{dY_j(1)}{dy}$	$\dfrac{\partial}{\partial\alpha_j}\left(\dfrac{dY_j(1)}{dy}\right)$	E_j
1	0.122015E+01	-0.852741E+00	-0.120537E+01	0.112623E+01
2	0.488090E+01	0.908862E+00	0.295200E+01	-0.171817E+00
3	0.874998E+01	-0.930076E+00	-0.477539E+01	0.688932E-01
4	0.126773E+02	0.942519E+00	0.653247E+01	-0.374843E-01
5	0.166300E+02	-0.952282E+00	-0.822439E+01	0.237466E-01
6	0.205964E+02	0.960877E+00	0.986142E+01	-0.164819E-01
7	0.245710E+02	-0.968801E+00	-0.114525E+02	0.121577E-01
8	0.285510E+02	0.976255E+00	0.130047E+02	-0.936669E-02
9	0.325348E+02	-0.983337E+00	-0.145235E+02	0.745568E-02
10	0.365214E+02	0.990106E+00	0.160129E+02	-0.608703E-02
11	0.405100E+02	-0.996599E+00	-0.174766E+02	0.507151E-02
12	0.445002E+02	0.100284E+01	0.189171E+02	-0.429615E-02
13	0.484917E+02	-0.100887E+01	-0.203367E+02	0.369002E-02
14	0.524842E+02	0.101468E+01	0.217374E+02	-0.320672E-02
15	0.564775E+02	-0.102030E+01	-0.231208E+02	0.281482E-02
16	0.604715E+02	0.102575E+01	0.244881E+02	-0.249238E-02
17	0.644661E+02	-0.103103E+01	-0.258407E+02	0.222372E-02
18	0.684613E+02	0.103616E+01	0.271796E+02	-0.199738E-02
19	0.724568E+02	-0.104114E+01	-0.285056E+02	0.180481E-02
20	0.764527E+02	0.104598E+01	0.298195E+02	-0.163853E-02

Table 1 continued

Bi = 10

j	α_j	$\dfrac{dY_j(1)}{dy}$	$\dfrac{\partial}{\partial \alpha_j}\left(\dfrac{dY_j(1)}{dy}\right)$	E_j
1	0.155181E+01	−0.965764E+00	−0.123633E+01	0.118305E+01
2	0.539775E+01	0.113374E+01	0.258474E+01	−0.266141E+00
3	0.930256E+01	−0.121755E+01	−0.404776E+01	0.132522E+00
4	0.132308E+02	0.126844E+01	0.553874E+01	−0.829508E−01
5	0.171731E+02	−0.130276E+01	−0.703411E+01	0.580516E−01
6	0.211250E+02	0.132737E+01	0.852376E+01	−0.434337E−01
7	0.250840E+02	−0.134579E+01	−0.100028E+02	0.339854E−01
8	0.290484E+02	0.136001E+01	0.114689E+02	−0.274645E−01
9	0.330171E+02	−0.137126E+01	−0.129208E+02	0.227439E−01
10	0.369892E+02	0.138034E+01	0.143584E+02	−0.191997E−01
11	0.409642E+02	−0.138781E+01	−0.157816E+02	0.164611E−01
12	0.449416E+02	0.139404E+01	0.171906E+02	−0.142951E−01
13	0.489211E+02	−0.139931E+01	−0.185860E+02	0.125486E−01
14	0.529023E+02	0.140383E+01	0.199682E+02	−0.111171E−01
15	0.568850E+02	−0.140775E+01	−0.213377E+02	0.992757E−02
16	0.608690E+02	0.141118E+01	0.226950E+02	−0.892701E−02
17	0.648542E+02	−0.141421E+01	−0.240406E+02	0.807653E−02
18	0.688404E+02	0.141693E+01	0.253750E+02	−0.734688E−02
19	0.728276E+02	−0.141937E+01	−0.266987E+02	0.671570E−02
20	0.768155E+02	0.142160E+01	0.280121E+02	−0.616566E−02

Table 2. Eigenvalues, Eigenconstants and Related Derivatives for Freezing Zone with $\varepsilon = 1$, 4, $k_\ell/k_s = 0.25$

$\varepsilon = 1$

j	β_j	$K_j(Bi = 1)$	$K_j(Bi = 2)$	$K_j(Bi = 10)$
1	0.168158E+01	0.654970E+00	0.107370E+01	0.120092E+01
2	0.566986E+01	-0.994100E-02	-0.909721E-01	-0.289388E+00
3	0.966824E+01	0.176365E-02	0.101645E-01	0.161183E+00
4	0.136677E+02	-0.585210E-03	-0.254599E-02	-0.107916E+00
5	0.176674E+02	0.258809E-03	0.105709E-02	0.802462E-01
6	0.216672E+02	-0.135493E-03	-0.535656E-03	-0.634875E-01
7	0.256671E+02	0.791797E-04	0.308331E-03	0.523656E-01
8	0.296670E+02	-0.500314E-04	-0.192815E-03	-0.444863E-01
9	0.336670E+02	0.335097E-04	0.128106E-03	0.386539E-01
10	0.376668E+02	-0.234795E-04	-0.891460E-04	-0.341916E-01
11	0.416669E+02	0.170542E-04	0.643446E-04	0.306928E-01
12	0.456668E+02	-0.127563E-04	-0.478386E-04	-0.279003E-01
13	0.496668E+02	0.977741E-05	0.364472E-04	0.256456E-01
14	0.536668E+02	-0.765034E-05	-0.283443E-04	-0.238164E-01
15	0.576668E+02	-0.544095E-05	0.224313E-04	0.223400E-01
16	0.616668E+02	0.572995E-05	-0.180207E-04	-0.211750E-01
17	0.656668E+02	-0.585895E-05	0.146677E-04	0.203137E-01
18	0.696668E+02	0.588349E-05	-0.120759E-04	-0.198041E-01
19	0.736668E+02	-0.583978E-05	0.100430E-04	0.198481E-01
20	0.776668E+02	0.575181E-05	-0.842759E-05	-0.215625E-01

$\varepsilon = 4$

j	β_j	$K_j(Bi = 1)$	$K_j(Bi = 2)$	$K_j(Bi = 10)$
1		0.164111E+00	0.333912E+00	0.113644E+01
2		-0.239915E-02	-0.363302E-02	-0.161154E+00
3		0.434408E-03	0.650903E-03	0.284912E-01
4		-0.144427E-03	-0.215809E-03	-0.475455E-02
5		0.639367E-04	0.954247E-04	0.121068E-02
6		-0.334678E-04	-0.499166E-04	-0.529474E-03
7		0.195599E-04	0.291593E-04	0.292206E-03
8		-0.123596E-04	-0.184180E-04	-0.179697E-03
9		0.827790E-05	0.123311E-04	0.113693E-03
10		-0.579981E-05	-0.863657E-05	-0.781662E-04
11		0.421230E-05	0.627033E-05	0.558245E-04
12		-0.315041E-05	-0.468787E-05	-0.410947E-04
13		0.241442E-05	0.359128E-05	0.310072E-04
14		-0.188890E-05	-0.280843E-05	-0.238791E-04
15		0.150407E-05	0.223528E-05	0.187081E-04
16		-0.121607E-05	-0.180642E-05	-0.148723E-04
17		0.996428E-06	0.147942E-05	0.119714E-04
18		-0.826122E-06	-0.122592E-05	-0.974059E-05
19		0.692120E-06	0.102650E-05	0.799963E-05
20		-0.585297E-06	-0.867569E-06	-0.662318E-05

Table 2 continued

j	$\dfrac{\partial N_j(1)}{\partial \beta_j}$	$\dfrac{dN_j(1)}{d\eta}$	j	$\dfrac{\partial N_j(1)}{\partial \beta_j}$	$\dfrac{dN_j(1)}{d\eta}$
1	-0.990437E+00	-0.142915E+01	11	-0.163960E+01	-0.189622E+02
2	0.117911E+01	0.380706E+01	12	0.166484E+01	0.215463E+02
3	-0.128625E+01	-0.592023E+01	13	-0.168831E+01	-0.231074E+02
4	0.136202E+01	0.789253E+01	14	0.171024E+01	0.246477E+02
5	-0.142133E+01	-0.977084E+01	15	-0.173086E+01	-0.261690E+02
6	0.147040E+01	0.115798E+02	16	0.175031E+01	0.276729E+02
7	-0.151246E+01	-0.133339E+02	17	-0.176875E+01	-0.291589E+02
8	0.154939E+01	0.150430E+02	18	0.178626E+01	0.306316E+02
9	-0.158238E+01	-0.167141E+02	19	-0.180296E+01	-0.320903E+02
10	0.161226E+01	0.183525E+02	20	0.181892E+01	0.335358E+02
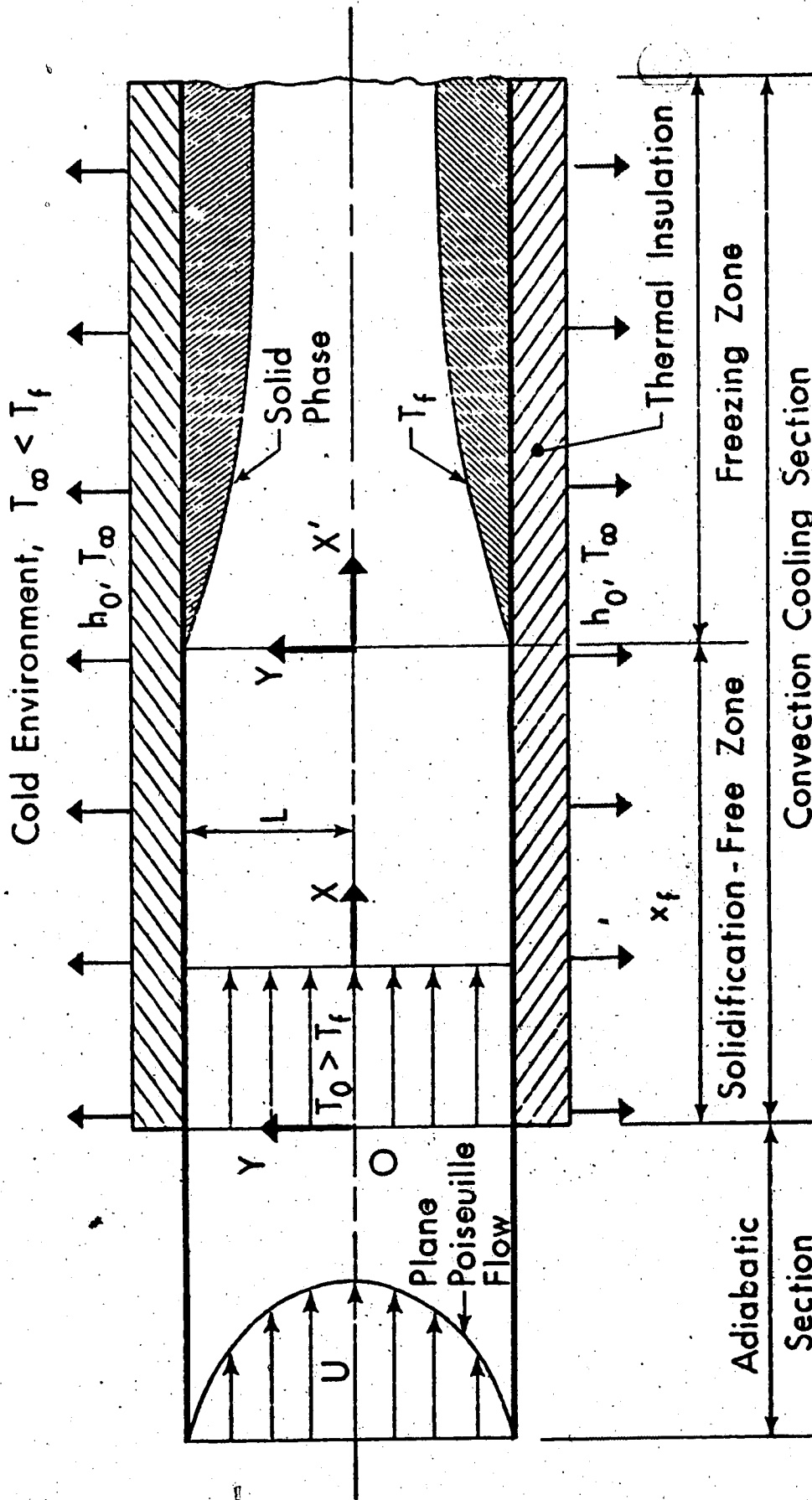
Figure 1. Physical model and coordinate system
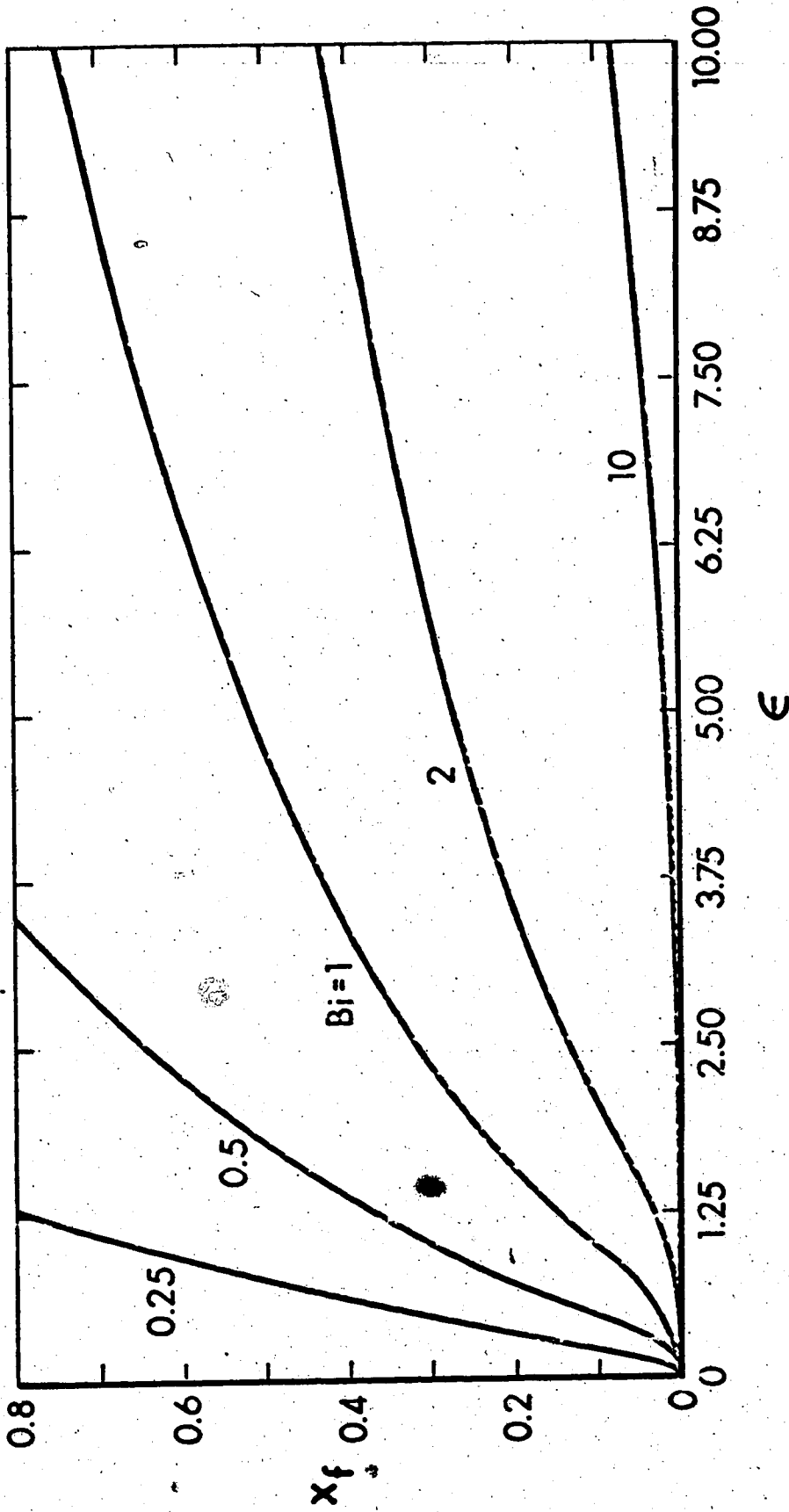
Figure 2.   Liquid solidification-free length as a function of superheat ratio for Bi=0.25,0.5,1,2,10
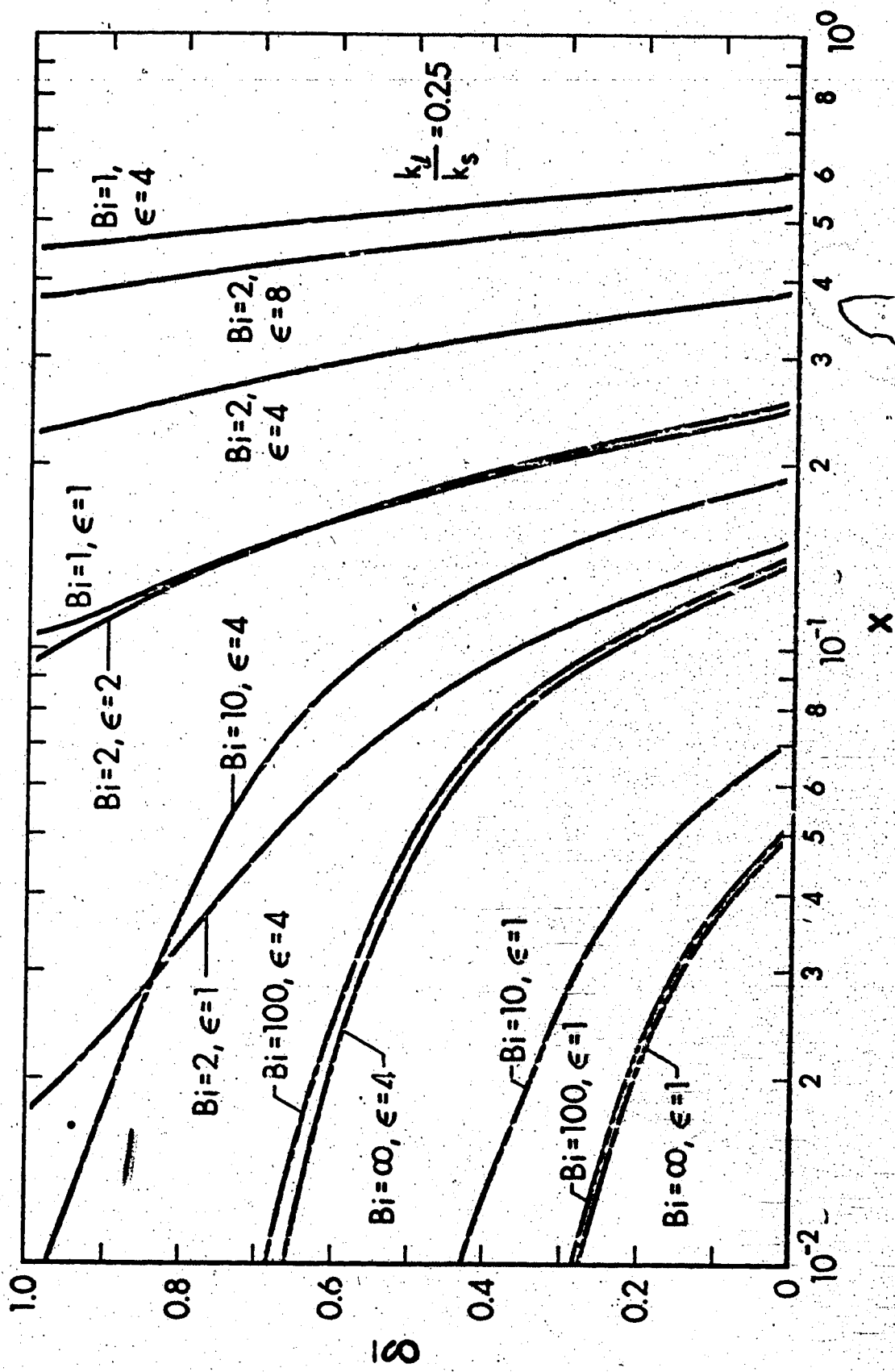
Figure 3. Steady state liquid-solid interface δ versus axial distance with Bi and ϵ as parameters for $k_\ell/k_s = 0.25$
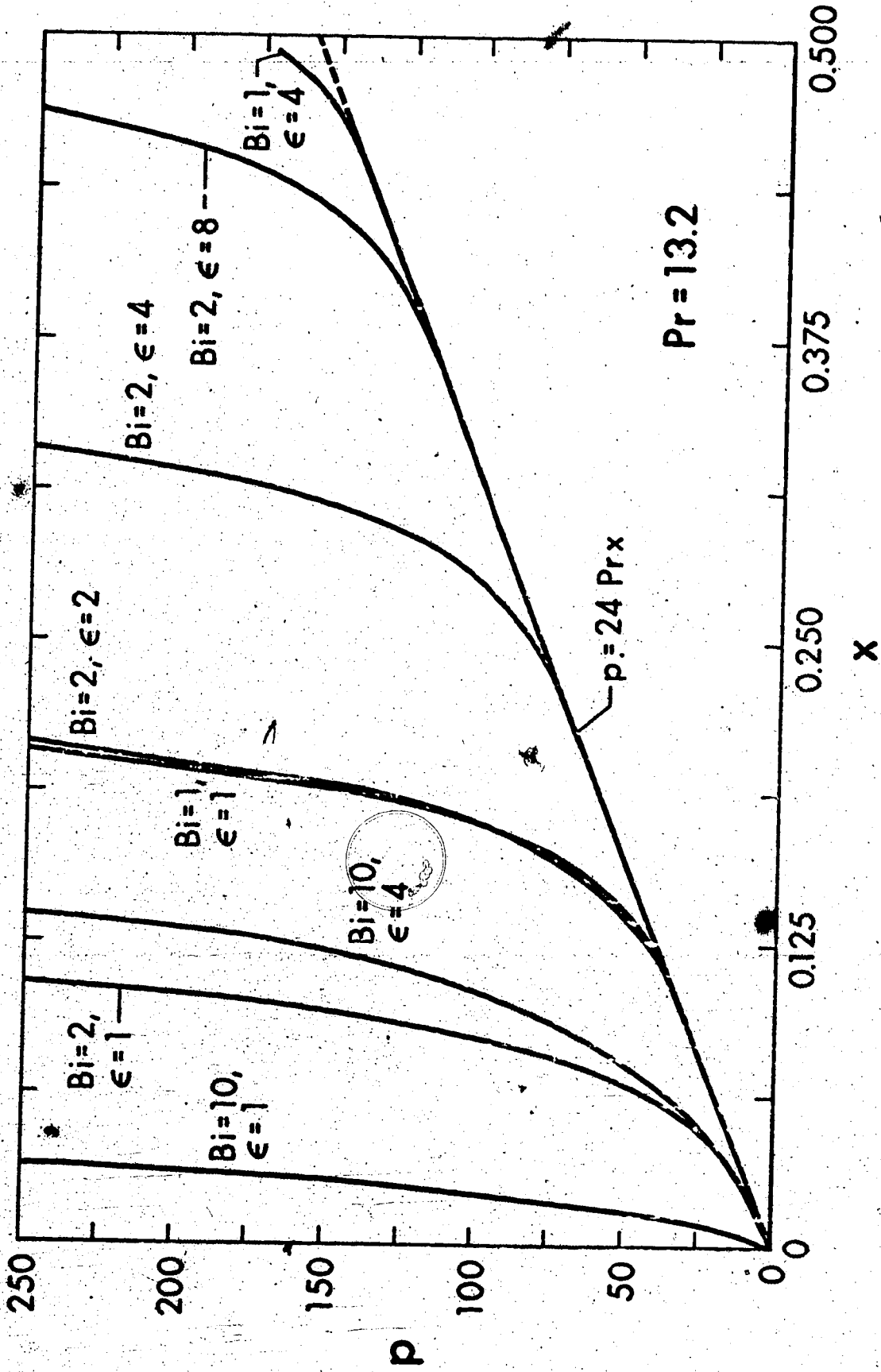
Figure 4. Steady state pressure drop p versus axial distance with Bi and ε as parameters
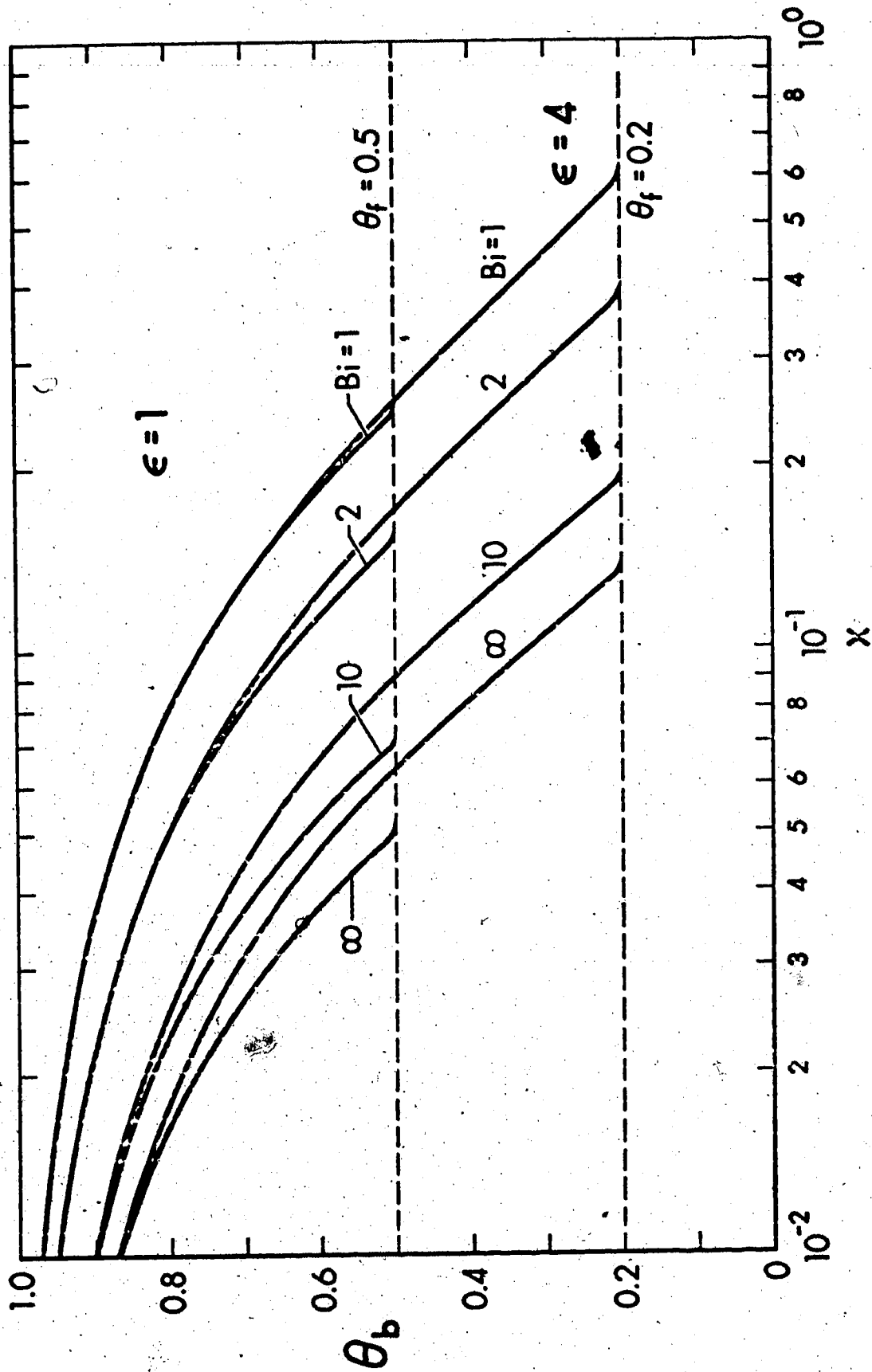
Figure 5. Axial bulk temperature distributions for Bi=1,2,10,∞ and ε=1,4
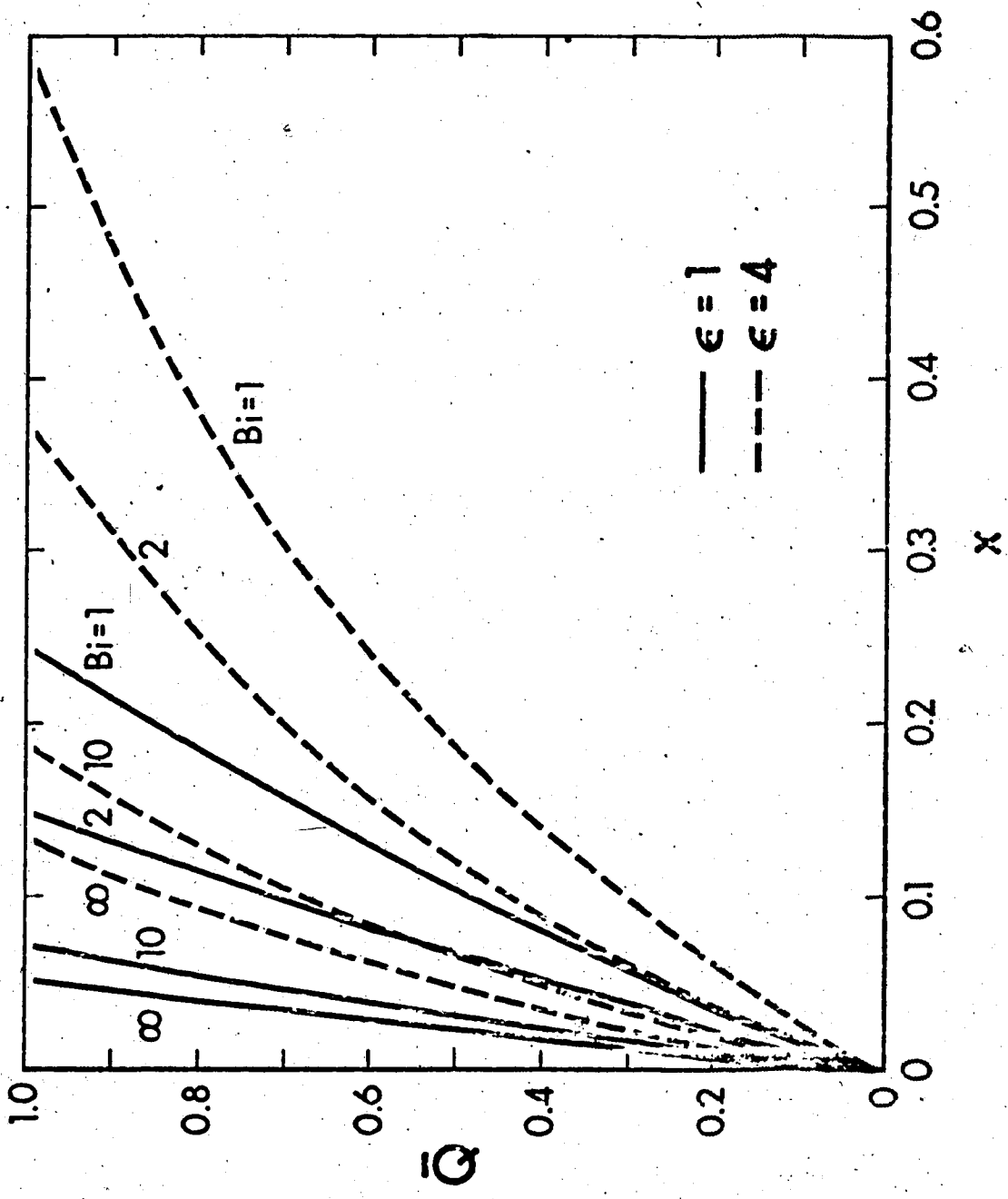
Figure 6. Total heat transfer rate $\bar{Q}$ versus axial position for $Bi=1,2,10,\infty$ and $\epsilon=1,4$
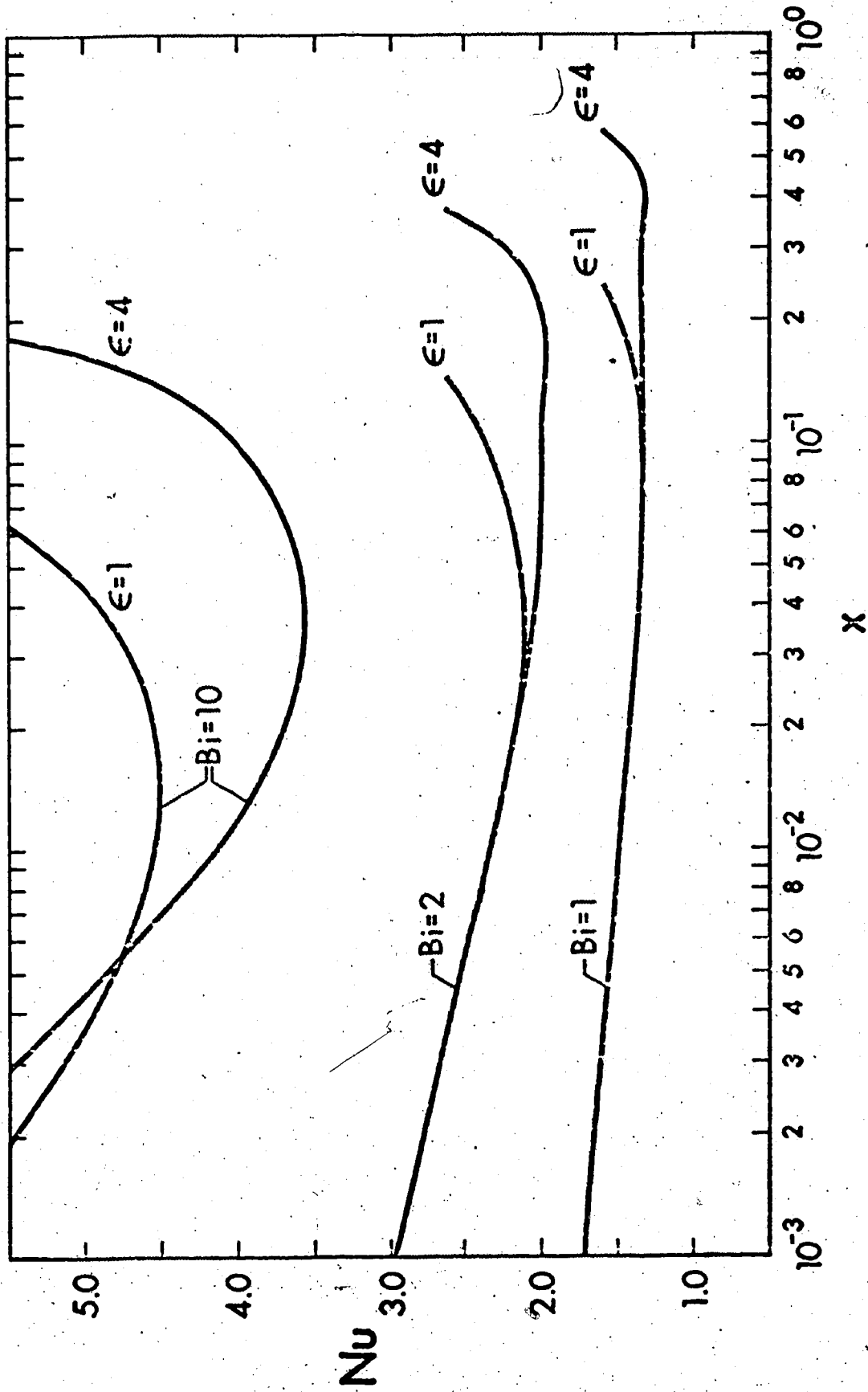
Figure 7. Local Nusselt number results for Bi=1,2,10 and ϵ=1,4 with T_∞ as reference temperature
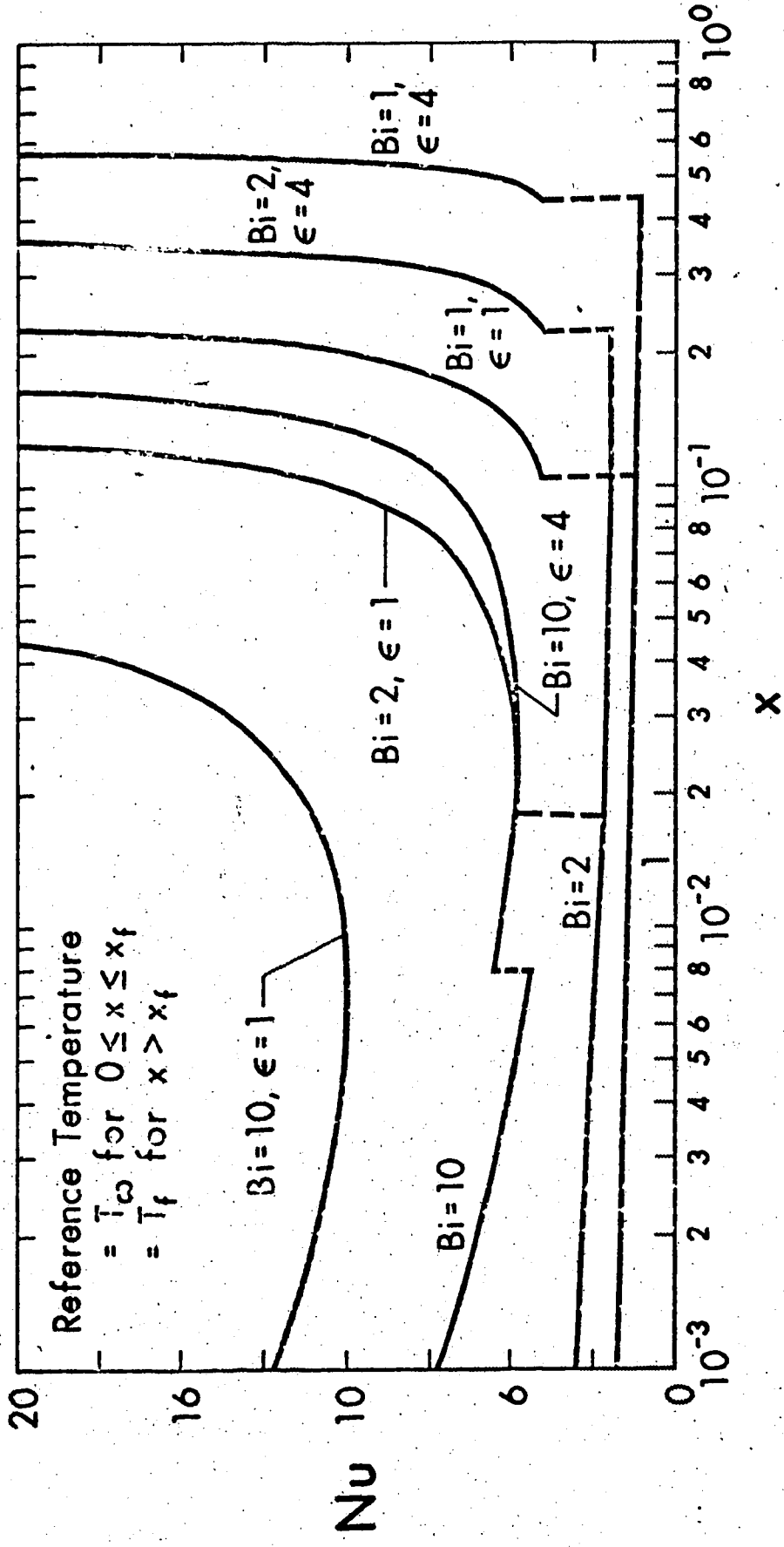
Figure 8. Local Nusselt number results for Bi=1,2,10 and ϵ=1,4 with T_f as reference temperature in the freezing zone

CHAPTER III

ASYMMETRIC SOLIDIFICATION OF FLOWING LIQUID IN
A CONVECTIVELY COOLED PARALLEL-PLATE CHANNEL

In this Chapter, an analysis is made of steady-state unsymmetric liquid solidification of forced laminar flow in a parallel-plate channel with different uniform external convection coolings at the upper and lower plates. The classical Graetz type analysis is made by using the confluent hypergeometric function. The case of one plate with perfect insulation and the other plate with a uniform external convection cooling is studied in detail. Numerical results are obtained for liquid solidification-free length, ice layer thickness, pressure drop, bulk temperature, heat transfer rate and local Nusselt number for $Bi_1 = 0$, $Bi_2 = 1$, 2, 10, 100, $\varepsilon = 0 \sim 10$, $Pr = 13.2$ and $k_\ell/k_s = 0.25$ using 10 eigenvalues. The configuration and thermal conditions may be encountered, for example, in heat exchangers using cryogenics and freezing of ice sheets on northern rivers and lakes.

NOMENCLATURE

a, b = parameters in Kummer's equation

Bi_1, Bi_2 = Biot numbers at lower and upper plates, $h_1 L/k$, $h_2 L/k$

Bi_s = $(k_\ell/k_s)Bi_2$

C_{1j}, C_{2j} = constants in eq. (8)

C_j, D_j = constants

c_p = specific heat at constant pressure

E_j, K_j = eigenconstants, eqs. (4) and (33)

H = function of $\bar{x}$ only, equation (31)

h = local heat transfer coefficient, eqs. (54) and (55)

h_1, h_2 = overall heat transfer coefficients defined by $k\partial T(X,0)/\partial Y$

$\quad = h_1[T(X,0)-T_\infty]$, $- k\partial T(X,L)/\partial Y = h_2[T(X,L)-T_\infty]$

k = thermal conductivity of liquid

L = distance between parallel plates

$M(a,b,z)$ = confluent hypergeometric function

N_j, Y_j = eigenfunctions

Nu = Nusselt number, hL/k

P, P_0 = Pressures at X and $X = 0$

Pe = Peclet number, $4 U_m L/\alpha$

Pr = Prandtl number, ν/α

p = dimensionless pressure drop, $(P_0-P)/(\rho U_m^2/2)$

$Q, \bar{Q}$ = total heat transfer rate and dimensionless Q, eq. (51)

q = local heat transfer rate, eqs. (54) and (55)

T, T_b, T_f = liquid temperature, bulk temperature and freezing temperature

T_0, T_∞ = uniform entrance temperature and ambient temperature

U, V	= axial and transverse velocities
U_m	= average axial velocity
v	= solution of Kummer's equation
X, Y	= rectangular coordinates
X'	= axial coordinate with origin at solid-phase entrance
x, y	= (X/3LPe), (Y/L)
$\bar{x}$, $\bar{y}$	= (X'/3LPe), (Y/L) in freezing zone
x_f	= dimensionless solidification-free length
z	= transformed variable
α	= thermal diffusivity
α_j, β_j	= eigenvalues
δ, $\bar{\delta}$	= transverse coordinate of liquid-solid interface and δ/L
ϵ	= superheat ratio, $(T_0-T_f)/(T_f-T_\infty)$
η	= dimensionless transverse coordinate, $\bar{y}/\bar{\delta} = Y/\delta$
θ	= dimensionless temperature difference, $(T-T_\infty)/(T_0-T_\infty)$
θ_b	= dimensionless bulk temperatures, eqs. (48) and (50)
θ_f	= $(T_f-T_\infty)/(T_0-T_\infty)$
μ, ν	= dynamic viscosity and kinematic viscosity
ρ	= density
ϕ	= dimensionless temperature difference, $(T-T_f)/(T_0-T_f)$

Subscripts

ℓ, s	= liquid and solid-phase.

3.1 Introduction

The freezing of liquids in forced laminar flow inside circular tubes is of technical importance and has been studied by Zerkle and Sunderland [1], DesRuisseaux and Zerkle [2], Özisik and Mulligan [3], Bilenas and Jiji [4, 5] and Hwang and Sheu [6] for uniform wall temperature condition and by Zerkle [7] and Lock, Freeborn and Nyren [8] for uniform external convection cooling. The analysis of Zerkle and Sunderland [1] employs the basic assumption of a parabolic axial velocity profile even in the presence of steady-state ice layer and reduces the problem to Graetz type analysis which proves to be a good approximation confirmed by numerical solutions [4, 6] and experiments [1, 6]. Lee and Zerkle [9] extended the analysis to steady-state liquid solidification in a parallel-plate channel with uniform wall temperature below the freezing temperature.

Turning to the one-plate problem, the transient freezing of a liquid flowing over a flat plate was treated by Lapadula and Mueller [10] and Beauboeuf and Chapman [11] for the case of constant wall temperature and by Miller and Jiji [12] for the case with constant heat removal. Savino and Siegel [13, 14] carried out experimental and analytical investigations on transient solidification of a warm liquid flowing over a convectively cooled flat plate. Their investigations where motivated by the application in liquid-liquid heat exchangers employing the coolant at a temperature below the freezing point of the warm liquid [13]. One notes that their test apparatus corresponds to the configuration with liquid flow between two parallel plates. Since the convective heat transfer decreases with length along the plate, the ice thickness increases in the downstream

direction and the ice-layer profile (see Fig. 6(b) of [13]) resembles that of Zerkle and Sunderland [1].

The purpose of this study is to analyze the steady-state two-dimensional asymmetric solidification of laminar forced liquid flow in a parallel-plate channel with different, uniform external convection coolings at the upper and lower plates. The investigation was motivated by the applications in solidification of metal castings in molds, freezing of northern rivers with ice cover, and solidification within liquid flow heat exchangers using a cryogen as the coolant such as plate coolers [13].

One notes that the two-plate problem represents a generalization of the one-plate problem since flow over a flat plate can be recovered when the distance between the two plates approaches infinity. On the other hand, the present investigation can be regarded to be the extension and generalization of the analysis by Lee and Zerkle [9] to the convective boundary conditions at the upper and lower plates. For the convective boundary condition, the limiting cases of Bi = 0 and ∞ represent the perfect insulation and the uniform wall temperature, respectively. The case Bi ≠ 0 represents a finite thermal resistance between the inner wall and the cold ambient. The present analysis is valid for any combination of Biot numbers at the upper and lower plates but numerical results are obtained for Bi_1 = 0 (perfect insulation) at lower plate and Bi_2 = 1, 2, 10, 100 at upper plate. This type of asymmetric solidification problem arises in freezing of northern rivers, discharge of warm water from power plants to the frozen northern lakes and various plate coolers.

For Graetz problem in parallel-plate channels with unsymme-

tric boundary conditions, one may mention the works by Schenk [15], Dennis and Poots [16], and Cess and Shaffer [17, 18] for reference. In this study, the solution to the thermal entry problem is obtained by the eigenfunction expansion method using the confluent hypergeometric function [19, 20].

3.2   The Liquid Solidification-Free Zone

3.2.1   Physical Problem and Analysis

The physical model is depicted in Fig. 1. The warm liquid with an established plane Poiseuille flow enters the thermal entrance ($X = 0$) at a uniform temperature T_∞. Different, but constant overall heat transfer coefficients, h_1 and h_2, between the inner wall and the cold ambient are prescribed at the lower and upper plates, respectively, in the cooling section. The liquid is cooled as it flows through the channel and eventually, at some downstream location, the freezing temperature is reached at the wall and solidification begins. With $h_1 \neq h_2$, the location of point of incipient solidification is different at the lower and upper plates. Thus, the thermal entrance region consists of a solidification-free zone and a freezing zone where the solid layer increases its thickness monotonically along the channel wall. It is assumed that the physical properties are constant and axial heat conduction, viscous energy dissipation and free convection are negligible. The fully developed velocity profile is given as

$$U(X,Y) = 6U_m(Y/L)[1-(Y/L)] \tag{1}$$

The energy equation in dimensionless form for the steady state and the thermal boundary conditions can be written as

$$y(1-y) \frac{\partial \theta}{\partial x} = \frac{\partial^2 \theta}{\partial y^2} \tag{2}$$

$$\theta(0,y) = 1, \quad \partial\theta(x,0)/\partial y = Bi_1 \theta(x,0), \quad \partial\theta(x,1)/\partial y = -Bi_2 \theta(x,1) \tag{3}$$

where $x = X/(3LPe)$, $y = Y/L$, $\theta = (T-T_\infty)/(T_0-T_\infty)$, $Bi_1 = h_1 L/k$,

$\quad Bi_2 = h_2 L/k$

and all other symbols are defined in Nomenclature. By using the method of separation of variables, the solution takes the form

$$\theta(x,y) = \sum_{j=1}^{\infty} E_j Y_j(y) \exp(-\alpha_j^2 x) \tag{4}$$

where α_j and Y_j are the eigenvalues and eigenfunctions which satisfy the following system of equations.

$$\frac{d^2 Y_j}{dy^2} + \alpha_j^2 y(1-y)Y_j = 0, \quad \frac{dY_j(0)}{dy} = Bi_1 Y_j(0), \quad \frac{dY_j(1)}{dy} = -Bi_2 Y_j(1) \tag{5}$$

3.2.2 Eigenvalues

In order to overcome the difficulty in obtaining the higher eigenvalues, the series solution is replaced by a solution using the confluent hypergeometric function [19, 20]. By introducing the transformations, $z = \alpha_j(y-1/2)^2$ and $v(z) = Y_j(y) \cdot \exp(z/2)$, equation (5) becomes

$$z\frac{d^2 v}{dz^2} + (1/2-z)\frac{dv}{dz} - (1/4 - \frac{\alpha_j}{16}) v = 0 \tag{6}$$

which is recognized to be Kummer's equation,

$$z\frac{d^2 v}{dz^2} + (b-z)\frac{dv}{dz} - av = 0 \tag{7}$$

with $a = (1/4)-(\alpha_j/16)$, $b = 1/2$. Noting that the general solution of equation (7) can be expressed in terms of the confluent hypergeometric function $M(a,b,z)$ [20], the expression for $Y_j(y)$ takes the form

$$Y_j(y) = \exp[-\alpha_j(y-1/2)^2/2] \cdot [C_{1j}M(a_j,1/2,\alpha_j(y-1/2)^2)$$

$$+ C_{2j}\alpha_j^{1/2}(y-1/2)M(a_j+1/2,3/2,\alpha_j(y-1/2)^2)] \tag{8}$$

where C_{1j} and C_{2j} are the constants. The series expansion for $M(a,b,z)$ is [20]

$$M(a,b,z) = 1 + \frac{a}{b}z + \frac{a(a+1)}{b(b+1)}\frac{z^2}{2!} + \cdots \frac{a(a+1)\cdots(a+n-1)}{b(b+1)\cdots(b+n-1)}\frac{z^n}{n!} + \cdots \tag{9}$$

Thus, one obtains

$$Y_j(y) = \exp[-\alpha_j(y-1/2)^2/2]$$

$$\cdot \{C_{1j}[1+ \sum_{n=1}^{\infty} \frac{(1-\alpha_j/4)\cdots(4n-3-\alpha_j/4)}{(2n)!} \alpha_j^n(y-1/2)^{2n}] + C_{2j}\alpha_j^{1/2}$$

$$\cdot [(y-1/2) + \sum_{n=1}^{\infty} \frac{(3-\alpha_j/4)\cdots(4n-1-\alpha_j/4)}{(2n+1)!} \alpha_j^n(y-1/2)^{2n+1}]\} \tag{10}$$

$$\frac{dY_j(y)}{dy} = \exp[-\alpha_j(y-1/2)^2/2]$$

$$\cdot \{-C_j\alpha_j(y-1/2)+\alpha_j^{1/2}[1-\alpha_j(y-1/2)^2]$$

$$+ C_j \sum_{n=1}^{\infty} \frac{(1-\alpha_j/4)\cdots(4n-3-\alpha_j/4)}{(2n)!} \alpha_j^n(y-1/2)^{2n}[-\alpha_j(y-1/2)+\frac{2n}{(y-1/2)}]$$

$$+ \alpha_j^{1/2} \sum_{n=1}^{\infty} \frac{(3-\alpha_j/4)\cdots(4n-1-\alpha_j/4)}{(2n+1)!} \alpha_j^n (y-1/2)^{2n}$$

$$\cdot [-\alpha_j(y-1/2)^2+2n+1]\} \tag{11}$$

where C_{2j} is being absorbed by the eigenconstant in equation (4) and C_j is the new constant. Substituting equations (10) and (11) into the convective boundary conditions in equation (3), one obtains

$$\frac{C_j \alpha_j}{2} - C_j Bi_1 + \alpha_j^{1/2}(\frac{Bi_1}{2} + 1 - \frac{\alpha_j}{4})$$

$$+ C_j \sum_{n=1}^{\infty} \frac{(1-\alpha_j/4)\cdots(4n-3-\alpha_j/4)}{(2n)!} (\frac{\alpha_j}{4})^n(\frac{\alpha_j}{2} - 4n-Bi_1)$$

$$+ \alpha_j^{1/2} \sum_{n=1}^{\infty} \frac{(3-\alpha_j/4)\cdots(4n-1-\alpha_j/4)}{(2n+1)!} (\frac{\alpha_j}{4})^n(\frac{Bi_1}{2} - \frac{\alpha_j}{4} + 2n + 1) = 0 \tag{12}$$

$$- \frac{C_j \alpha_j}{2} + C_j Bi_2 + \alpha_j^{1/2} (\frac{Bi_2}{2} + 1 - \frac{\alpha_j}{4})$$

$$+ C_j \sum_{n=1}^{\infty} \frac{(1-\alpha_j/4)\cdots(4n-3-\alpha_j/4)}{(2n)!} (\frac{\alpha_j}{4})^n(Bi_2 - \frac{\alpha_j}{2} + 4n)$$

$$+ \alpha_j^{1/2} \sum_{n=1}^{\infty} \frac{(3-\alpha_j/4)\cdots(4n-1-\alpha_j/4)}{(2n+1)!} (\frac{\alpha_j}{4})^n(\frac{Bi_2}{2} - \frac{\alpha_j}{4} + 2n + 1) = 0 \tag{13}$$

By adding and subtracting the above two equations, one can solve for C_j and obtain the equation for α_j. The subtraction of equation (12) from (13) yields

$$C_j = \frac{(Bi_2-Bi_1)\alpha_j^{1/2}[1+ \sum_{n=1}^{\infty} \frac{(3-\alpha_j/4)\cdots(4n-1-\alpha_j/4)}{(2n+1)!}(\frac{\alpha_j}{4})^n]}{2Bi_1} \tag{14}$$

while the addition of the two equations gives

$$C_j = \frac{2\alpha_j^{1/2}\phi_2}{(Bi_1-Bi_2)[1+\sum\limits_{n=1}^{\infty}\frac{(1-\alpha_j/4)\cdots(4n-3-\alpha_j/4)}{(2n)!}(\frac{\alpha_j}{4})^n]} \tag{15}$$

where

$$\phi_1 = \alpha_j-(Bi_1+Bi_2) + \sum\limits_{n=1}^{\infty}\frac{(1-\alpha_j/4)\cdots(4n-3-\alpha_j/4)}{(2n)!}(\frac{\alpha_j}{4})^n[\alpha_j-8n-Bi_1-Bi_2],$$

$$\phi_2 = 1 - \frac{\alpha_j}{4} + \frac{Bi_1+Bi_2}{2} + \sum\limits_{n=1}^{\infty}\frac{(3-\alpha_j/4)\cdots(4n-1-\alpha_j/4)}{(2n+1)!}(\frac{\alpha_j}{4})^n$$

$$\cdot[\frac{Bi_1+Bi_2}{4} - \frac{\alpha_j}{4} + 2n + 1]$$

Equating equations (14) and (15), one obtains

$$4\phi_1\phi_2 + (Bi_1-Bi_2)^2[1+\sum\limits_{n=1}^{\infty}\frac{(3-\alpha_j/4)\cdots(4n-1-\alpha_j/4)}{(2n+1)!}(\frac{\alpha_j}{4})^n]$$

$$\cdot[1+\sum\limits_{n=1}^{\infty}\frac{(1-\alpha_j/4)\cdots(4n-3-\alpha_j/4)}{(2n)!}(\frac{\alpha_j}{4})^n] = 0 \tag{16}$$

In present study, only the specific case of $Bi_1 = 0$ (perfect insulation at bottom plate) will be studied in detail. With $Bi_1 = 0$, equation (16) becomes

$$4\phi_1\phi_2 + Bi_2^2[1+\sum\limits_{n=1}^{\infty}\frac{(3-\alpha_j/4)\cdots(4n-1-\alpha_j/4)}{(2n+1)!}(\frac{\alpha_j}{4})^n]$$

$$\cdot[1+\sum\limits_{n=1}^{\infty}\frac{(1-\alpha_j/4)\cdots(4n-3-\alpha_j/4)}{(2n)!}(\frac{\alpha_j}{4})^n] = 0 \tag{17}$$

where one notes that $Bi_1 = 0$ in the expressions for Φ_1 and Φ_2. The eigenvalues α_j are the roots of equation (17) and initial estimates of the roots can be obtained by tabulating the value of the left-hand side of equation (17) versus a sequence of closely spaced values of α_j's. The values of α_j's at which the sign of the left-hand side of equation (17) changes give the upper and lower bounds of the root and may serve as a starting point in computing the eigenvalue using the variable secant method.

The limiting case with $Bi_1 = Bi_2 = Bi$ (symmetric boundary conditions) are of special interest since comparison of the eigen-values with the published results can be made. From the symmetry condition $Y_j(0)=Y_j(1)$, one notes from equation (10) that all odd terms vanish. Thus, the eigenfunction $Y_j(y)$ becomes

$$Y_j(y)=C_{1j} \exp[-\alpha_j(y-1/2)^2/2] \cdot [1+ \sum_{n=1}^{\infty} \frac{(1-\alpha_j/4)\cdots(4n-3-\alpha_j/4)}{(2n)!} \alpha_j^n(y-1/2)^{2n}]$$

$$(18)$$

After applying the convective boundary condition $dY_j(1)/dy = -BiY_j(1)$, one obtains $\Phi_1 = 0$, i.e.

$$\frac{\alpha_j}{2} - Bi + \sum_{n=1}^{\infty} \frac{(1-\alpha_j/4)\cdots(4n-3-\alpha_j/4)}{(2n)!} (\frac{\alpha_j}{4})^n[\frac{\alpha_j}{2} - 4n - Bi] = 0 \qquad (19)$$

The first three eigenvalues are obtained for $Bi = 2,20$ and the results are listed in Table 1 where the resluts from Van Der Does De Bye and Schenk [21] and the approximate values of Dennis and Poots [16] are also given for comparison.

3.2.3 Eigenconstants

From the orthogonality of the eigenfunctions, the eigen-constants can be determined from

$$E_j = \int_0^1 y(1-y)Y_j(y)dy / \int_0^1 y(1-y)Y_j^2(y)dy \tag{20}$$

The integrals appearing in the numerator and denominator can be written as

$$\int_0^1 y(1-y)Y_j(y)dy = -\frac{1}{\alpha_j^2}\frac{dY_j(1)}{dy}$$

$$\int_0^1 y(1-y)Y_j^2(y)dy = \frac{1}{2\alpha_j}\left[\frac{\partial Y_j}{\partial \alpha_j}\frac{dY_j}{dy} - Y_j\frac{d}{dy}\left(\frac{\partial Y_j}{\partial \alpha_j}\right)\right]_{y=0}^1$$

Thus, the eigenconstants for the case $Bi_1 = 0$ are

$$E_j = -\frac{2}{\alpha_j}\left[\frac{1}{\left[\frac{\partial Y_j}{\partial \alpha_j} + \frac{1}{Bi_2}\frac{d}{dy}\left(\frac{\partial Y_j}{\partial \alpha_j}\right)\right]_{y=1} + S}\right] \tag{21}$$

where $S = Y_j(0)\frac{d}{dy}\left(\frac{\partial Y_j(0)}{\partial \alpha_j}\right) / \frac{dY_j(1)}{dy}$

The first ten eigenvalues, eigenconstants together with $C_1 \sim C_{10}$ and $Y_1 \sim Y_{10}$ are listed in Table 2 for $Bi_1 = 0$ and $Bi_2 = 1, 2, 10, 100$. The ten eigenvalues are found to give sufficiently accurate solution.

3.2.4 Location of Point of Incipient Solidification

Noting that the solidification starts at the location where the wall temperature at the upper plate reaches the freezing temperature, the liquid soldification-free length x_f can be evaluated

from

$$\theta(x_f,1)=\theta_f=\sum_{j=1}^{10} E_j Y_j(1)\exp(-\alpha_j^2 x_f) \tag{22}$$

where $\theta_f=(T_f-T_\infty)/(T_0-T_\infty)$. For the determination of x_f, it is convenient to define a superheat ratio ϵ as

$$\epsilon = (T_0-T_f)/(T_f-T_\infty) = \theta_f^{-1} -1 \tag{23}$$

One observes that $x_f = f(\epsilon,Bi_2)$.

3.3   Analysis of Freezing Zone

3.3.1.   Flow Field Solution

The basic assumption that the axial velocity profile remains parabolic in form even in the presence of axially increasing solid layer is well discussed in [1, 7]. In present analysis, only steady state solution for $Bi_1=0$ (perfect insulation at bottom plate) is sought and no soldification occurs at the bottom plate. The velocity components satisfying the continuity equation $\partial U/\partial X'+\partial V/\partial Y=0$, $\int_0^\delta U(X',Y)dY=LU_m$ and the no-slip boundary conditions are found to be

$$U(X',Y)= \frac{6LU_m}{\delta} \left(\frac{Y}{\delta}\right)\left(1 - \frac{Y}{\delta}\right) \tag{24}$$

$$V(X',Y)= \frac{6LU_m}{\delta} \left(\frac{Y}{\delta}\right)^2\left(1 - \frac{Y}{\delta}\right)\frac{d\delta}{dX'}$$

Substitution equation (24) into energy equation, $U\partial T/\partial X'+V\partial T/\partial Y$ $= \alpha\partial^2 T/\partial Y^2$ and introducing the dimensionless variables,
$\bar{x} = X'/(3LPe)$, $\bar{y} = Y/L$, $\bar{\delta} =\delta/L$, $\phi = (T-T_f)/(T_0-T_f)$
one obtains

$$\frac{1}{\bar{\delta}} [\frac{\bar{Y}}{\bar{\delta}}(1 - \frac{\bar{Y}}{\bar{\delta}}) \frac{\partial \phi}{\partial \bar{x}} + (\frac{\bar{Y}}{\bar{\delta}})^2 (1 - \frac{\bar{Y}}{\bar{\delta}}) \frac{\partial \phi}{\partial \bar{y}}] = \frac{\partial^2 \phi}{\partial \bar{y}^2} \qquad (25)$$

with boundary conditions

$$\phi(\bar{x},\bar{\delta})=0 \text{ (interface)}, \quad \partial\phi(\bar{x},0)/\partial y=0 \text{ (insulation)} \qquad (26)$$

$$\phi(0,\bar{y})=[(1+\epsilon)/\epsilon]\theta(x_f,y)-(1/\epsilon) \text{ (initial condition)} \qquad (27)$$

Applying the variable transformation [1, 9] from $\phi(\bar{x},\bar{y})$ to $\phi(\bar{x},n)$ with $n=\bar{y}/\bar{\delta}=Y/\delta,\bar{\delta}$ can be eliminated from the boundary condition and one obtains the following system of equations which is similar in form to the classical Graetz problem.

$$\bar{\delta} \frac{\partial \phi}{\partial \bar{x}} = \frac{1}{n(1-n)} \frac{\partial^2 \phi}{\partial \bar{y}^2} \qquad (28)$$

$$\phi(\bar{x},1)=0, \quad \partial\phi(\bar{x},0)/\partial \bar{y}=0 \qquad (29)$$

$$\phi(0,n)=[(1+\epsilon)/\epsilon]\theta(x_f,y)-(1/\epsilon) \qquad (30)$$

Using the method of separation of variables by setting $\phi=H(\bar{x})N(n)$, one obtains

$$\bar{\delta} \frac{dH}{d\bar{x}} + \beta^2 H = 0, \quad H(0) = \frac{1+\epsilon}{\epsilon} \theta(x_f,y) - \frac{1}{\epsilon} \qquad (31)$$

$$\frac{d^2 N}{dn^2} + n(1-n)\beta^2 N=0, \quad dN(0)/dn=0, \quad N(1)=0 \qquad (32)$$

The solution to equation (31) is

$$H(\bar{x}) = \exp [-\beta^2 \int_0^{\bar{x}} \frac{d\bar{x}}{\bar{\delta}}]$$

Hence, the series solution for $\phi(\bar{x},n)$ is

$$\phi(\bar{x},\eta) = \sum_{j=1}^{\infty} K_j N_j(\eta) \exp[-\beta_j^2 \int_0^{\bar{x}} \frac{d\bar{x}}{\delta}] \qquad (33)$$

where β_j and N_j are the eigenvalues and eigenfunctions.

Using the transformations, $z=\beta_j(\eta-1/2)^2$ and $N_j(\eta)=w(z)\exp(-z/2)$, equation (32) is reduced to Kummer's equation and one obtains

$$N_j(\eta)=\exp[-\beta_j(\eta-1/2)^2/2]\cdot[D_j(1+\sum_{n=1}^{\infty} \frac{(1-\beta_j/4)\cdots(4n-3-\beta_j/4)}{(2n)!} \beta_j^n(\eta-1/2)^{2n})$$

$$+ \beta_j^{1/2}(\eta-1/2)(1+\sum_{n=1}^{\infty} \frac{(3-\beta_j/4)\cdots(4n-1-\beta_j/4)}{(2n+1)!} \beta_j^n(\eta-1/2)^{2n})] \qquad (34)$$

From the boundary condition $N_j(1)=0$, D_j can be found as

$$D_j = - (\beta_j^{1/2}/2)\Phi_3/\Phi_4 \qquad (35)$$

where $\Phi_3 = 1+\sum_{n=1}^{\infty} \frac{(3-\beta_j/4)\cdots(4n-1-\beta_j/4)}{(2n+1)!} (\frac{\beta_j}{4})^n$,

$$\Phi_4 = 1+\sum_{n=1}^{\infty} \frac{(1-\beta_j/4)\cdots(4n-3-\beta_j/4)}{(2n)!} (\frac{\beta_j}{4})^n$$

The other boundary condition $dN_j(0)/d\eta = 0$ yields the following equation from which the eigenvalues β_j can be evaluated.

$$\frac{dN_j(0)}{d\eta} = \exp(-\beta_j/8)\{\beta_j^{1/2} - \frac{\beta_j^{3/2}}{4}$$

$$+ D_j[\frac{\beta_j}{2} + \sum_{n=1}^{\infty} \frac{(1-\beta_j/4)\cdots(4n-3-\beta_j/4)}{(2n)!} (\frac{\beta_j}{4})^n(\frac{\beta_j}{2} - 4n)$$

$$+ \beta_j \sum_{n=1}^{\infty} \frac{(3-\beta_j/4)\cdots(4n-1-\beta_j/4)}{(2n+1)!} (\frac{\beta_j}{4})^n(- \frac{\beta_j}{4} + 2n + 1)]\} = 0$$

Thus, one has

$$F(\beta_j)=\phi_3[\frac{\beta_j}{2} + \sum_{n=1}^{\infty} \frac{(1-\beta_j/4)\cdots(4n-3-\beta_j/4)}{(2n)!} (\frac{\beta_j}{4})^n(\frac{\beta_j}{2} - 4n)]$$

$$+ 2\phi_4[\frac{\beta_j}{4} - 1 - \sum_{n=1}^{\infty} \frac{(3-\beta_j/4)\cdots(4n-1-\beta_j/4)}{(2n+1)!} (\frac{\beta_j}{4})^n$$

$$\cdot(- \frac{\beta_j}{4}+ 2n + 1)] = 0 \tag{36}$$

The roots representing the eigenvalues can be determined by using the procedure described in Section 3.2.2.

The eigenconstants K_j can be evaluated from

$$K_j = \int_0^1 n(1-n)N_j(n)\phi(0,n)dn/\int_0^1 n(1-n)N_j^2(n)\,dn \tag{37}$$

It is noted that $\phi(0,n)$ depends on the superheat ratio as well as the Biot number. The integration in equation (37) is evaluated by a Simpson's rule (IBM-SSP-DQSF) employing 200 equal step sizes. The first ten eigenvalues, constants $D_1 \sim D_{10}$ and values for $dN_1(1)/dn$ $\sim dN_{10}(1)/dn$ are given in Table 3. Table 4 lists eigenconstants for the case $Bi_1 = 0$, $Bi_2 = 1, 2, 10$ with $\epsilon = 1, 1.91, 4, 9.5$. The eigenvalues in freezing zone can be compared with those given by Schenk [15] for the case $Bi_j = 0$, $Bi_2 = \infty$ (constant wall temperature) and the agreement is found to be very good.

3.3.2 Steady-State Frozen Layer Growth

Application of the energy balance at the liquid-solid interface for steady state yields

$$k_\ell \partial T_\ell(X',\delta)/\partial Y = k_s \partial T_s(X',\delta)/\partial Y \tag{38}$$

$$\text{where } \frac{\partial T_\ell(X',\delta)}{\partial Y} = \frac{(T_0 - T_f')}{L\bar{\delta}} \frac{\partial\phi(\bar{x},1)}{\partial\eta} \qquad (39)$$

The temperature in the solid-phase layer is described by the following system of equations

$$\frac{d^2 T_s}{dY^2} = 0, \quad T_s(X',\delta) = 0, \quad K_s \frac{dT_s(X',L)}{dY} + h_2[T(X',L) - T_\infty] = 0 \qquad (40)$$

The solution is

$$T_s = T_f - \frac{Bi_s[(T_{\infty} - T_{\infty})/L]}{1 + Bi_s[1 - (\delta/L)]} (y - \delta) \qquad (41)$$

where $Bi_s = h_2 L/k_s$.

Using the above result, the steady-state thickness of frozen layer $\delta(\bar{x})$ can be found from equation (38) as

$$\delta(\bar{x}) = \frac{(1 + Bi_s)\partial\phi(\bar{x},1)/\partial\eta}{Bi_s[\partial\phi(\bar{x},1)/\partial\eta - (k_s/k_\ell \epsilon)]} \qquad (42)$$

3.4 Pressure Drop and Heat Transfer Characteristics

3.4.1 Pressure Drop

The information on pressure drop is of practical interest to prevent the channel from "freeze-shut". The pressure drop is linear in the solidification-free zone with a pressure gradient $dP/dX = (-12\mu U_m)/L^2$. Defining the dimensionless pressure difference $p = (P_0 - P)/(\rho U_m^2/2)$, one obtains

$$p = 144 \, Pr \, x, \qquad 0 \leq x \leq x_f \qquad (43)$$

In order to determine the pressure drop in the freezing zone, one integrates the axial momentum equation, $U\partial U/\partial X' + V\partial U/\partial Y = -\partial P/\partial X' + \nu(\partial^2 U/\partial X'^2 + \partial^2 U/\partial Y^2)$, from $Y = 0$ to $Y = \delta$ and obtains

$$\frac{d}{dX'}\int_0^\delta U^2 dY + \frac{\delta}{\rho}\frac{dP}{dX'} = \nu\int_0^\delta \frac{\partial^2 U}{\partial X'^2} dY + \nu[\frac{\partial U(X',\delta)}{\partial Y} - \frac{\partial U(X',0)}{\partial Y}] \tag{44}$$

It is now assumed that the axial variation of the solid layer thickness is gradual so that $d^2\delta/dX'^2$, $(d\delta/dX')^2 \ll 1$. Substituting the expression for U into equation (44), one obtains the momentum equation in dimensionless form as

$$\frac{dp}{d\bar{x}} = -\frac{12}{5}\frac{1}{\bar{\delta}^3}\frac{d\bar{\delta}}{d\bar{x}} + \frac{144\ Pr}{\bar{\delta}^3} \tag{45}$$

Integrating from $\bar{x} = 0$ to $\bar{x}$ and applying the initial condition p =144 Pr x at $\bar{x} = 0$, one obtains

$$p(\bar{x}) = \frac{6}{5}(\frac{1}{\bar{\delta}^2} - 1) + 144\ Pr\ (x_f + \int_0^{\bar{x}} \frac{d\bar{x}}{\bar{\delta}^3}) \tag{46}$$

It is noted that the first term represents the momentum effect and the second term denotes the viscous effect.

3.4.2 Bulk Temperature

The dimensionless bulk temperature in the solidification-free zone is

$$\theta_b = (T_b-T_\infty)/(T_0-T_\infty) = \int_0^1 U\theta dy/\int_0^1 U dy \tag{47}$$

where $U = 6U_m y(1-y)$. Using equations (4) and (5), one has

$$\theta_b = -6 \sum_{j=1}^{10} E_j \, dY_j(1)/dy \cdot \exp(-\alpha_j^2 x)/\alpha_j^2, \quad 0 \leq x \leq x_f \tag{48}$$

where $dY_j(1)/dy = -Bi_2 \, Y_j(1)$.

For the freezing zone, it can be shown similarly that

$$\phi_b = (T_b - T_f)/(T_0 - T_f) = -6 \sum_{j=1}^{10} K_j \, dN_j(1)/dn \cdot \exp[-\beta_j^2 \int_0^{\bar{x}} \frac{d\bar{x}}{\bar{\delta}}]/\beta_j^2 \tag{49}$$

Noting that $\phi_b = (T_b - T_f)/(T_0 - T_f) = (1+\varepsilon)\theta_b/\varepsilon - 1/\varepsilon$, the expression for bulk temperature θ_b becomes

$$\theta_b = \frac{1}{1+\varepsilon} - \frac{6\varepsilon}{1+\varepsilon} \sum_{j=1}^{10} K_j \frac{dN_j(1)}{dn} \cdot \exp[-\beta_j^2 \int_0^{\bar{x}} \frac{\bar{x}d\bar{x}}{\bar{\delta}}]/\beta_j^2, \qquad x > x_f \tag{50}$$

3.4.3 Heat Transfer

The dimensionless total rate of heat transfer from the liquid per unit depth of the channel in the solidification-free zone from X = 0 to X is

$$\bar{Q}_1 = Q/LU_m \rho c_p (T_0 - T_f), \quad 0 \leq x \leq x_f \tag{51}$$

where $Q = \int_0^X - k\partial T(X,L)/\partial Y \cdot dX$.

The value of $\bar{Q}_1$ becomes 1 when the liquid is cooled to its freezing temperature. Using equation (4), one obtains

$$\bar{Q}_1 = 6(\frac{1+\varepsilon}{\varepsilon})[\sum_{j=1}^{10} E_j \frac{dY_j(1)}{dy} (\exp(-\alpha_j^2 x) - 1)/\alpha_j^2], \quad 0 \leq x \leq x_f \tag{52}$$

Similarly, the dimensionless heat transfer rate in the freezing zone

from $\bar{x} = 0$ to $\bar{x}$ is found as

$$\bar{Q}_2 = -6\int_0^{\bar{x}} \frac{1}{\delta} \frac{\partial\phi(\bar{x},1)}{\partial\eta} d\bar{x} \tag{53}$$

Thus, $(\bar{Q}_1 + \bar{Q}_2)$ represents the total heat transfer rate between the thermal entrance (x=0) to any axial location ($\bar{x}=\bar{x}$) in the freezing zone.

3.4.4 Local Nusselt number

The local heat transfer coefficient, h, is defined by

$$q = -k\frac{\partial T(X,L)}{\partial Y} = h(T_b - T(X,L)) \qquad 0 \leq x \leq x_f \tag{54}$$

$$q = -k\frac{\partial T(X',\delta)}{\partial Y} = h(T_b - T_f), \qquad x \geq x_f \tag{55}$$

Thus, the local Nusselt number, Nu = hL/k, becomes

$$Nu = [-\partial\theta(x,1)/\partial y]/[\theta_b(x)-\theta(x,1)] \qquad 0 \leq x \leq x_f \tag{56}$$

$$Nu = [(-1/\delta)\partial\phi(\bar{x},1)/\partial\eta]/\phi_b, \qquad x > x_f \tag{57}$$

The local Nusselt number provides further insight into the heat transfer mechanism particularly in the freezing zone.

3.5 Results and Discussion

3.5.1 Temperature Distributions

The developing temperature profiles in both the solidification-free and freezing zones for $Bi_1 = 0$, $Bi_2 = 2$, $\varepsilon = 4$ are shown in Fig. 2. The difference between the temperatures at the upper and lower plates is of interest. The profile at $x_f = 0.15$ represents the entrance

temperature distribution for the freezing zone. For $x \geq 0.15$, the ice-water interface is at the equilibrium freezing temperature T_f whereas the temperature at the insulated lower plate decreases toward T_f. At $x = 0.220$, the temperature profile becomes fully developed and is relatively flat.

Numerical results for liquid-solidification-free length x_f versus superheat ratio ε are plotted in Fig. 3 for both the symmetric case ($Bi_1 = Bi_2 = Bi$) and the unsymmetric case with $Bi_1 = 0$, $Bi_2 = 1$, 2, 10. As expected, x_f decreases with the increase in Biot number, and increases with the superheat ratio. For a given Biot number, x_f for the unsymmetric case ($Bi_1 = 0$) is seen to be about 2 to 3 times longer than that of the symmetric case ($Bi_1 = Bi_2$).

The axial distributions of the dimensionless bulk temperatures θ_b for $Bi_1 = 0$ and $\varepsilon = 1,4$ with $Bi_2 = 1$, 2, 10, 100 are shown in Fig. 4. Noting that $\theta_b = \theta_f = 1/(1+\varepsilon)$ as $\bar{x} \to \infty$ in equation (50), all the curves approach the same asymptotic value depending on ε. The development length required to reach the freezing temperature $\theta_b \to \theta_f$ depends on Biot number and superheat ratio.

3.5.2 Steady-State Ice Layer Thickness

The shape of the steady-state ice layer growth along the convectively cooled upper plate is of considerable interest. The axial variation of the ice layer thickness for $Bi_1 = 0$, $Bi_2 = 1$, 2, 10 with $\varepsilon = 1$, 1.9, 9.5 and $k_\ell/k_s = 0.25$ is presented in Fig. 5. The effects of Biot number and superheat ratio on the ice layer profile can be seen clearly. The solution is terminated when $\bar{\delta}$ reaches a value of 10^{-3} and the complete "freeze shut" of the channel will not occur be-

cause of a constant mass flow rate assumption. With further reduction

of δ, the assumptions employed in the analysis may not be valid. As

can be inferred from the characteristic of flat-plate boundary-layer

heat transfer, the convective heat-transfer coefficient of the warm

water is high near the solid-phase entrance and the ice layer is seen

to have zero thickness at $x = x_f$. Further downstream, the convective

heat transfer decreases with length along the plate and thus the ice

thickness increases in the downstream direction. The ice-water inter-

face contour apparently resembles that of forced flow over a flat

plate [12, 13].

3.5.3 Pressure Drop and Heat Transfer

The pressure drop results are given in Fig. 6 for $Pr = 13.2$

(water). After the onset of ice formation, the pressure drop increases

rapidly and the deviation from the curve representing a linear pressure

drop ($p=144$ Pr x) occurs. The pressure drop is caused by the flow

acceleration due to the reduction of the flow area. It is apparent

that the channel will freeze shut if the pressure gradient is not high

enough.

The removal of the sensible heat before the bulk temperature

approaches the freezing temperature is of practical interest. The

dimensionless total heat transfer rate $\bar{Q}$ as a function of x is shown in

Fig. 7 where the effects of Biot number and superheat ratio are also

clearly seen: One notes that $\bar{Q} \to 1$ as $\theta_b \to \theta_f$ (see Fig. 4).

Further insight regarding heat transfer mechanism can be

gained by studying the local Nusselt number behavior. The effects of

Biot number and superheat ratio on local Nusselt number results are

shown in Fig. 8. As in the case of classical Graetz problem, the local Nusselt number decreases with the axial distance in the solidification-free zone. The increase of local Nusselt number in the freezing zone is related to the increased axial velocity due to the presence of the growing ice layer. Apparently, the increase in Nusselt number in the freezing zone is related to the corresponding increase in the pressure drop. For the cases, $Bi_1 = 0$, $Bi_2 = 1$, 2 and $\epsilon = 4$, the liquid-solidification free zone is long enough so that the fully developed Nusselt number is already reached before the freezing zone begins. It is noted that the local Nusselt number in the solidification-free zone is independent of superheat ratio.

The local Nusselt number can also be defined using the ambient temperature T_∞ as the reference temperature throughout the whole convection cooling section. The numberical results for Nu thus defined are plotted in Fig. 9 where the effects of Biot number and superheat ratio are seen more distinctively than those shown in Fig. 8 but the trend is generally similar. It is of interest to note that the asymptotic Nusselt number, $Nu_\infty = 1.126$, in the solidification-free zone for $Bi_1 = 0$, $Bi_2 = 2$ agrees well with the asymptotic value $Nu_\infty = 1.13$ given by Schenk [15].

3.6   Concluding Remarks

The solution of the steady-state liquid solidification problem for laminar forced flow in a parallel-plate channel with uniform external convection cooling at the upper plate and, perfect insulation at the lower plate is obtained by the classical Graetz method using the confluent hypergeometric function. The use of the

confluent-hypergeometric function is particularly effective when the boundary conditions are unsymmetric and a large number of eigenvalues is required.

The configuration and the thermal conditions considered in the present solidification analysis are encountered in various impor- tant engineering applications such as casting of metals in molds, heat exchangers using cryogenics, and freezing of ice sheets on north- ern rivers, estuaries, waterways and lakes with thermal discharge. It must be pointed out that the real physical problems mentioned above are of great complexity and the present physical model represents a somewhat idealized one. However, the analysis does provide consider- able insight into the conditions under which the northern river, for example, may freeze completely. In this connection, the pressure-drop and heat transfer results presented are useful in estimating the con- ditions for the complete blockage of the flow in channels.

The transient solidification analysis to reach the present steady-state solidification problem is not the subject of present study. However, the method described in [8] can be applied to the transient solidification analysis involving a parallel-plate channel.

The developing temperature profiles in Fig. 2 show that the flow field is potentially unstable because of top-heavy situation in the case of a horizontal channel. For laminar forced convection in horizontal parallel-plate channels, the free convection effects will appear only after the onset of a secondary flow in the form of longi- tudinal vortex rolls [22,23]. However, the free convection effects in the freezing zone are not expected to be important since the tempera- ture difference between the lower and upper plates is rather small.

The thermal instability analysis is beyond the scope of present investigation.

The experimental investigation for the present problem does not appear to have been reported in the past. Thus, the experimental investigation is apparently in order.

REFERENCES

1. Zerkle, R.D. and Sunderland, J.E., "The effect of liquid solidification in a tube upon laminar-flow heat transfer and pressure drop", J. Heat Transfer 90C, 1968, pp. 183-190.

2. DesRuisseaux, N. and Zerkle, R.D., "Freezing of hydraulic systems", Can. J. Chem. Eng. 47, 1969, pp. 233-237.

3. Özisik, M.N. and Mulligan, J.C., "Transient freezing of liquids in forced flow inside circular tubes", J. Heat Transfer 91C, 1969, pp. 385-390.

4. Bilenas, J.A. and Jiji, L.M., "Numerical solution of a nonlinear free boundary problem of axisymmetric fluid flow in tubes with surface solidification", Heat Transfer 1970, Vol. 1, Cu 2.1.

5. Bilenas, J.A. and Jiji, L.M., "Variational solution of axisymmetric fluid flow in tubes with surface solidification", J. Franklin Inst. 289, 1970, pp. 265-279.

6. Hwang, G.J. and Sheu, J.P., "Liquid solidification in combined hydrodynamic and thermal entrance region of a circular tube", Can. J. Chem. Eng. 54, 1976, pp. 66-71.

7. Zerkle, R.D., "The effect of external thermal insulation on liquid solidification in a tube", Proc. 6th Southeastern Seminar on Thermal Sciences, 1970, pp. 1-19.

8. Lock, G.S.H., Freeborn, R.D.J. and Nyren, R.H., "Analysis of ice formation in a convectively-cooled pipe", Heat Transfer 1970, Vol. 1, Cu 2.9.

9. Lee, D.G. and Zerkle, R.D., "The effect of liquid solidification in a parallel plate channel upon laminar-flow heat transfer and

pressure drop", J. Heat Transfer 91C, 1969, pp. 583-585.

10. Lapadula, C. and Mueller, W.K., "Heat conduction with solidification and a convective boundary condition at the freezing front", Int. J. Heat Mass Transfer 9, 1966, pp. 702-704.

11. Beaubouef, R.T. and Chapman,A.J., "Freezing of fluids in forced flow",Int. J. Heat Mass Transfer 10, 1967, pp. 1581-1587.

12. Miller, M.L. and Jiji, L.M., "Two-dimensional solidification of viscous flow over a semi infinite-plate constant heat removal", Appl. Sci. Res. 22, 1970, pp. 141-149.

13. Siegel, R. and Savino, J., "Experimental and analytical study of the transient solidification of a warm liquid flowing over a chilled flat plate", NASA TN D-4015, 1967, Washington (D.C.).

14. Savino, J. and Siegel, R., "Transient solidification of a flowing liquid on a cold plate including heat capacities of frozen layer and plate", NASA TN D-4353, 1968, Washington (D.C.).

15. Schenk, J., "A problem of heat transfer in laminar flow between parallel plates", Appl. Sci. Res. 5A, 1955, pp. 241-244.

16. Dennis, S.C.R. and Poots, G., "An approximate treatment of forced heat convection in laminar flow between parallel plates", Appl. Sci. Res. 5A, 1955, pp. 453-457.

17. Cess, R.D. and Shaffer, E.C., "Laminar heat transfer between parallel plates with an unsymmetrically prescribed heat flux at the walls", Appl. Sci. Res. 9A, 1959, pp. 64-70.

18. Cess, R.D. and Shaffer, E.C., "Summary of laminar heat transfer between parallel plates with unsymmetrical wall temperatures", J. Aero/Space Sciences 26, 1959, pp. 538.

19. Pirkle, J.C. and Sigillito, V.G., "A variational approach to low

Peclet number heat transfer in laminar flow", J. Comp. Phys. 9, 1972, pp. 207-221.

20. Davis, E.J., "Exact solutions for a class of heat and mass transfer problems", Can. J. Chem. Eng. 51, 1973, pp. 562-572.

21. Van Der Does De Bye, J.A.W. and Schenk, J., "Heat transfer in laminary flow between parallel plates", Appl. Sci. Res. 3A, 1953, pp. 308-316.

22. Hwang, G.J. and Cheng, K.C., "Convective instability in the thermal entrance region of a horizontal parallel-plate channel heated from below", J. Heat Transfer 95C, 1973, pp. 72-77.

23. Kamotani, Y. and Ostrach, S., "Effect of thermal instability on thermally developing laminar channel flow", J. Heat Transfer 98C, 1976, pp. 62-66.

Table 1. Comparison of Eigenvalues for Symmetric Case

$Bi_1 = Bi_2 = 20$		
	Present Study	Dennis and Poots [16]	Van Der Does De Bye and Schenk [21]
α_1	6.20725	6.224	6.208
α_2	21.59102	21.62	21.60
α_3	37.21023	36.46	37.20

$Bi_1 = Bi_2 = 2$		
	Present Study	Dennis and Poots [16]	Van Der Does De Bye and Schenk [12]
α_1	4.00000	4.016	4.000
α_2	18.62455	17.870	18.624
α_3	34.24808	32.16	34.24

Table 2. Eigenvalues, Eigenconstants and Related Constants in Solidification-Free Zone

$Bi_1 = 0$, $Bi_2 = 1$

j	α_j	Dennis and Poots [16]	E_j	C_j	$Y_j(1)$
1	2.08371	2.087	-0.266524	-3.817806	-2.693650
2	9.67057	9.839	0.165483	0.074425	0.628723
3	17.57230	16.533	0.006485	-5.699476	6.557491
4	25.52443	23.857	-0.048682	0.023727	-0.489415
5	33.49519	31.362	-0.001886	-6.266131	-8.231765
6	41.47513	38.943	0.026014	0.014845	0.424599
7	49.46036	46.561	0.000885	-6.639342	9.414833
8	57.44894	54.201	-0.017021	0.010229	-0.384612
9	65.43980	61.854	-0.000512	-6.925514	-10.359363
10	73.43228	69.517	0.012347	0.007717	0.356496

$Bi_1 = 0$, $Bi_2 = 2$

j	α_j	Dennis and Poots [16]	E_j	C_j	$Y_j(1)$
1	2.59909	2.606	-0.381679	-2.676988	-1.445367
2	10.08976	10.210	0.258106	0.123702	0.534025
3	17.90334	16.973	0.019919	-3.154053	3.276071
4	25.80165	24.200	-0.086986	0.047010	-0.448958
5	33.73615	31.634	-0.006426	-3.349224	-4.110774
6	41.68979	39.166	0.048246	0.027876	0.399227
7	49.65494	46.749	0.003143	-3.495190	4.702609
8	57.62760	54.364	-0.032126	0.019466	-0.366187
9	65.60547	61.998	-0.001860	-3.613963	-5.175385
10	73.58712	69.645	0.023546	0.054805	0.342048

$Bi_1 = 0$, $Bi_2 = 10$

j	α_j	Dennis and Poots [16]	E_j	C_j	$Y_j(1)$
1	3.45364	3.474	-0.608023	1.644730	-0.304813
2	11.21113	11.047	0.425776	0.257615	0.226343
3	19.03138	18.425	0.107894	-1.179940	0.631750
4	26.89229	25.762	-0.209015	0.132651	-0.249886
5	34.78045	33.123	-0.052630	-1.067455	-0.796217
6	42.68794	40.531	0.137480	0.389697	0.252473
7	50.60973	47.987	0.032103	-1.021619	0.915821
8	58.54248	55.485	-0.101285	0.067588	-0.250126
9	66.48386	63.017	-0.021863	-0.999274	-1.012189
10	74.43218	70.576	0.079425	0.054065	0.246122

Table 2 continued

$Bi_1 = 0$, $Bi_2 = 100$

j	α_j	Dennis and Poots [16]	E_j	C_j	$Y_j(1)$
1	3.77767	3.806	-0.700620	-1.397823	-0.030563
2	11.81415	11.479	0.474645	0.335600	0.028993
3	19.80861	19.141	0.189993	-0.279486	0.059614
4	27.79490	26.800	-0.264012	0.240920	-0.037700
5	35.79886	34.458	-0.122062	-0.606870	-0.073920
6	43.76219	42.116	0.193609	0.163351	0.043027
7	51.74554	49.773	0.092247	-0.519361	0.084397
8	59.72914	57.430	-0.156325	0.136585	-0.046948
9	67.71311	65.087	-0.074927	-0.464541	-0.092936
10	75.69749	72.742	0.132657	0.118884	0.050059

Table 3. Eigenvalues and Related Constants and Derivatives in Freezing Zone

j	B_j	D_j	$dN_j(1)/d\eta$
1	3.81867	-1.870122	3.055443
2	11.89723	0.346941	-2.985555
3	19.92414	-0.738129	-5.895183
4	27.93834	0.224488	3.964931
5	35.94732	-0.560772	7.265630
6	43.95360	0.177917	-4.604755
7	51.95828	-0.470026	-8.255711
8	59.96194	0.151776	5.102194
9	67.96488	-0.412671	9.053809
10	75.96731	0.134516	-5.517327

Table 4. Eigenconstants in Freezing Zone

$Bi_1 = 0,\ Bi_2 = 1$

j	$K_j(\varepsilon=1)$	$K_j(\varepsilon=1.91)$	$K_j(\varepsilon=4)$
1	-0.302819	0.157806	-0.075654
2	0.015254	0.007904	0.003789
3	0.002251	0.001170	0.000561
4	-0.001508	-0.000784	-0.000376
5	-0.000455	-0.000237	-0.000114
6	0.000449	0.000233	0.000112
7	0.000169	0.000088	0.000042
8	-0.000196	-0.000102	-0.000049
9	-0.000082	-0.000043	-0.000020
10	0.000104	0.000054	0.000026

$Bi_1 = 0,\ Bi_2 = 10$

j			
1	-0.712624	-0.700665	-0.631491
2	0.479844	0.407427	0.153353
3	0.204661	0.129882	0.011515
4	-0.274210	-0.113691	-0.003852
5	-0.139614	-0.033684	-0.000981
6	0.210474	0.027218	0.000911
7	0.114456	0.007704	0.000330
8	-0.184592	-0.006681	-0.000370
9	-0.107191	-0.002230	-0.000151
10	0.198241	0.002395	0.000185

Table 4 continued

$Bi_1 = 0, Bi_2 = 2$,

j	$K_j(\epsilon=4)$	$K_j(\epsilon=1.91)$	$K_j(\epsilon=4)$	$K_j(\epsilon=9.5)$
1	-0.562605	-0.322037	-0.154147	-0.064745
2	0.067028	0.012761	0.006158	0.002532
3	0.006094	0.001848	0.000945	0.000373
4	-0.003773	-0.001234	-0.000676	-0.000252
5	-0.001118	-0.000372	-0.000222	-0.000077
6	0.000095	0.000366	0.000241	0.000077
7	-0.000413	0.000138	0.000101	0.000030
8	-0.000480	-0.000159	-0.000130	-0.000035
9	-0.000203	-0.000077	-0.000061	-0.000015
10	0.000260		0.000086	0.000020
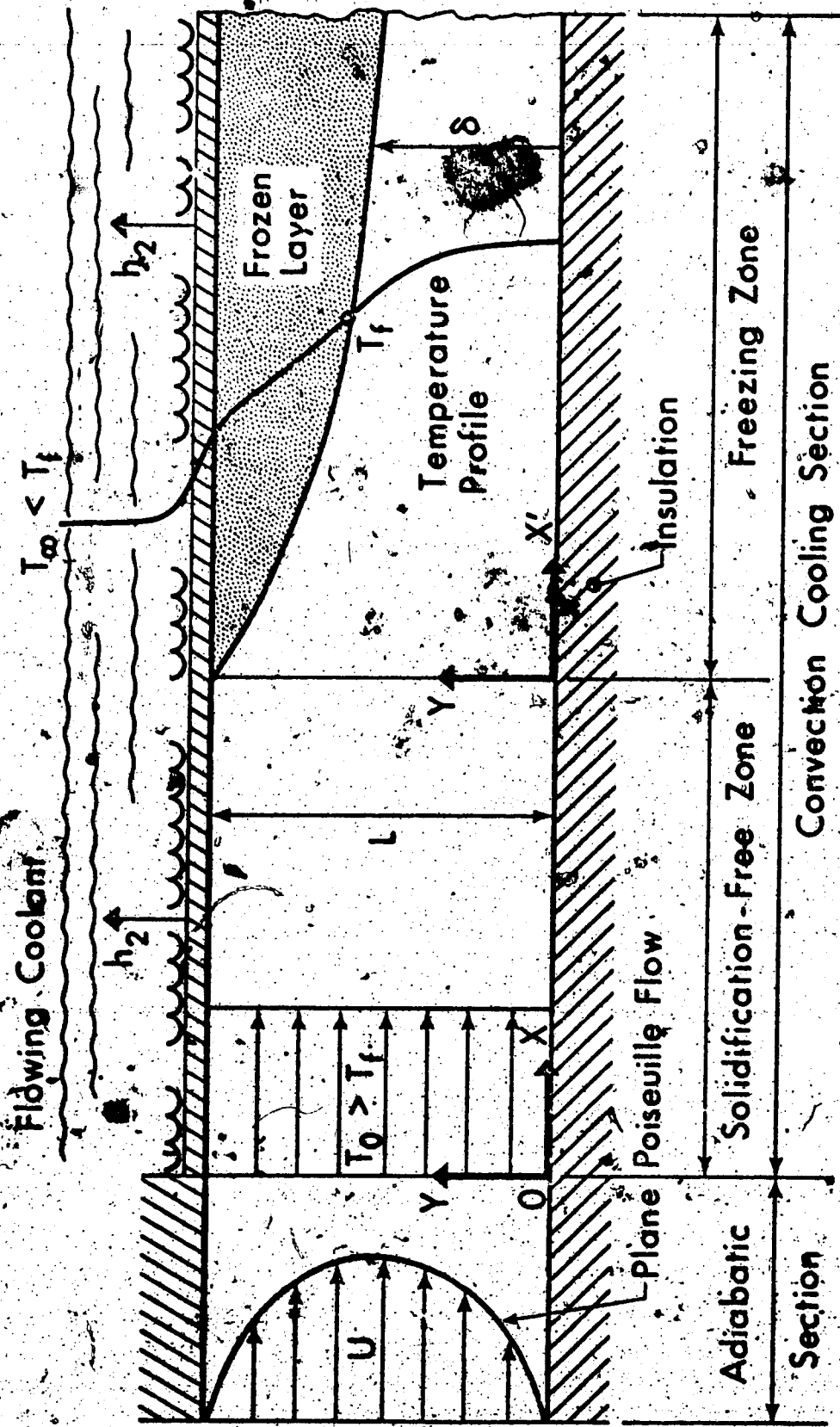
Figure 1. Physical model and coordinate system
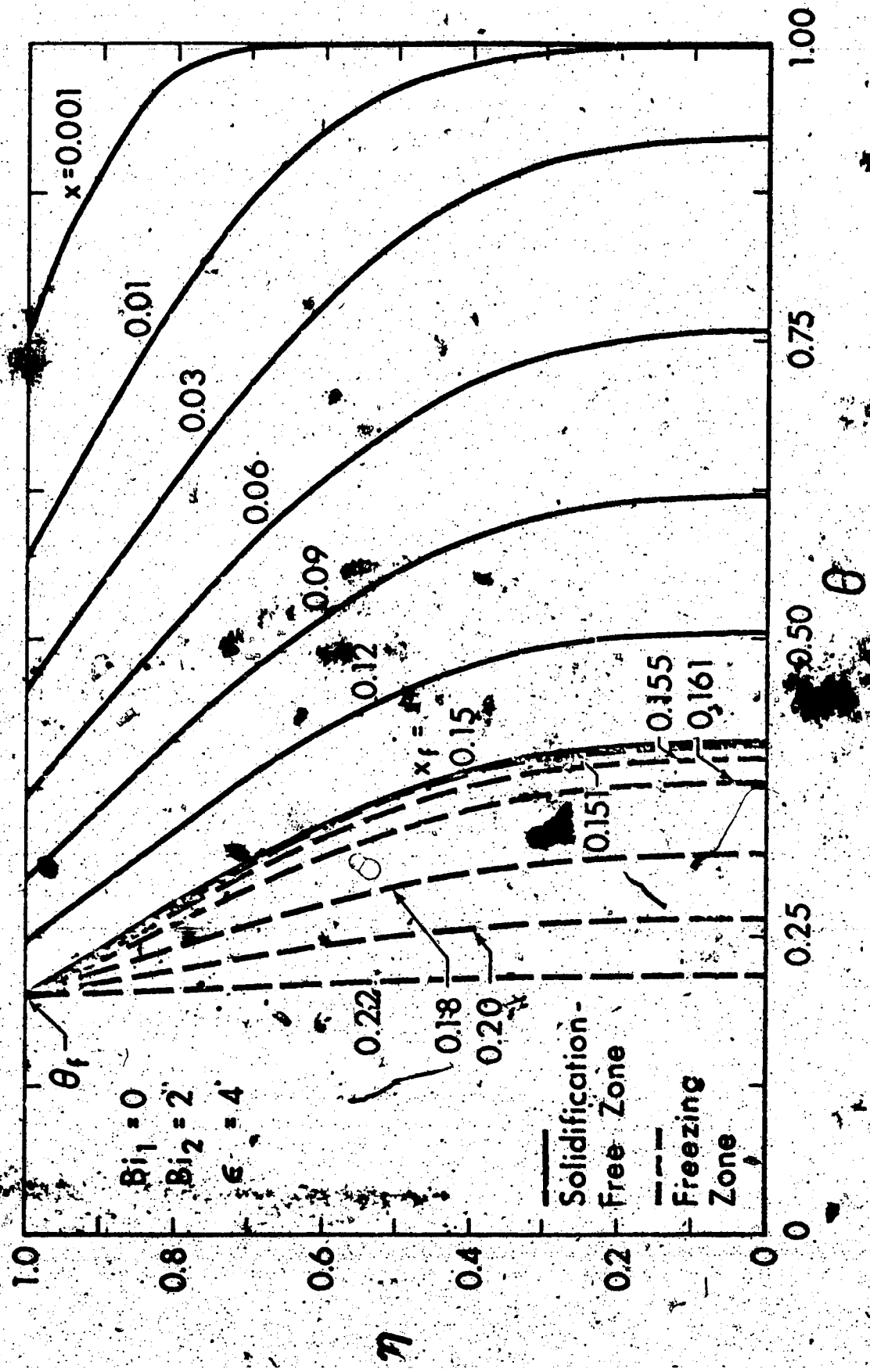
Figure 2. Developing temperature profiles for $Bi_1 = 0$, $Bi_2 = 2$ and $\epsilon = 4$
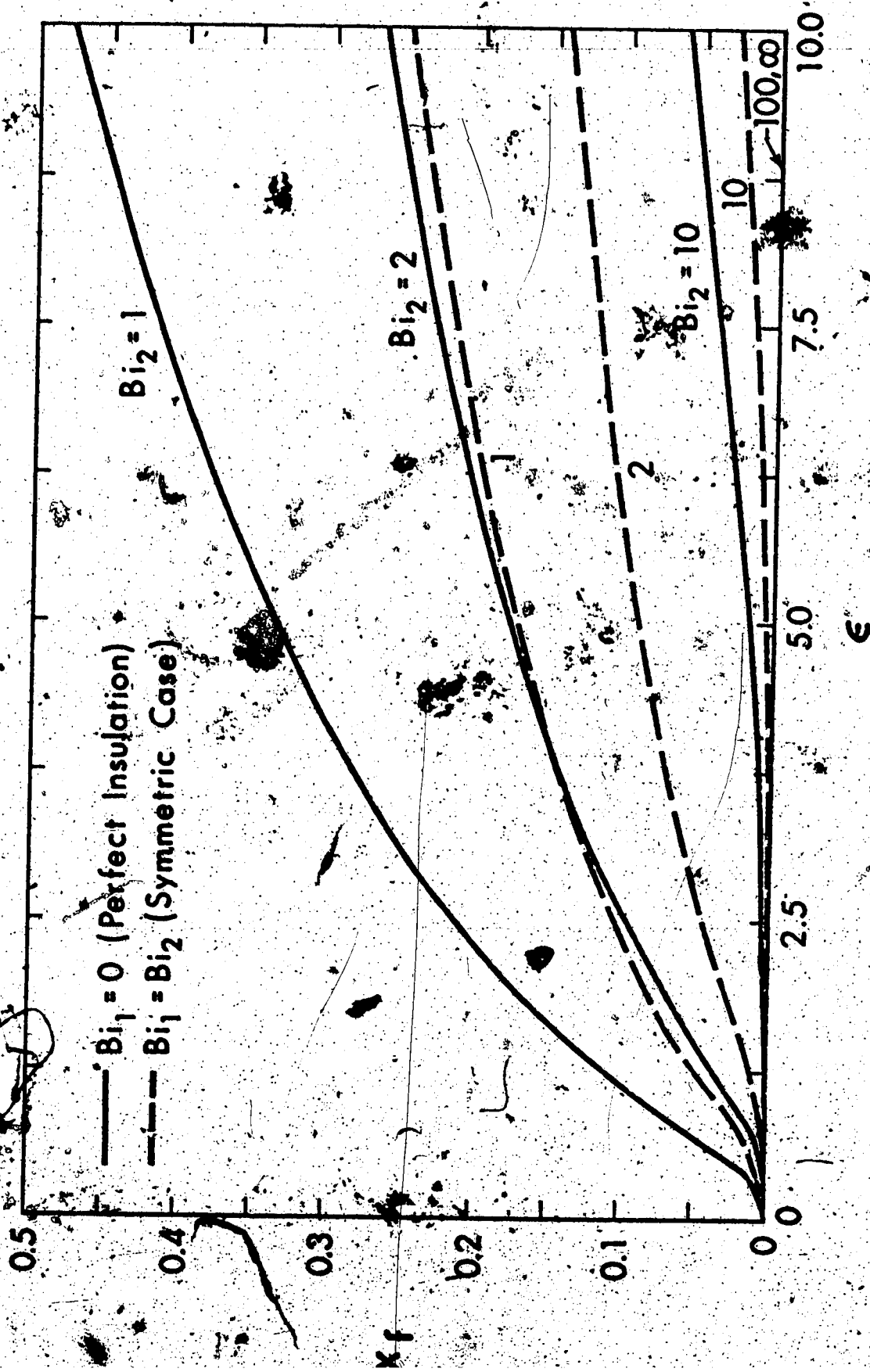
Figure 3. Liquid solidification-free length as a function of superheat ratio for $Bi_1=0$, $Bi_2=1,2,10$ and $Bi_1=Bi_2=1,2,10$
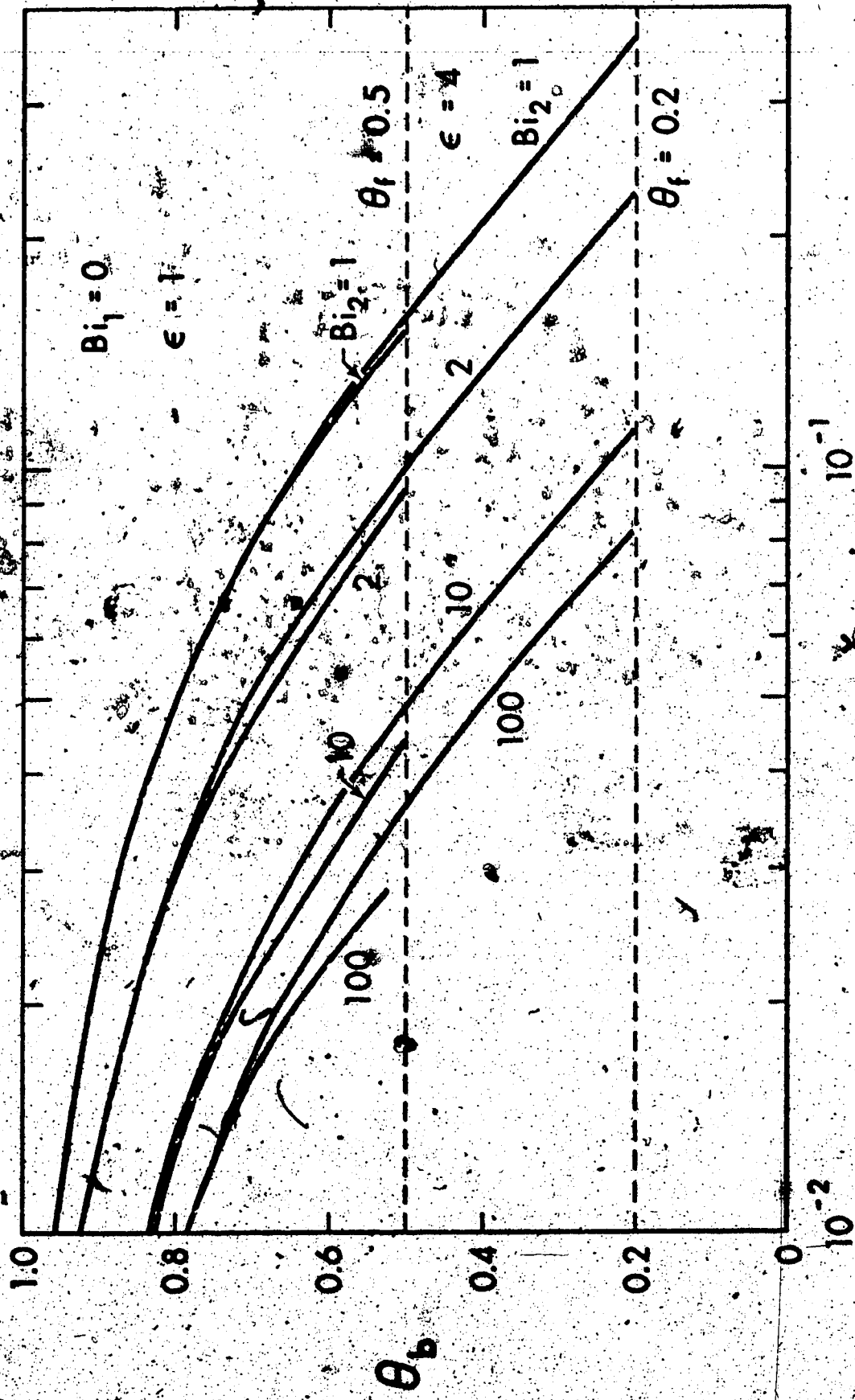
Figure 4. Axial bulk temperature distributions for $Bi_1=0$, $Bi_2=1,2,10,100$ and $\epsilon=1,4$
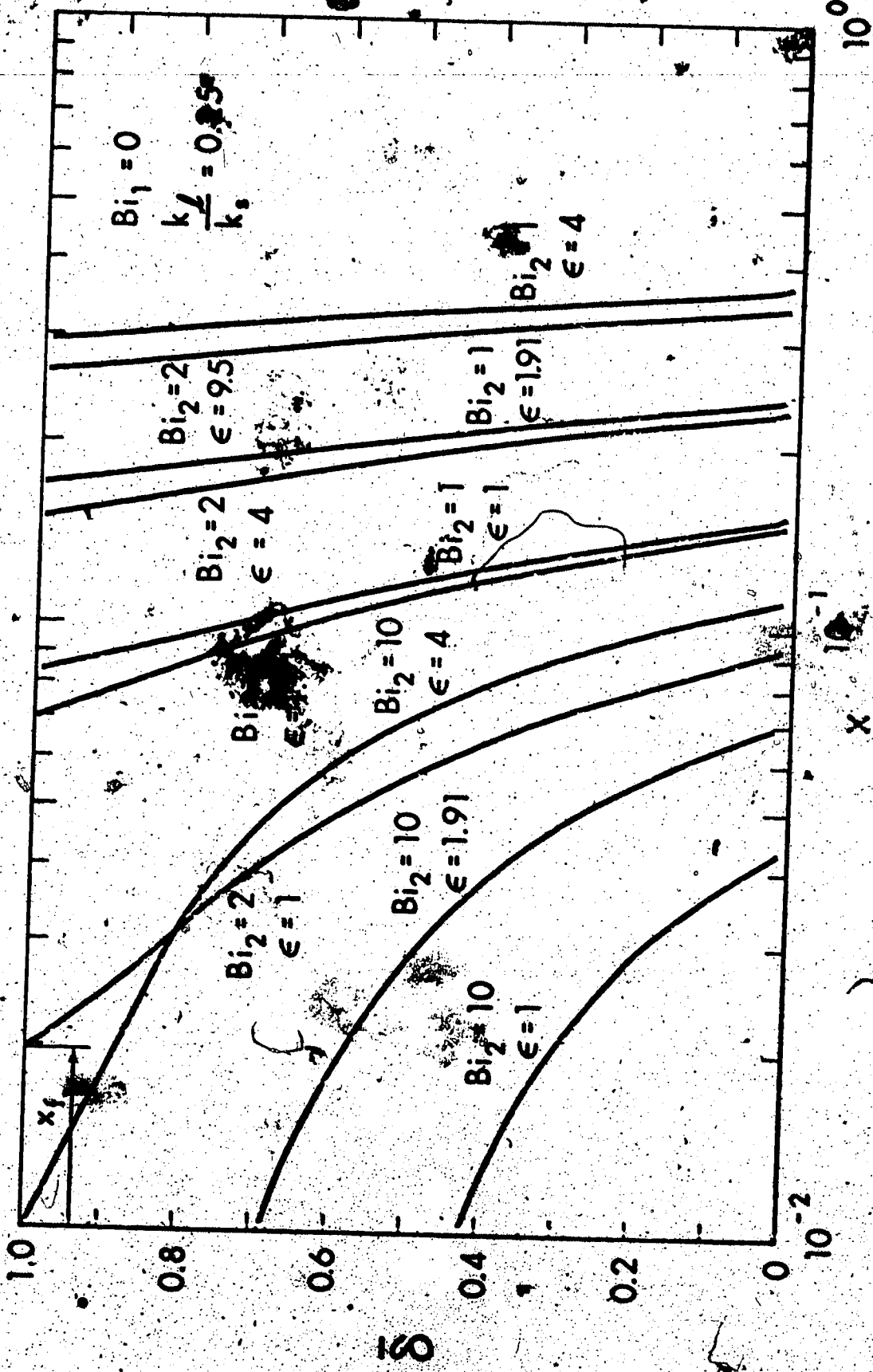
Figure 5. Axial variation of steady state ice layer thickness for $Bi_1 = 0$, $Bi_2 = 1, 2, 10$ and $\epsilon = 1, 1.91, 4, 9.5$ with $k_\ell / k_s = 0.25$
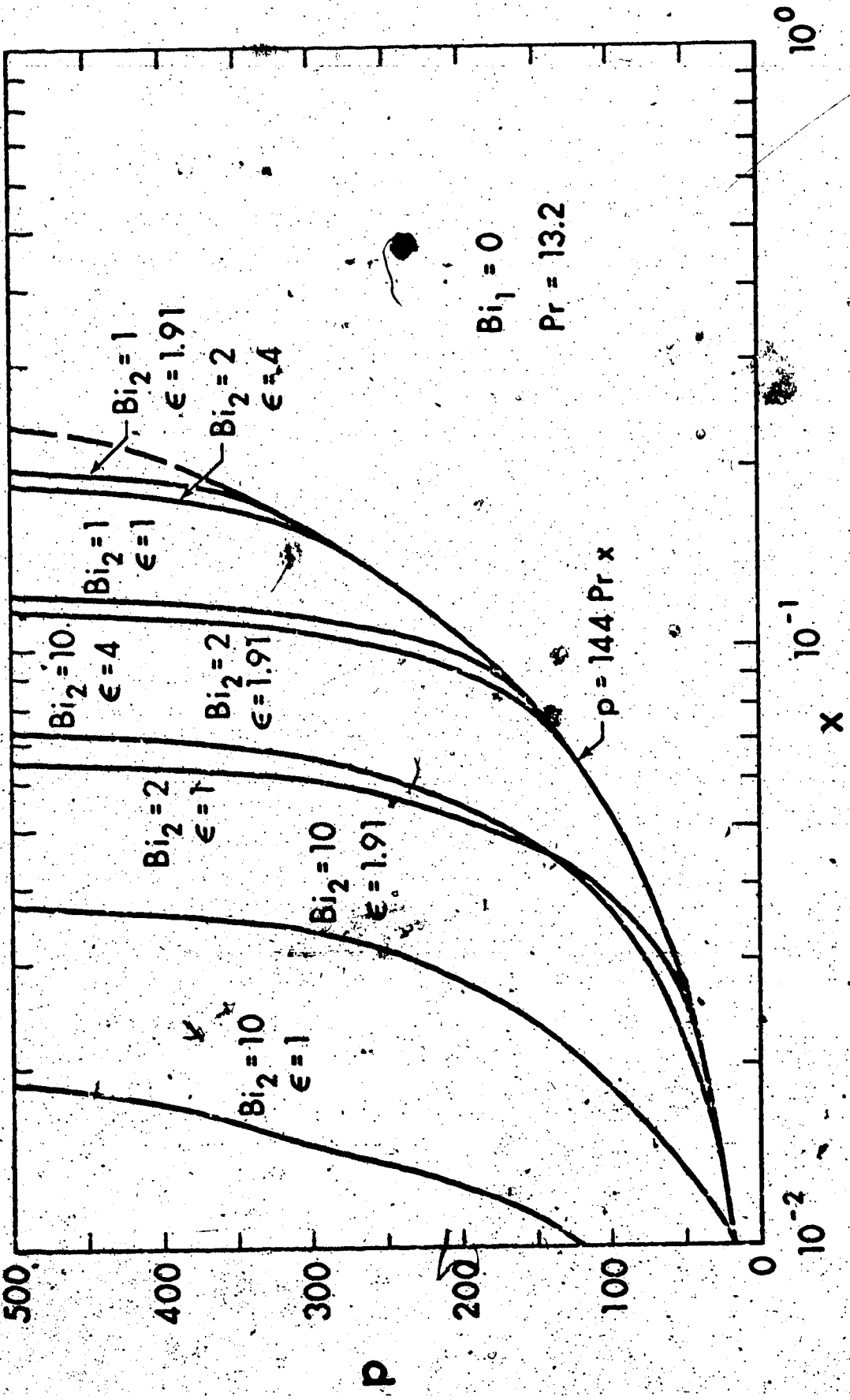
Figure 6. Steady state pressure drop versus axial distance for $Bi_1=0$, $Pr=13.2$ with Bi_2 and ϵ as parameters
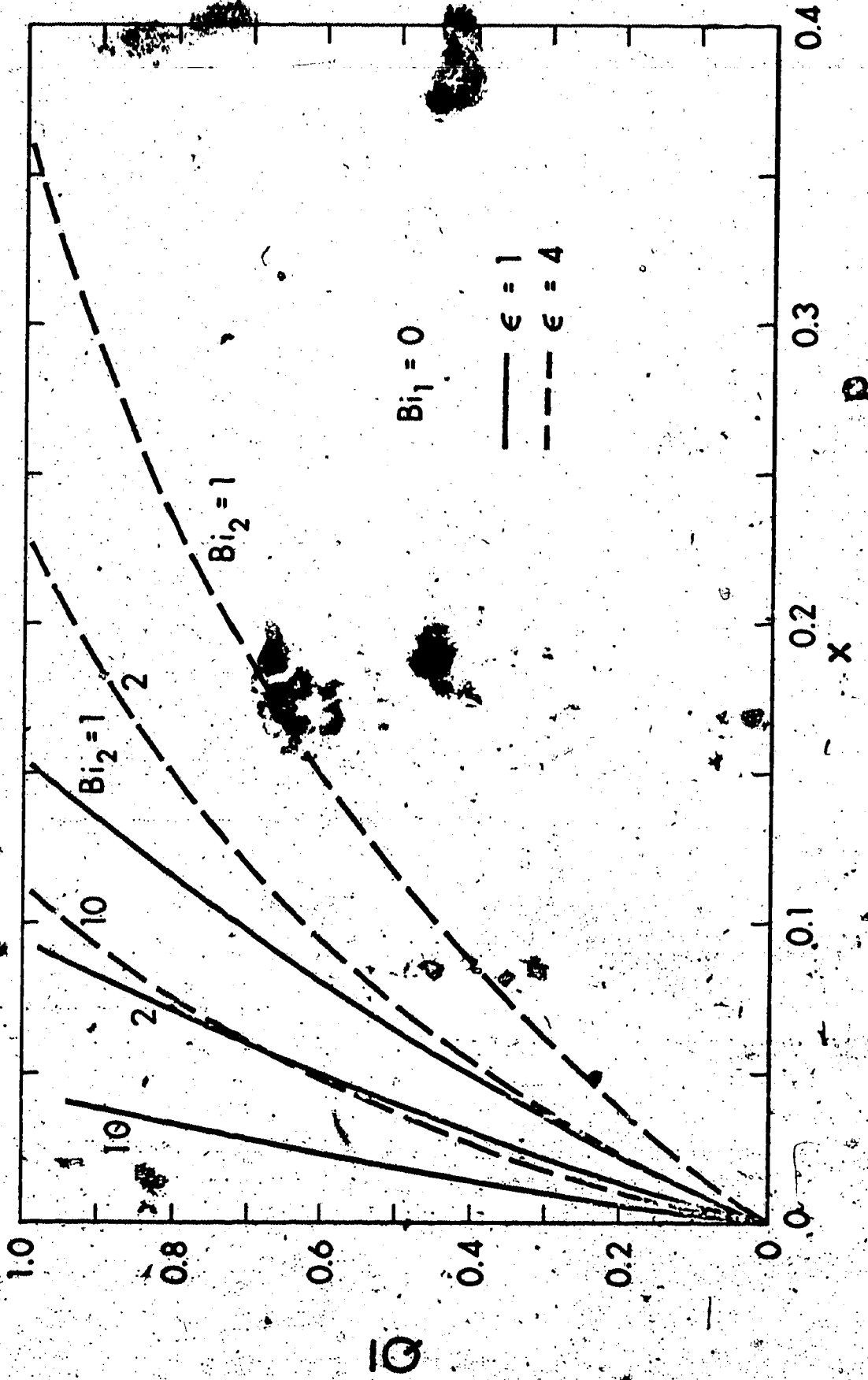
Figure 7. Total heat transfer rate $\bar{Q}$ versus axial position
for $Bi_1=0$, $Bi_2=1,2,10$ and $\epsilon=1,4$

82
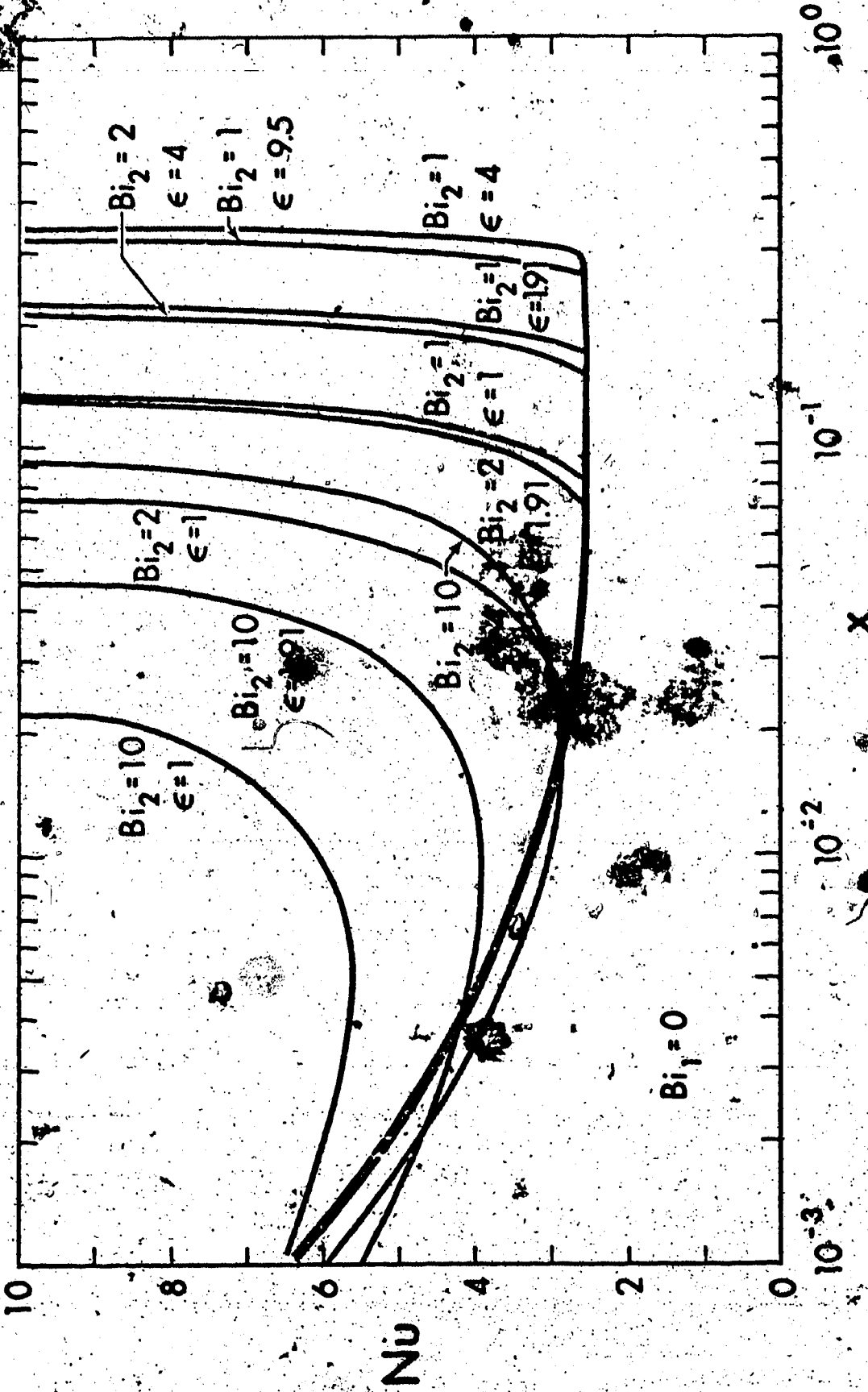
Figure 8. Local Nusselt number results for $Bi_1 = 0$, $Bi_2 = 1, 2, 10$ and $\epsilon = 1, 1.91, 4, 9.5$
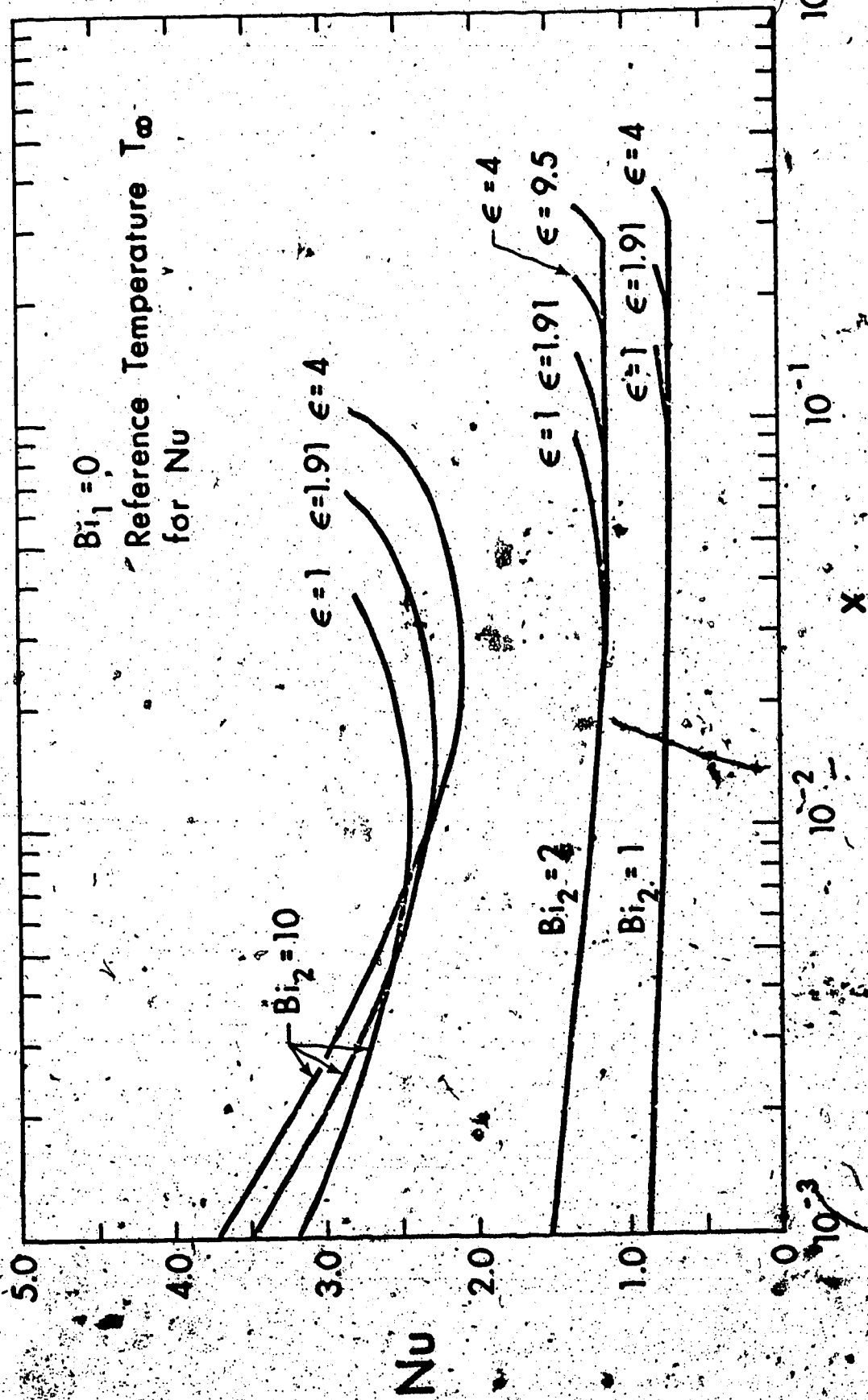
Figure 9. Local Nusselt number results with T_∞ as reference temperature for $Bi_1=0$, $Bi_2=1,2,10$ and $\epsilon=1$, 1.91, 4, 9.5

CHAPTER IV

EXTENDED GRAETZ PROBLEM AND LIQUID SOLIDIFICATION-FREE
ZONE IN CONVECTIVELY-COOLED PARALLEL-PLATE CHANNELS

The extended Graetz problem with axial heat conduction is considered for the infinite region consisting of the upstream adiabatic region ($-\infty < x \leq 0$) and the downstream convectively-cooled region ($0 < x < \infty$) in parallel-plate channels with fully developed laminar flow. The solution is obtained by the eigenfunction expansion method using the confluent hypergeometric function and the Galerkin method for eigenconstants. Heat transfer results are obtained for Peclet numbers 1, 5, 10, 50 and Biot numbers 1, 2, 10, ∞ by using the first twenty eigenvalues and the related constants. The axial heat conduction effects on the length of liquid solidification-free zone are studied and the implications on liquid solidification problem in low Peclet number flow regime are pointed out.

NOMENCLATURE

a,b   = parameters in Kummer's equation

Bi   = Biot number, $h_0 L/k$

B_n, C_n = eigenconstants, eqs. (3) and (4)

C_{1j}, C_{2j} = constants in eq. (10)

h_0 = overall heat transfer coefficient between inner wall and ambient defined by $-k(\partial T/\partial Y)_{Y=L} = h_0(T_{Y=L} - T_\infty)$

k   = thermal conductivity of fluid

L   = half-distance between parallel plates

M(a,b,z)   = confluent hypergeometric function

Nu   = Nusselt number, $h(2L)/k$

Pe   = Peclet number, $4U_m L/\alpha$

R_n, Y_n = eigenfunctions, eqs. (5) and (6)

T, T_f = fluid temperature and liquid freezing temperature

T_0, T_∞ = uniform entrance temperature and ambient temperature

U_m = average velocity

w   = solution of Kummer's equation

X, Y   = rectangular coordinates

x, y   = (X/LPe), (Y/L)

x_f = liquid solidification-free length

Greek Letters

α = thermal diffusivity

α_n, β_n = eigenvalues in eqs. (3) and (4)

ϵ = superheat ratio, $(T_0 - T_f)/(T_f - T_\infty)$

θ = dimensionless temperature difference, $(T - T_\infty)/(T_0 - T_\infty)$

θ_b = bulk temperature, eqs. (22) and (23)

$\theta_f \qquad = (T_f - T_\infty)/(T_0 - T_\infty)$

$\theta_\infty \qquad =$ asymptotic temperature solution

4.1 Introduction

Theoretical analysis on liquid solidification inside circular tubes [1-5] or parallel plates [6] with forced flow is of considerable practical interest. The prediction of solid phase formation within the tubes or channels is closely related to the well-known Graetz problem [1,6]. The analyses [1-6] are all based on the assumption that the liquid temperature is uniform at the thermal entrance $X = 0$. Recent theoretical investigations [7-12] on Graetz problem with axial heat conduction considering both the adiabatic region ($X = -\infty \sim 0$) and the thermal entrance region ($X = 0 \sim \infty$) show clearly the importance of up-stream heat penetration through $X = 0$ for low Peclet number flow regime. The analyses [7-12] reported in literature are all limited to the cases of either uniform wall temperature or uniform wall heat flux for the heated or cooled section. In many practical situations involving a cold environment, one may wish to evaluate the effects of the thermal insulation and the surrounding sink temperature. Thus, the convective boundary condition is important and was considered in [7,13,14] for thermal entrance region problem.

The purpose of this investigation is to study the axial heat conduction effects on thermal entrance region heat transfer and liquid solidification-free zone in convectively-cooled parallel-plate channels. The problem does not appear to have been studied in the past. The investigation was motivated by a desire to determine the conditions under which the assumption of uniform liquid temperature at the thermal entrance $X = 0$ is applicable for liquid solidification analysis in parallel-plate channels. This investigation will shed some light on liquid solidification in ducts or channels with forced flow for low Peclet

number flow regime where the axial heat conduction is important.

The elliptic-type energy equation is solved by the method of separation of variables and the eigenvalues and eigenfunctions are obtained by using the confluent hypergeometric function [15-18]. The eigenconstants are determined by using the Galerkin method [19].

4.2 Theoretical Analysis

4.2.1 Problem and Solution

Consider a fluid with constant physical properties flowing between parallel plates from the upstream adiabatic section to the downstream convectively-cooled section (see Fig. 1). It $\clubsuit$ assumed that the flow is a steady plane Poiseuille flow with uniform temperature T_0 at $X = -\infty$. The Poiseuille velocity is given by $U = 3U_m[1-(Y/L)^2]/2$. Neglecting viscous dissipation, the energy equation with axial heat conduction in dimensionless form can be written as

$$\frac{3}{8}(1-y^2)\frac{\partial\theta}{\partial x} = \frac{1}{Pe^2}\frac{\partial^2\theta}{\partial x^2} + \frac{\partial^2\theta}{\partial y^2}$$

(1)

with the boundary conditions

$\theta_1 = 1$ at $x = -\infty$, $\partial\theta/\partial y = 0$ at $y = 0$ and 1,

$\partial\theta_2/\partial y = 0$ at $y = 0$, $\partial\theta_2/\partial y = -Bi\theta_2$ at $y = 1$ 　　　(2)

$\theta_2 = \theta_\infty$ at $x = \infty$

$\theta_1 = \theta_2$, $\partial\theta_1/\partial x = \partial\theta_2/\partial x$ at $x = 0$

where $x = X/LPe$, $y = Y/L$, $\theta = (T - T_\infty)/(T_0 - T_\infty)$ and $Bi = h_0 L/k$

and all other symbols are defined in Nomenclature. For the present problem, it is shown in Appendix 3 that $\theta_\infty = 0$ (asymptotic solution).

The solution to the system of eqs. (1) and (2) can be obtained by the separation of variables method and the expressions for temperature fields, θ_1 and θ_2, in the upstream adiabatic and downstream entry regions, respectively, are

$$\theta_1 = 1 + \sum_{n=1}^{\infty} B_n Y_n(y)\exp(8\alpha_n^2 x/3), \quad -\infty < x \leq 0 \tag{3}$$

$$\theta_2 = \sum_{n=1}^{\infty} C_n R_n(y)\exp(-8\beta_n^2 x/3), \quad 0 \leq x < \infty \tag{4}$$

where the eigenfunctions and eigenvalues satisfy the following system of equations:

$$\frac{d^2 Y_n}{dy^2} + \alpha_n^2 [\frac{64}{9Pe^2} \alpha_n^2 - (1 - y^2)]Y_n = 0, \quad \frac{dY_n(0)}{dy} = 0, \quad \frac{dY_n(1)}{dy} = 0 \tag{5}$$

$$\frac{d^2 R_n}{dy^2} + \beta_n^2 [\frac{64}{9Pe^2} \beta_n^2 + (1 - y^2)] R_n = 0 \tag{6}$$

$$\frac{dR_n(0)}{dy} = 0, \quad \frac{dR_n(1)}{dy} = -BiR_n(1) \tag{7}$$

By introducing the transformations

$$z = \beta_n y^2 \text{ and } w(z) = \exp(z/2)R_n(y)$$

equation (6) becomes

$$z\frac{d^2 w}{dz^2} + (\frac{1}{2} - z) \frac{dw}{dz} - [\frac{1}{4} - \frac{\beta_n}{4} (1 + \frac{64}{9Pe^2} \beta_n^2)]w = 0 \tag{8}$$

which is seen to be Kummer's equation,

$$z \frac{d^2 w}{dz^2} + (b - z) \frac{dw}{dz} - aw = 0 \qquad (9)$$

where $a = (1/4) - [1 + (64\beta_m^2/9Pe^2)](\beta_n/4)$ and $b = 1/2$.

The general solution of eq. (9) can be expressed in terms of the confluent hypergeometric function $M(a,b,z)$ [17]. Thus, the eigenfunctions $R_j(y)$ are given by

$$R_j(y) = \exp(-\beta_j y^2/2)[C_{1j}M(a_j,1/2,\beta_j y^2)$$

$$+ C_{2j}\beta_j^{1/2} yM(a_j+1/2,3/2,\beta_j y^2) \qquad (10)$$

where C_{1j} and C_{2j} are the constants.

4.2.2 Eigenvalues and Eigenfunctions

The first twenty eigenvalues and eigenfunctions accurate to seven significant figures for eq. (5) with Pe = 1, 5, 10 and 50 are obtained in a recent related study [14,20] and will be utilized in this study. The first twenty eigenvalues only are listed in Table 1. Equation (5) was solved by a fourth-order Runge-Kutta method employing two hundred equal steps.

For the downstream region, the eigenvalues are found by application of eq. (7). From eq. (10), one obtains

$$dR_j(y)/dy = \exp(-\beta_j y^2/2)[-C_{1j}\beta_j yM(a_j,1/2,\beta_j y^2)$$

$$+ C_{2j}\beta_j^{1/2}(1 - \beta_j y^2)M(a_j + 1/2, 3/2, \beta_j y^2)$$

$$+ 4C_{1j}a_j\beta_j yM(a_j + 1, 3/2, \beta_j y^2)$$

$$+ (4/3)(C_{2j}\beta_j^{3/2}y^2(a_j + 1/2)M(a_j + 3/2, 5/2, \beta_j y^2)] \qquad (11)$$

From the symmetry condition $dR_j(0)/dy = 0$, one obtains $C_{2j} = 0$ (all odd terms vanish). It is interesting to note that the constants C_{2j} correspond to odd eigenfunctions in [12,20] where the upper and lower plates are at unequal but constant wall temperatures. Equations (10) and (11) now become:

$$R_j(y) = \exp(-\beta_j y^2/2)M(a_j, 1/2, \beta_j y^2) \qquad (11)$$

$$dR_j(y)/dy = \exp(-\beta_j y^2/2)[-\beta_j yM(a_j, 1/2, \beta_j y^2)$$

$$+ 4a_j\beta_j yM(a_j + 1, 3/2, \beta_j y^2)] \qquad (12)$$

where the constants C_{1j} are being absorbed in the eigenconstants C_n in eq. (4).

Substituting eqs. (11) and (12) into the convective boundary condition of eq. (7), one obtains

$$(Bi - \beta_j - 2a_j)M(a_j, 1/2, \beta_j) + 2a_j M(a_j + 1, 1/2, \beta_j) = 0 \qquad (13)$$

where the following recurrence formula is utilized.

$$z\, M(a, b+1, z) = b\, M(a, b, z) - b\, M(a-1, b, z) \qquad (14)$$

The first estimates of the roots of eq. (13) can be obtained by tabulating the value of the left-hand side of eq. (13) versus a sequence of closely spaced values of β_j. The values of β_j at which the sign of the left-hand side of eq. (13) changes give the upper and lower ends of the root and may serve as the starting points for computation. Thus, one may inspect the whole spectrum of eigenvalues before the eigenvalues are improved by using the variable secant method.

The series expansion for $M(a,b,z)$ is

$$M(a,b,z) = 1 + \frac{a}{b}z + \frac{a(a+1)}{b(b+1)}\frac{z^2}{2!} + \cdots + \frac{a(a+1)\cdots(a+n-1)}{b(b+1)\cdots(b+n-1)}\frac{z^n}{n!} + \cdots \quad (15)$$

With $b = 1/2$, $a_j = (1 - A\beta_j)/4$ and $A = 1 + (64\beta_j^2)/(9Pe^2)$, eq. (15) becomes

$$M(a_j,1/2,\beta_j) = 1 + \sum_{n=1}^{\infty} \frac{(1-A\beta_j)\cdots(4n-3-A\beta_j)}{(2n)!} \beta_j^n \quad (16)$$

The above expression is used in evaluating Kummer's function $M(a,b,z)$ for $-2 \le a_j \le 2$ where the values of a_j's are mostly negative in this study. For large a_j's and β_j's, the value of Kummer's function evaluated tends to be very large and one cannot maintain the same computational accuracy as for smaller a_j's if the series expansion formula from eq. (16) is used. For $a_j < -2$, eq. (16) is used in conjunction with the recurrence formula [16].

$$(b - a)M(a - 1, b, z) = aM(a + 1, b, z) - (2a - b + z)M(a,b,z) \quad (17)$$

The Kummer's function is thus evaluated at two smaller a_j's utilizing eq. (17).

4.2.3 Eigenconstants

The series expansion coefficients B_n, C_n are determined by applying the matching conditions at $x = 0$ given in eq. (2) as

$$\sum_{n=1}^{\infty} C_n R_n - \sum_{n=1}^{\infty} B_n Y_n = 1 \tag{18}$$

$$\sum_{n=1}^{\infty} C_n \beta_n^2 R_n + \sum_{n=1}^{\infty} B_n \alpha_n^2 Y_n = 0 \tag{19}$$

With the axial conduction term, the eigenfunctions are nonorthogonal and the eigenfunction expansion technique commonly used for the Sturm-Liouville system is not applicable. To overcome the difficulty, the Galerkin method [19] is used in this study. After multiplying eq. (18) by Y_m and eq. (19) by R_m and integrating from 0 to 1, one obtains the following system of equations by taking the first N terms of the series.

$$\sum_{n=1}^{N} C_n \int_0^1 R_n Y_m dy - \sum_{n=1}^{N} B_n \int_0^1 Y_n Y_m dy = \int_0^1 Y_m dy \tag{20}$$

$$\sum_{n=1}^{N} C_n \beta_n^2 \int_0^1 R_n R_m dy + \sum_{n=1}^{N} B_n \alpha_n^2 \int_0^1 Y_n R_m dy = 0 \tag{21}$$

where $m = 1, \ldots N$. The system of simulataneous linear equations for $N = 20$ is solved by using the Gaussian elimination method (IBM-SSP-DGELG) with a relative tolerance of 10^{-8}. The numerical integration is performed with Simpson's rule. The first twenty eigenvalues, eigenconstants $B_1 \sim B_{20}$, $C_1 \sim C_{20}$ along with $dR_1(1)/dy \sim dR_{20}(1)/dy$ for Bi = 1, 2, 10, ∞ and Pe = 1, 5, 10, 50 are listed in Table 2.

The first matching condition $\theta_1 = \theta_2$ at $x = 0$ is checked for all combinations of Peclet and Biot numbers, and it is found that

three significant figures agree except at points on the upper and lower plates where two significant figures agree. The agreement for $\partial\theta_1/\partial x = \partial\theta_2/\partial x$ at $x = 0$ is generally one order lower than that for $\theta_1 = \theta_2$. One notes that a discontinuity from zero to a finite value exists for $(\partial\theta/\partial y)_{y=1}$ at $\bar{x} = 0$ and this causes the discrepancy. For bulk temperature, four significant figures agree at $x = 0$. Thus, one may conclude that the Galerkin method is very satisfactory in determining the eigenconstants involving nonorthogonal eigenfunctions.

4.2.4 Bulk Temperature and Local Nusselt Number

The expressions for bulk temperature and local Nusselt number are

$$\theta_{1b} = \frac{3}{2}\int_0^1 (1-y^2)\theta_1 dy = 1 - \frac{3}{2}\int_0^1 (1-y^2) \sum_{n=1}^{N} B_n Y_n \exp(8\alpha_n^2 x/3)dy, \quad -\infty < x \leq 0$$

$$(22)$$

$$\theta_{2b} = \frac{3}{2}\int_0^1 (1-y^2) \sum_{n=1}^{N} C_n R_n \exp(-8\beta_n^2 x/3)dy, \quad 0 \leq x < \infty \qquad (23)$$

$$Nu = 2(-\partial\theta_2/\partial y)_{y=1}/\theta_{2b}$$

$$= [-2 \sum_{n=1}^{N} C_n dR_n(1)/dy \exp(-8\beta_n^2 x/3)]/\theta_{2b}, \quad 0 \leq x < \infty \qquad (24)$$

The integration is performed using a Simpson's rule (IBM-SSP-DQSF) using 200 equal step sizes. One notes that Nusselt number in the upstream region is zero.

4.2.5 Solidification-Free Length

The prediction of liquid solidification-free length is important when a severe cold environment is involved. The solidification starts when the wall temperature reaches the freezing temperature. Beacuse of upstream heat penetration for low Peclet number flow regime, solidification may start in the adiabatic region. Using eqs. (3) and (4), one may determine the liquid solidification-free length x_f from the following equations.

$$\theta_1(x_f,1) = \theta_f = 1 + \sum_{n=1}^{N} B_n Y_n(1)\exp(8\alpha_n^2 x_f/3), \quad -\infty < x_f \leq 0 \tag{25}$$

$$\theta_2(x_f,1) = \theta_f = \sum_{n=1}^{N} C_n R_n(1)\exp(-8\beta_n^2 x_f/3), \quad 0 \leq x_f < \infty \tag{26}$$

where $\theta_f = (T_f - T_\infty)/(T_0 - T_\infty)$ is the dimensionless freezing temperature. For the determination of x_f, it is convenient to define the superheat ratio ε as

$$\varepsilon = (T_0 - T_f)/(T_f - T_\infty) = \theta_f^{-1} - 1 \tag{27}$$

It is readily seen that $x_f = f(\varepsilon, Bi, Pe)$. In evaluating x_f for given values of Bi and Pe, the superheat ratio ε at which $x_f = 0$ is determined first. For ε less than this value, the upstream solution is used. Otherwise, the solidification occurs in the downstream region.

4.3 Results and Discussion

4.3.1 Developing Temperature Profiles

The temperature profiles at x = 0 with Biot and Peclet

numbers as parameter are shown in Figs. 2 and 3 where the extent of upstream heat penetration can be assessed from the degree of deviation from the uniform profile $\theta(0,y) = 1$. It is useful to note that $Bi = \infty$ is equivalent to a constant temperature boundary condition, and $Bi = 0$ represents perfect insulation. The effects of Biot and Peclet numbers on the wall temperature $\theta(0,1)$ are of particular interest. At $Pe = 1$, the axial heat conduction effect on entrance temperature $\theta(0,y)$ is considerable. At $Pe = 50$ and $Bi = 1$, the profile for $\theta(0,y)$ is not yet uniform.

The developing temperature profiles with $Pe = 1$, 5, 50 in both the upstream and downstream regions are shown in Figs. 4 and 5 for $Bi = 1$ and 10, respectively. At $Pe = 1$, it is seen that the uniform temperature profile representing the pure axial conduction regime is approached at the upstream location $x \approx -0.5$ but the uniform entrance temperature $\theta = 1$ is nearly approached only at $x = -20$. The extent of upstream heat penetration is considerable with $Pe = 1$. At $Pe = 50$, the uniform entrance temperature $\theta = 1$ is reached at $x = -0.1$. The developing temperature profiles shown are useful in understanding the heat transfer characteristics in the thermal entrance region.

4.3.2 Heat Transfer Characteristics

The effect of Peclet number on the axial distribution of the bulk temperature is shown in Figs. 6 and 7 for $Bi = 1$, 10 and $Bi = 2$, ∞, respectively. At $Pe = 1$, the axial heat conduction effect is quite appreciable but at $Pe = 50$ the effect is rather small. The bulk temperature curves for various Peclet numbers cross one another at some downstream location before approaching the asymptotic value $\theta_{2b} = 0$.

The asymptotic trend is reasonable since the thermal entrance length is longer for lower Peclet number. The upstream and downstream development lengths for approaching the asymptotic values $\theta_b = 1$ and 0, respectively, depend on both Biot and Peclet numbers. The downstream development length increases with the decrease of Biot number but the opposite trend is observed for the upstream development length.

The local Nusselt number results for $Bi = 1$, 2 and $Bi = 10$, ∞ are shown in Figs. 8 and 9, respectively, with Peclet number as parameter. For a given Peclet number, the Biot number effect on local Nusselt number is quite appreciable. Near the thermal entrance $x = 0$, the Nusselt number curve is nearly flat for $Pe < 50$ excluding the case of $Bi = \infty$. For the semi-infinite region analysis [14] with axial heat conduction effect, $Nu \to \infty$ as $x \to 0$ since the entrance temperature is assumed to be uniform. This model is apparently not correct when $Pe < 50$ because of "back" heat diffusion through $x = 0$. In contrast, Nu is finite at $x = 0$ for the present infinite region analysis. The limiting case of $Bi = \infty$ (constant wall temperature) is similar to low Peclet number mass transfer in laminar flow through circular tubes considered in [21].

The asymptotic Nusselt numbers based on the agreement of four figures for Nu at the consecutive axial locations are listed in Table 3. On this basis, the asymptotic value is already approached at $x \approx 5$ for $Pe = 1$ and $x \approx 0.2$ for $Pe = 50$. The asymptotic value $Nu_\infty = 3.773$ for $Bi = \infty$, $Pe = 50$ from this study agrees well with $Nu_\infty = 3.77$ for $Bi = \infty$, $Pe = \infty$ (no axial conduction) given in [13].

TABLE 3. Asymptotic Nusselt Numbers

Bi	Pe = 1	5	10	50
1	1.385	1.350	1.339	1.334
2	2.097	2.026	2.000	1.986
10	3.434	3.305	3.250	3.213
∞	4.003	3.874	3.815	3.773

4.3.3 Liquid Soldification-Free Length

The computed results for the solidification-free length x_f as a function of the superheat ratio ε are shown in Fig. 10 for Bi = 1, 2, 10 with Peclet number as parameter. At Pe = 1, Bi = 10, for example, the solidification occurs entirely in the upstream adiabatic region for the range of superheat ratios $\varepsilon = 0 \sim 10$ under consideration. On the other hand, with Pe = 50, Bi = 1, the solidification occurs mostly in the downstream region. With Pe ≥ 10, Bi = 10, one obtains $x_f = 0$. Fig. 9 provides some insight into the liquid solidification inside the tubes or channels with forced laminar flow in the low Peclet number flow regime.

4.4   Concluding Remarks

Use of the confluent hypergeometric function for the solution of the characteristic eq. (6) involving the infinite region proves to be very efficient computationally and requires considerably less computing time than the Runge-Kutta procedure used in [10, 12].

The Galerkin method of obtaining the series expansion coefficients involving the nonorthagonal eigenfunctions is direct, simple

and more efficient as compared with the rather tedious Gram-Schmidt orthonormalization procedure used in [10, 12].

Present numerical results show that when the axial heat conduction is included in the energy equation for the extended Graetz problem, the assumption of a uniform entrance fluid temperature at $x = 0$ is incompatible with the physical situation and a uniform temperature must be prescribed at $x = -\infty$.

The present analysis does not consider the region $x > x_f$ where the prediction of the solid-phase profile is of primary interest [1-6]. However, the present investigation does provide some insight into the scope of the problem to be expected when solving liquid solidification problem with axial heat conduction in a convectively-cooled pipe or channel by a numerical method. The heat transfer results presented are useful in assessing both the Peclet and Biot numbers effects. A discussion on the analysis in the freezing zone $(x > x_f)$ is given in Appendix 4 for future reference.

The Biot number in this analysis corresponds to the wall Nusselt number defined in [13] and the ambient side Nusselt number used in [7]. The problem of laminar flow mass transfer in a flat channel with permeable walls [18] is analogous to the present heat transfer problem with a convective boundary condition. Thus, the wall Sherwood number is analogous to the Biot number. The theoretical technique used in this analysis can also be applied to problems of heat and mass transfer in a circular pipe. The relevant equations for the case of circular pipe are given in Appendix 5.

REFERENCES

1. Zerkle, R.D. and Sunderland, J.E., "The effect of liquid solidi-
    fication in a tube upon laminar-flow heat transfer and pressure
    drop", J. Heat Transfer 90C, 1968, pp. 183-190.

2. DesRuisseaux, N. and Zerkle, R.D., "Freezing of hydraulic systems",
    Can. J. Chem. Eng. 47, 1969, pp. 233-237.

3. Zerkle, R.D., "The effect of external thermal insulation on liquid
    solidification in a tube", Proc. 6th Southeastern Seminar on Ther-
    mal Sciences, 1970, pp. 1-19.

4. Lock, G.S.H., Freeborn, R.D.J. and Nyren, R.H., "Analysis of ice
    formation in a convectively-cooled pipe", Heat Transfer 1970, Vol.
    1, Elsevier, Amsterdam, Cu 2.9.

5. Hwang, G.J. and Sheu, J.P., "Liquid solidification in combined
    hydrodynamic and thermal entrance region of a circular tube",
    Can. J. Chem. Eng. 54, 1976, pp. 66-71.

6. Lee, D.G. and Zerkle R.D., "The effect of liquid solidification
    in a parallel plate channel upon laminar-flow heat transfer and
    pressure drop", J. Heat Transfer 91C, 1969, pp. 583-585.

7. Schneider, P.J., "Effect of axial fluid conduction on heat trans-
    fer in the entrance regions of parallel plates and tubes", Trans.
    Am. Soc. Mech. Engrs. 79, 1957, pp. 765-773.

8. Agrawal, H.C., "Heat transfer in laminar flow between parallel
    plates of small Peclet numbers", Appl. Sc. Res. A9, 1960, pp. 177-
    189.

9. Hennecke, D.K., "Heat transfer by Hagen-Poiseuille flow in the
    thermal development region with axial conduction", Wärme -

Stoffübertragung, Vol. 1, 1968, pp. 177-184.

10. Hsu, C.J., "An exact analysis of low Peclet number thermal entry region heat transfer in transversely non-uniform velocity fields", AIChE Journal, Vol. 7, 1971, pp 732-740.

11. Deavours, C.A., "An exact solution for the temperature distribution in parallel plate Poiseuille flow", J. Heat Transfer 96C, 1974, pp. 489-495.

12. Wu, R.S., Cheng, K.C. and Ou, J.W., "Low Peclet number heat transfer in the thermal entrance region of parallel-plate channels with unequal wall temperatures", Can. J. Chem. Eng. 54, 1976.

13. Van Der Does De Bye, J.A.W. and Schenk, J., " Heat transfer in laminary flow between parallel plates", Appl. Sci. Res. 3A, 1952, pp. 308-316.

14. Hsu, C.J., "Exact solution to entry-region laminar heat transfer with axial conduction and the boundary condition of the third kind", Chem. Eng. Sci. 23, 1968, pp. 457-468.

15. Lauwerier, H.A., "The use of confluent hypergeometric function in mathematical physics and the solution of an eigenvalue problem", Appl. Sci. Res. 2A, 1950, pp. 184-204.

16. Pirkle, J.C. and Sigillito, V.G., "A variational approach to low Peclet number heat transfer in laminar flow", J. Comp. Phys. 9, 1972, pp. 207-221.

17. Davis, E.J., "Exact solutions for a class of heat and mass transfer problems", Can. J. Chem. Eng. 51, 1973, pp. 562-572.

18. Walker, G. and Davies, T., "Mass transfer in laminar flow between parallel permeable plates", AIChE Journal 20, 1974, pp. 881-889.

19. Kantorovich, L.V. and Krylov, V.I., "Approximate Methods of Higher

Analysis", Interscience Publishers, 1958, pp. 54-56.

20. Wu, R.S., Ph. D. Thesis, 1976, Dept. Mechanical Engineering, University of Alberta, Edmonton, Alberta, Canada.

21. Tan, C.W. and Hsu, C.J., "Low Peclet number mass transfer in laminar flow through circular tubes", Int. J. Heat Mass Transfer 15, 1972, pp. 2187-2201.

Table 1.　Eigenvalues for Adiabatic Region

n	Pe = 1	5	10	50
1	0.3060400E+00	0.1508323E+01	0.2891829E+01	0.1051927E+02
2	0.1105802E+01	0.2678328E+01	0.4236301E+01	0.1584147E+02
3	0.1550091E+01	0.3606607E+01	0.5365803E+01	0.1786702E+02
4	0.1892395E+01	0.4345400E+01	0.6355316E+01	0.1885437E+02
5	0.2181588E+01	0.4976393E+01	0.7216786E+01	0.1982894E+02
6	0.2436687E+01	0.5536188E+01	0.7988097E+01	0.2104313E+02
7	0.2667499E+01	0.6044506E+01	0.8692240E+01	0.2227199E+02
8	0.2879869E+01	0.6513350E+01	0.9344008E+01	0.2347410E+02
9	0.3077619E+01	0.6950688E+01	0.9953504E+01	0.2463882E+02
10	0.3263408E+01	0.7362123E+01	0.1052797E+02	0.2576402E+02
11	0.3439175E+01	0.7751771E+01	0.1107281E+02	0.2685069E+02
12	0.3606386E+01	0.8122765E+01	0.1159217E+02	0.2790096E+02
13	0.3766180E+01	0.8477549E+01	0.1208929E+02	0.2891733E+02
14	0.3919465E+01	0.8818078E+01	0.1256682E+02	0.2990226E+02
15	0.4066977E+01	0.9145943E+01	0.1302690E+02	0.3085812E+02
16	0.4209322E+01	0.9462460E+01	0.1347129E+02	0.3178705E+02
17	0.4347009E+01	0.9768730E+01	0.1390152E+02	0.3269101E+02
18	0.4480467E+01	0.1006569E+02	0.1431884E+02	0.3357178E+02
19	0.4610063E+01	0.1035414E+02	0.1472435E+02	0.3443091E+02
20	0.4736114E+01	0.1063477E+02	0.1511900E+02	0.3526995E+02

Table 2. Eigenvalues and Related Constants for
Bi = 1, 2, 10, ∞ with Pe = 1, 5, 10, 50

Bi=1, Pe=1

n	β_n	$dR_n(1)/dy$	B_n	C_n
1	0.5244216E+00	-0.6392275E+00	-0.7524885E+00	0.2776517E+00
2	0.1115477E+01	0.9785680E+00	0.1554215E-01	-0.2201501E-01
3	0.1539333E+01	-0.1001277E+01	-0.4429145E-02	0.6091974E-02
4	0.1878266E+01	0.1003929E+01	0.2078580E-02	-0.2693922E-02
5	0.2167001E+01	-0.1004108E+01	-0.1204935E-02	0.1496491E-02
6	0.2422377E+01	0.1003840E+01	0.7861793E-03	-0.9471816E-03
7	0.2653666E+01	-0.1003504E+01	-0.5533766E-03	0.6518684E-03
8	0.2866555E+01	0.1003189E+01	0.4106531E-03	-0.4754652E-03
9	0.3064810E+01	-0.1002911E+01	-0.3168507E-03	0.3618938E-03
10	0.3251072E+01	0.1002670E+01	0.2519028E-03	-0.2845650E-03
11	0.3427275E+01	-0.1002463E+01	-0.2050752E-03	0.2295801E-03
12	0.3594886E+01	0.1002283E+01	0.1701994E-03	-0.1891075E-03
13	0.3755047E+01	-0.1002126E+01	-0.1435267E-03	0.1584657E-03
14	0.3908670E+01	0.1001988E+01	0.1226706E-03	-0.1347182E-03
15	0.4056492E+01	-0.1001867E+01	-0.1060545E-03	0.1159498E-03
16	0.4199125E+01	0.1001760E+01	0.9260096E-04	-0.1008691E-03
17	0.4337077E+01	-0.1001663E+01	-0.8155575E-04	0.8858623E-04
18	0.4470782E+01	0.1001577E+01	0.7237496E-04	-0.7848445E-04
19	0.4600608E+01	-0.1001498E+01	-0.6466155E-04	0.7019801E-04
20	0.4726874E+01	0.1001429E+01	0.5812442E-04	-0.6457625E-04

Bi=1, Pe=5

n	β_n	$dR_n(1)/dy$	B_n	C_n
1	0.8787878E+00	-0.6165786E+00	-0.2641423E+00	0.8170123E+00
2	0.2345772E+01	0.1030799E+01	0.4000128E-01	-0.6231960E-01
3	0.3318760E+01	-0.1050364E+01	-0.1208564E-01	0.1799514E-01
4	0.4094426E+01	0.1041576E+01	0.5759726E-02	-0.7948064E-02
5	0.4752435E+01	-0.1032621E+01	-0.3366117E-02	0.4394690E-02
6	0.5332484E+01	0.1027023E+01	0.2207274E-02	-0.2770800E-02
7	0.5856544E+01	-0.1022990E+01	-0.1558902E-02	0.1901311E-02
8	0.6338035E+01	0.1019977E+01	0.1159645E-02	-0.1383683E-02
9	0.6785803E+01	-0.1017650E+01	-0.8963862E-03	0.1051333E-02
10	0.7206022E+01	0.1015802E+01	0.7136556E-03	-0.8255451E-03
11	0.7603197E+01	-0.1014300E+01	-0.5816457E-03	0.6652909E-03
12	0.7980731E+01	0.1013058E+01	0.4831712E-03	-0.5475161E-03
13	0.8341266E+01	-0.1012013E+01	-0.4077574E-03	0.4584705E-03
14	0.8686903E+01	0.1011121E+01	0.3487222E-03	-0.3895494E-03
15	0.9019343E+01	-0.1010353E+01	-0.3016407E-03	0.3351532E-03
16	0.9339990E+01	0.1009683E+01	0.2634872E-03	-0.2915259E-03
17	0.9650011E+01	-0.1009095E+01	-0.2321386E-03	0.2561068E-03
18	0.9950397E+01	0.1008574E+01	0.2060779E-03	-0.2272137E-03
19	0.1024199E+02	-0.1008107E+01	-0.1842780E-03	0.2040766E-03
20	0.1052553E+02	0.1007694E+01	0.1665507E-03	-0.2047998E-03

Table 2 continued

B1=1, Pe=10

n	β_n	$dR_n(1)/dy$	B_n	C_n
1	0.9588549E+00	-0.6100638E+00	-0.9679815E-01	0.9886881E+00
2	0.3084710E+01	0.1060758E+01	0.3317524E-01	-0.7676043E-01
3	0.4491519E+01	-0.1103029E+01	0.7904728E-02	0.2558956E-01
4	0.5612634E+01	0.1084070E+01	-0.1057131E-01	-0.9523924E-02
5	0.6561905E+01	-0.1067366E+01	-0.3867406E-02	0.5450691E-02
6	0.7396513E+01	0.1055551E+01	0.2575463E-02	-0.3474181E-02
7	0.8148843E+01	-0.1047080E+01	-0.1832555E-02	0.2382968E-02
8	0.8839795E+01	0.1040785E+01	0.1370105E-02	-0.1729613E-02
9	0.9479480E+01	-0.1035946E+01	-0.1063004E-02	0.1310616E-02
10	0.1008003E+02	0.1032120E+01	0.8487263E-03	-0.1026718E-02
11	0.1064710E+02	-0.1029022E+01	-0.6933500E-03	0.8257740E-03
12	0.1113568E+02	0.1026465E+01	0.5769831E-03	-0.6784669E-03
13	0.1169965E+02	-0.1024320E+01	-0.4876694E-03	0.5673445E-03
14	0.1219210E+02	0.1022496E+01	0.4176003E-03	-0.4815139E-03
15	0.1266550E+02	-0.1020923E+01	-0.3616202E-03	0.4139075E-03
16	0.1312191E+02	0.1019557E+01	0.3161995E-03	-0.3598028E-03
17	0.1356302E+02	-0.1018356E+01	-0.2788834E-03	0.3160028E-03
18	0.1399027E+02	0.1017295E+01	0.2480179E-03	-0.2804661E-03
19	0.1440488E+02	-0.1016349E+01	-0.2229359E-03	0.2502431E-03
20	0.1480793E+02	0.1015501E+01	0.2052633E-03	-0.2805005E-03

Bi=1, Pe=50

n	β_n	$dR_n(1)/dy$	B_n	C_n
1	0.9981068E+00	-0.6066959E+00	-0.2965549E-03	0.1083281E+01
2	0.4429122E+01	0.1053174E+01	0.2492789E-03	-0.1080273E+00
3	0.7486342E+01	-0.1244283E+01	-0.1258323E-02	0.3520996E-01
4	0.1006235E+02	0.1303495E+01	0.2620914E-02	-0.1633908E-01
5	0.1230085E+02	-0.1291197E+01	-0.2698127E-02	0.8954873E-02
6	0.1429260E+02	0.1258689E+01	0.1988914E-02	-0.5475571E-02
7	0.1609381E+02	-0.1226433E+01	-0.1519342E-02	0.3633079E-02
8	0.1774397E+02	0.1199161E+01	0.1196967E-02	-0.2564836E-02
9	0.1927201E+02	-0.1176913E+01	-0.9661946E-03	0.1898833E-02
10	0.2069950E+02	0.1158778E+01	0.7958934E-03	-0.1458775E-02
11	0.2204275E+02	-0.1143846E+01	-0.6671596E-03	0.1154124E-02
12	0.2331433E+02	0.1131398E+01	0.5680932E-03	-0.9350813E-03
13	0.2452409E+02	-0.1120882E+01	-0.4911451E-03	0.7726224E-03
14	0.2567992E+02	0.1111901E+01	0.4317840E-03	-0.6489935E-03
15	0.2678820E+02	-0.1104158E+01	-0.3880232E-03	0.5527517E-03
16	0.2785417E+02	0.1097470E+01	0.3605911E-03	-0.4778923E-03
17	0.2888222E+02	-0.1091278E+01	-0.3532824E-03	0.4062569E-03
18	0.2987599E+02	0.1084962E+01	0.3711478E-03	-0.4159654E-03
19	0.3083863E+02	0.1079902E+01	-0.4086764E-03	0.1671461E-03
20	0.3177291E+02	0.1079176E+01	0.4096598E-03	-0.5221364E-03

Table 2 continued

Bi=2, Pe=1

n	β_n	$dR_n(1)/dy$	B_n	C_n
1	0.5942047E+00	-0.9265640E+00	-0.8018682E+00	0.2355142E+00
2	0.1151607E+01	0.1774416E+01	0.1983371E-01	-0.2778959E-01
3	0.1556622E+01	-0.1935231E+01	-0.5883518E-02	0.8781252E-02
4	0.1888351E+01	0.1975359E+01	0.2814536E-02	-0.4013791E-02
5	0.2173713E+01	-0.1989438E+01	-0.1650659E-02	0.2249949E-02
6	0.2427232E+01	0.1995531E+01	0.1085592E-02	-0.1427062E-02
7	0.2657380E+01	-0.1998531E+01	-0.7685927E-03	0.9819252E-03
8	0.2869512E+01	0.2000134E+01	0.5729242E-03	-0.7154890E-03
9	0.3067235E+01	-0.2001036E+01	-0.4436366E-03	0.5439171E-03
10	0.3253106E+01	0.2001557E+01	0.3537323E-03	-0.4271694E-03
11	0.3429013E+01	-0.2001861E+01	-0.2886791E-03	0.3442395E-03
12	0.3596393E+01	0.2002033E+01	0.2400837E-03	-0.2832704E-03
13	0.3756371E+01	-0.2002124E+01	-0.2028226E-03	0.2371704E-03
14	0.3909844E+01	0.2002165E+01	0.1736226E-03	-0.2014918E-03
15	0.4057543E+01	-0.2002172E+01	-0.1503141E-03	0.1733353E-03
16	0.4200072E+01	0.2002158E+01	0.1314107E-03	-0.1507495E-03
17	0.4337938E+01	-0.2002130E+01	-0.1158693E-03	0.1323928E-03
18	0.4471567E+01	0.2002095E+01	0.1029376E-03	-0.1173432E-03
19	0.4601329E+01	-0.2002053E+01	-0.9207030E-04	0.1050736E-03
20	0.4727539E+01	0.2002008E+01	0.8291077E-04	-0.9696313E-04

Bi=2, Pe=5

n	β_n	$dR_n(1)/dy$	B_n	C_n
1	0.1035311E+01	-0.8844404E+00	-0.3430053E+00	0.7664347E+00
2	0.2429733E+01	0.1824403E+01	0.5661982E-01	-0.8461467E-01
3	0.3360409E+01	-0.2013896E+01	-0.1767858E-01	0.2799449E-01
4	0.4118470E+01	0.2041562E+01	0.8567198E-02	-0.1286779E-01
5	0.4768254E+01	-0.2043287E+01	-0.5059287E-02	0.7199226E-02
6	0.5343827E+01	0.2040234E+01	0.3341589E-02	-0.4554065E-02
7	0.5865165E+01	-0.2036532E+01	-0.2372682E-02	0.3126262E-02
8	0.6344865E+01	0.2033097E+01	0.1772342E-02	-0.2273684E-02
9	0.6791382E+01	-0.2030102E+01	-0.1374554E-02	0.1725836E-02
10	0.7210690E+01	0.2027531E+01	0.1097345E-02	-0.1353733E-02
11	0.7607176E+01	-0.2025325E+01	-0.8964170E-03	0.1089828E-02
12	0.7984174E+01	0.2023424E+01	0.7461131E-03	-0.8960718E-03
13	0.8344284E+01	-0.2021775E+01	-0.6307318E-03	0.7497454E-03
14	0.8689576E+01	0.2020334E+01	0.5402232E-03	-0.6366286E-03
15	0.9021733E+01	-0.2019066E+01	-0.4679138E-03	0.5474706E-03
16	0.9342142E+01	0.2017944E+01	0.4092292E-03	-0.4760721E-03
17	0.9651964E+01	-0.2016942E+01	-0.3609583E-03	0.4182156E-03
18	0.9952179E+01	0.2016045E+01	0.3208173E-03	-0.3711446E-03
19	0.1024363E+02	-0.2015239E+01	-0.2873317E-03	0.3336256E-03
20	0.1052703E+02	0.2014502E+01	0.2607667E-03	-0.3353907E-03

Table 2 continued

Bi=2, Pe=10

n	β_n	$dR_n(1)/dy$	B_n	C_n
1	0.1152744E+01	-0.8699626E+00	-0.1406812E+00	0.9791802E+00
2	0.3204189E+01	0.1837647E+01	0.5046375E-01	-0.1076118E+00
3	0.4554698E+01	-0.2092915E+01	0.1246043E-01	0.4100793E-01
4	0.5649146E+01	0.2118419E+01	-0.1644055E-01	-0.1629191E-01
5	0.6585693E+01	-0.2108278E+01	-0.6151661E-02	0.9386051E-02
6	0.7413416E+01	0.2094973E+01	0.4122499E-02	-0.6000108E-02
7	0.8161599E+01	-0.2083377E+01	-0.2947328E-02	0.4119488E-02
8	0.8848843E+01	0.2073879E+01	0.2211809E-02	-0.2989511E-02
9	0.9497653E+01	-0.2066141E+01	-0.1721239E-02	0.2263775E-02
10	0.1008684E+02	0.2059781E+01	0.1377725E-02	-0.1771900E-02
11	0.1065288E+02	-0.2054490E+01	-0.1127811E-02	0.1423873E-02
12	0.1119067E+02	0.2050031E+01	0.9403075E-03	-0.1168925E-02
13	0.1170402E+02	-0.2046232E+01	-0.7960215E-03	0.9767787E-03
14	0.1219596E+02	0.2042956E+01	0.6826155E-03	-0.8285198E-03
15	0.1266895E+02	-0.2040109E+01	-0.5918722E-03	0.7118763E-03
16	0.1312501E+02	0.2037610E+01	0.5181588E-03	-0.6186516E-03
17	0.1356583E+02	-0.2035400E+01	-0.4575665E-03	0.5433037E-03
18	0.1399283E+02	0.2033436E+01	0.4075121E-03	-0.4823042E-03
19	0.1440723E+02	-0.2031675E+01	-0.3671927E-03	0.4305662E-03
20	0.1481009E+02	0.2030088E+01	0.3403517E-03	-0.4828713E-03

Bi=2, Pe=50

n	β_n	$dR_n(1)/dy$	B_n	C_n
1	0.1216892E+01	-0.8615370E+00	-0.4974878E-03	0.1117993E+01
2	0.4634373E+01	0.1740219E+01	0.4296820E-03	-0.1577561E+00
3	0.7635944E+01	-0.2227868E+01	-0.2182913E-02	0.5775639E-01
4	0.1016738E+02	0.2454515E+01	0.4558777E-02	-0.2846094E-01
5	0.1237364E+02	-0.2500024E+01	-0.4704227E-02	0.1611470E-01
6	0.1434431E+02	0.2471480E+01	0.3476974E-02	-0.1001358E-01
7	0.1613204E+02	-0.2425363E+01	-0.2662555E-02	0.6693736E-02
8	0.1777335E+02	0.2380583E+01	0.2102180E-02	-0.4740881E-02
9	0.1929536E+02	-0.2341652E+01	-0.1700220E-02	0.3514124E-02
10	0.2071857E+02	0.2308772E+01	0.1403080E-02	-0.2700401E-02
11	0.2205866E+02	-0.2281099E+01	-0.1178173E-02	0.2135998E-02
12	0.2332785E+02	0.2257683E+01	0.1004973E-02	-0.1729879E-02
13	0.2453576E+02	-0.2237708E+01	-0.8704793E-03	0.1428625E-02
14	0.2569012E+02	0.2220511E+01	0.7669594E-03	-0.1199428E-02
15	0.2679720E+02	-0.2205532E+01	-0.6911903E-03	0.1021085E-02
16	0.2786220E+02	0.2192366E+01	0.6448287E-03	-0.8824472E-03
17	0.2888943E+02	-0.2180821E+01	-0.6350628E-03	0.7499564E-03
18	0.2988251E+02	0.2173576E+01	0.6712105E-03	-0.7677941E-03
19	0.3084457E+02	-0.2160303E+01	-0.7428653E-03	0.3108554E-03
20	0.3177833E+02	0.2154883E+01	0.7463652E-03	-0.9583752E-03

Table 2 continued

Bi=10, Pe=1

n	β_n	$dR_n(1)/dy$	B_n	C_n
1	0.6926418E+00	-0.1384287E+01	-0.8636188E+00	0.1807202E+00
2	0.1253301E+01	0.3936592E+01	0.2887543E-01	-0.3086735E-01
3	0.1633024E+01	-0.5861049E+01	-0.9474614E-02	0.1376716E-01
4	0.1944412E+01	0.7158693E+01	0.4794428E-02	-0.7742185E-02
5	0.2215943E+01	-0.7999682E+01	-0.2918983E-02	0.4880063E-02
6	0.2460063E+01	0.8546646E+01	0.1972744E-02	-0.3311993E-02
7	0.2683648E+01	-0.8910807E+01	-0.1426306E-02	0.2372584E-02
8	0.2891049E+01	0.9160629E+01	0.1081218E-02	-0.1772100E-02
9	0.3085257E+01	-0.9337292E+01	-0.8489188E-03	0.1368385E-02
10	0.3268448E+01	0.9465759E+01	0.6848595E-03	-0.1085676E-02
11	0.3442263E+01	-0.9561588E+01	-0.5645821E-03	0.8809555E-03
12	0.3607977E+01	0.9634677E+01	0.4737204E-03	-0.7285074E-03
13	0.3766605E+01	-0.9691529E+01	-0.4033771E-03	0.6122893E-03
14	0.3918967E+01	0.9736521E+01	0.3477968E-03	-0.5219273E-03
15	0.4065739E+01	-0.9772676E+01	-0.3031245E-03	0.4505131E-03
16	0.4207487E+01	0.9802125E+01	0.2667005E-03	-0.3933446E-03
17	0.4344687E+01	-0.9826400E+01	-0.2366571E-03	0.3472054E-03
18	0.4477744E+01	0.9846630E+01	0.2116752E-03	-0.3100067E-03
19	0.4607008E+01	-0.9863651E+01	-0.1909257E-03	0.2809938E-03
20	0.4732784E+01	0.9878096E+01	0.1747065E-03	-0.2665986E-03

Bi=10, Pe=5

n	β_n	$dR_n(1)/dy$	B_n	C_n
1	0.1255729E+01	-0.1318149E+01	-0.4747655E+00	0.6704588E+00
2	0.2653116E+01	0.384362E+01	0.9369382E-01	-0.1037169E+00
3	0.3535772E+01	-0.5851900E+01	-0.3197363E-01	0.4712713E-01
4	0.4248441E+01	0.7215799E+01	0.1631811E-01	-0.2684494E-01
5	0.4866173E+01	-0.8093221E+01	-0.9980659E-02	0.1702844E-01
6	0.5419770E+01	0.8655882E+01	0.6764605E-02	-0.1158942E-01
7	0.5925749E+01	-0.9024171E+01	-0.4900471E-02	0.8311004E-02
8	0.6394398E+01	0.9272311E+01	0.3720177E-02	-0.6208806E-02
9	0.6832730E+01	-0.9444606E+01	-0.2924131E-02	0.4793351E-02
10	0.7245811E+01	0.9567667E+01	0.2361111E-02	-0.3801566E-02
11	0.7637450E+01	-0.9657827E+01	-0.1947867E-02	0.3083299E-02
12	0.8010598E+01	0.9725388E+01	0.1635405E-02	-0.2548517E-02
13	0.8367594E+01	-0.9777024E+01	-0.1393332E-02	0.2140952E-02
14	0.8710330E+01	0.9817181E+01	0.1201965E-02	-0.1824189E-02
15	0.9040359E+01	-0.9848892E+01	-0.1048119E-02	0.1573974E-02
16	0.9358976E+01	0.9874273E+01	0.9227153E-03	-0.1373827E-02
17	0.9667273E+01	-0.9894832E+01	-0.8194446E-03	0.1212547E-02
18	0.9966177E+01	0.9911662E+01	0.7341168E-03	-0.1083123E-02
19	0.1025649E+02	-0.9925574E+01	-0.6653545E-03	0.9833906E-03
20	0.1053890E+02	0.9937168E+01	0.6223528E-03	-0.1010893E-02

Table 2 continued

Bi=10, Pe=10

n	β_n	$dR_n(1)/dy$	B_n	C_n
1	0.1433665E+01	-0.1290536E+01	-0.2329176E+00	0.9346199E+00
2	0.3508055E+01	0.3716410E+01	0.9382434E-01	-0.1378446E+00
3	0.4806640E+01	-0.5802546E+01	0.2591372E-01	0.7192631E-01
4	0.5839725E+01	0.7256938E+01	-0.3267986E-01	-0.3655905E-01
5	0.6729877E+01	-0.8190195E+01	-0.1321577E-01	0.2358690E-01
6	0.7525123E+01	0.8779734E+01	0.9070243E-02	-0.1624276E-01
7	0.8250481E+01	-0.9157704E+01	-0.6607769E-02	0.1169244E-01
8	0.8921302E+01	0.9406496E+01	0.5035249E-02	-0.8740877E-02
9	0.9547971E+01	-0.9575045E+01	-0.3968900E-02	0.6745069E-02
10	0.1013795E+02	0.9692416E+01	0.3211742E-02	-0.5344810E-02
11	0.1069684E+02	-0.9776198E+01	-0.2654346E-02	0.4330657E-02
12	0.1122897E+02	0.9837325E+01	0.2231910E-02	-0.3575942E-02
13	0.1173775E+02	-0.9682774E+01	-0.1904055E-02	0.3001180E-02
14	0.1222594E+02	0.9917124E+01	0.1644557E-02	-0.2554831E-02
15	0.1269582E+02	-0.9943453E+01	-0.1435834E-02	0.2202551E-02
16	0.1314927E+02	0.9963876E+01	0.1265863E-02	-0.1921002E-02
17	0.1358786E+02	-0.9979887E+01	-0.1126582E-02	0.1694335E-02
18	0.1401296E+02	0.9992545E+01	0.1013668E-02	-0.1512761E-02
19	0.1442571E+02	-0.1000262E+02	-0.9300202E-03	0.1360423E-02
20	0.1482713E+02	0.1001070E+02	0.9016691E-03	-0.1552778E-02

Bi=10, Pe=50

n	β_n	$dR_n(1)/dy$	B_n	C_n
1	0.1545663E+01	-0.1271709E+01	-0.1133542E-02	0.1164415E+01
2	0.5112520E+01	0.3268026E+01	0.1086195E-02	-0.2325519E+00
3	0.8116373E+01	-0.5144398E+01	-0.5672956E-02	0.1046635E+00
4	0.1060631E+02	0.6307335E+01	0.1198956E-01	-0.6149086E-01
5	0.1274611E+02	-0.8315110E+01	-0.1250854E-01	0.4051010E-01
6	0.1464845E+02	0.9282812E+01	0.9363708E-02	-0.2823629E-01
7	0.1637828E+02	-0.9888682E+01	-0.7257337E-02	0.2042779E-01
8	0.1797416E+02	0.1025007E+02	0.5794559E-02	-0.1524133E-01
9	0.1946132E+02	-0.1045979E+02	-0.4736506E-02	0.1168706E-01
10	0.2085777E+02	0.1057813E+02	0.3949192E-02	-0.9182287E-02
11	0.2217709E+02	-0.1064161E+02	-0.3350885E-02	0.7370603E-02
12	0.2342991E+02	0.1067200E+02	0.2890190E-02	-0.6028511E-02
13	0.2462474E+02	-0.1068227E+02	-0.2535169E-02	0.5012588E-02
14	0.2576848E+02	0.1068031E+02	0.2269244E-02	-0.4228706E-02
15	0.2686683E+02	-0.1067095E+02	-0.2085129E-02	0.3612733E-02
16	0.2792456E+02	0.1065717E+02	0.1996795E-02	-0.3131589E-02
17	0.2894571E+02	-0.1064178E+02	-0.2031162E-02	0.2665728E-02
18	0.2993355E+02	0.1062339E+02	0.2218553E-02	-0.2736190E-02
19	0.3089117E+02	-0.1060372E+02	-0.2511068E-02	0.1140741E-02
20	0.3182111E+02	0.1058797E+02	0.2531075E-02	-0.3341952E-02

Table 2 continued

Bi=∞, Pe=1

n	β_n	$dR_n(1)/dy$	B_n	C_n
1	0.7287309E+00	-0.1542929E+01	-0.8925384E+00	0.1525937E+00
2	0.1311250E+01	0.4680637E+01	0.3689196E-01	-0.2432326E-01
3	0.1702419E+01	-0.7822316E+01	-0.1371363E-01	0.1102643E-01
4	0.2019032E+01	0.1096400E+02	0.7617861E-02	-0.6615073E-02
5	0.2292299E+01	-0.1410566E+02	-0.5008130E-02	0.4541284E-02
6	0.2536285E+01	0.1724730E+02	0.3647687E-02	-0.3377582E-02
7	0.2758776E+01	-0.2038892E+02	-0.2776724E-02	0.2650224E-02
8	0.2964615E+01	0.2353054E+02	0.2224118E-02	-0.2161536E-02
9	0.3157061E+01	-0.2667215E+02	-0.1839238E-02	0.1815989E-02
10	0.3338432E+01	0.2981375E+02	0.1559511E-02	-0.1562440E-02
11	0.3510444E+01	-0.3295536E+02	-0.1349645E-02	0.1371400E-02
12	0.3674413E+01	0.3609696E+02	0.1188441E-02	-0.1224936E-02
13	0.3831371E+01	-0.3923856E+02	-0.1062575E-02	0.1111784E-02
14	0.3982148E+01	0.4238016E+02	0.9634121E-03	-0.1024863E-02
15	0.4127420E+01	-0.4552176E+02	-0.8853425E-03	0.9600609E-03
16	0.4267750E+01	0.4866336E+02	0.8248987E-03	-0.9159050E-03
17	0.4403610E+01	-0.5180496E+02	-0.7804948E-03	0.8943686E-03
18	0.4535403E+01	0.5494655E+02	0.7528367E-03	-0.9046658E-03
19	0.4663472E+01	-0.5808815E+02	-0.7472849E-03	0.9815463E-03
20	0.4788118E+01	0.6122974E+02	0.7846638E-03	-0.1483502E-02

Bi=∞, Pe=5

n	β_n	$dR_n(1)/dy$	B_n	C_n
1	0.1337162E+01	-0.1479343E+01	-0.5525819E+00	0.6043114E+00
2	0.2776457E+01	0.4550386E+01	0.1272379E+00	-0.8691208E-01
3	0.3686892E+01	-0.7689307E+01	-0.4884889E-01	0.3936687E-01
4	0.4413191E+01	0.1083221E+02	0.2729398E-01	-0.2365227E-01
5	0.5036002E+01	-0.1397501E+02	-0.1800209E-01	0.1624685E-01
6	0.5589979E+01	0.1711751E+02	0.1303296E-01	-0.1208336E-01
7	0.6093883E+01	-0.2025979E+02	-0.1002090E-01	0.9477545E-02
8	0.6559240E+01	0.2340191E+02	0.8038947E-02	-0.7724966E-02
9	0.6993735E+01	-0.2654391E+02	-0.6657483E-02	0.6484522E-02
10	0.7402794E+01	0.2968584E+02	0.5653177E-02	-0.5573307E-02
11	0.7790420E+01	-0.3282771E+02	-0.4899887E-02	0.4885672E-02
12	0.8159665E+01	0.3596953E+02	0.4321822E-02	-0.4357222E-02
13	0.8512917E+01	-0.3911132E+02	-0.3871382E-02	0.3947316E-02
14	0.8852091E+01	0.4225308E+02	0.3517860E-02	-0.3630110E-02
15	0.9178745E+01	-0.4539481E+02	-0.3241548E-02	0.3390025E-02
16	0.9494171E+01	0.4853653E+02	0.3030764E-02	-0.3220117E-02
17	0.9799452E+01	-0.5167824E+02	-0.2881285E-02	0.3123593E-02
18	0.1009551E+02	0.5481993E+02	0.2798807E-02	-0.3122113E-02
19	0.1038313E+02	-0.5796112E+02	-0.2809788E-02	0.3248209E-02
20	0.1066300E+02	0.6110328E+02	0.2995387E-02	-0.5470049E-02

Table 2 continued

Bi=∞, Pe=10

n	β_n	$dR_n(1)/dy$	B_n	C_n
1	0.1539808E+01	-0.1450941E+01	-0.3006565E+00	0.8840305E+00
2	0.3672146E+01	0.4399766E+01	0.1373854E+00	-0.1158858E+00
3	0.5012257E+01	-0.7516604E+01	0.4569652E-01	0.6700212E-01
4	0.6068040E+01	0.1065870E+02	-0.5288004E-01	-0.3345774E-01
5	0.6967728E+01	-0.1380338E+02	-0.2511067E-01	0.2285940E-01
6	0.7764920E+01	0.1694779E+02	0.1838886E-01	-0.1710898E-01
7	0.8488152E+01	-0.2009167E+02	-0.1421489E-01	0.1345200E-01
8	0.9154773E+01	0.2323509E+02	0.1144878E-01	-0.1096662E-01
9	0.9776265E+01	-0.2637816E+02	-0.9513107E-02	0.9197831E-02
10	0.1036069E+02	0.2952096E+02	0.8102664E-02	-0.7894128E-02
11	0.1091397E+02	-0.3266356E+02	-0.7043729E-02	0.6907557E-02
12	0.1144059E+02	0.3580601E+02	0.6231489E-02	-0.6146889E-02
13	0.1194408E+02	-0.3894833E+02	-0.5600088E-02	0.5553966E-02
14	0.1242722E+02	0.4209055E+02	0.5107276E-02	-0.5091244E-02
15	0.1289230E+02	-0.4523269E+02	-0.4726509E-02	0.4735196E-02
16	0.1334120E+02	0.4837476E+02	0.4443242E-02	-0.4473398E-02
17	0.1377551E+02	-0.5151678E+02	-0.4254994E-02	0.4304846E-02
18	0.1419654E+02	0.5465875E+02	0.4176433E-02	-0.4252113E-02
19	0.1460546E+02	-0.5780069E+02	-0.4254995E-02	0.4068500E-02
20	0.1500325E+02	0.6094259E+02	0.4574340E-02	-0.7922288E-02

Bi=∞, Pe=50

n	β_n	$dR_n(1)/dy$	B_n	C_n
1	0.1673994E+01	-0.1430361E+01	-0.1918076E-02	0.1170031E+01
2	0.5363987E+01	0.3921668E+01	0.2300059E-02	-0.2399337E+00
3	0.8447450E+01	-0.6526332E+01	-0.1307021E-01	0.1055891E+00
4	0.1100647E+02	0.9381546E+01	0.2879166E-01	-0.6114074E-01
5	0.1319919E+02	-0.1240030E+02	-0.3130428E-01	0.4087946E-01
6	0.1513469E+02	0.1549773E+02	0.2469202E-01	-0.2973800E-01
7	0.1688097E+02	-0.1862879E+02	-0.2020556E-01	0.2285706E-01
8	0.1848174E+02	0.2177356E+02	0.1704496E-01	-0.1826900E-01
9	0.1996659E+02	-0.2492366E+02	-0.1472975E-01	0.1503953E-01
10	0.2135654E+02	0.2807555E+02	0.1299626E-01	-0.1267265E-01
11	0.2266705E+02	-0.3122770E+02	-0.1168459E-01	0.1088294E-01
12	0.2390992E+02	0.3437949E+02	0.1069487E-01	-0.9495947E-02
13	0.2509433E+02	-0.3753062E+02	-0.9965693E-02	0.8399862E-02
14	0.2622759E+02	0.4068101E+02	0.9462239E-02	-0.7520742E-02
15	0.2731565E+02	-0.4383103E+02	-0.9168216E-02	0.6802648E-02
16	0.2836340E+02	0.4698034E+02	0.9073949E-02	-0.6264548E-02
17	0.2937492E+02	-0.5012817E+02	-0.9144719E-02	0.5469595E-02
18	0.3035362E+02	0.5327020E+02	0.9233490E-02	-0.6540433E-02
19	0.3130247E+02	-0.5641846E+02	-0.8892392E-02	0.2242008E-02
20	0.3222405E+02	0.5957436E+02	0.7104719E-02	-0.7333617E-02
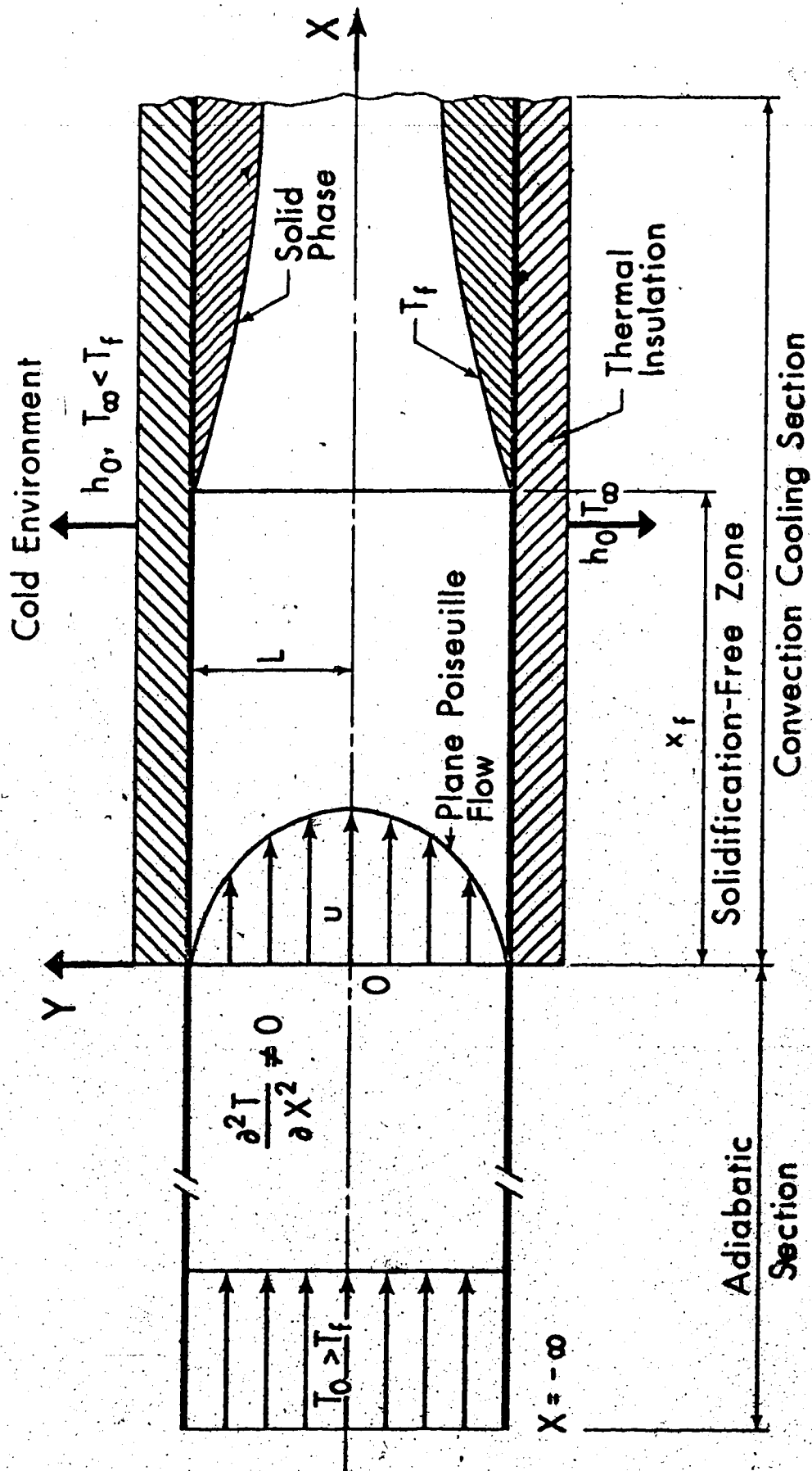
Figure 1. Coordinate system for extended Graetz problem
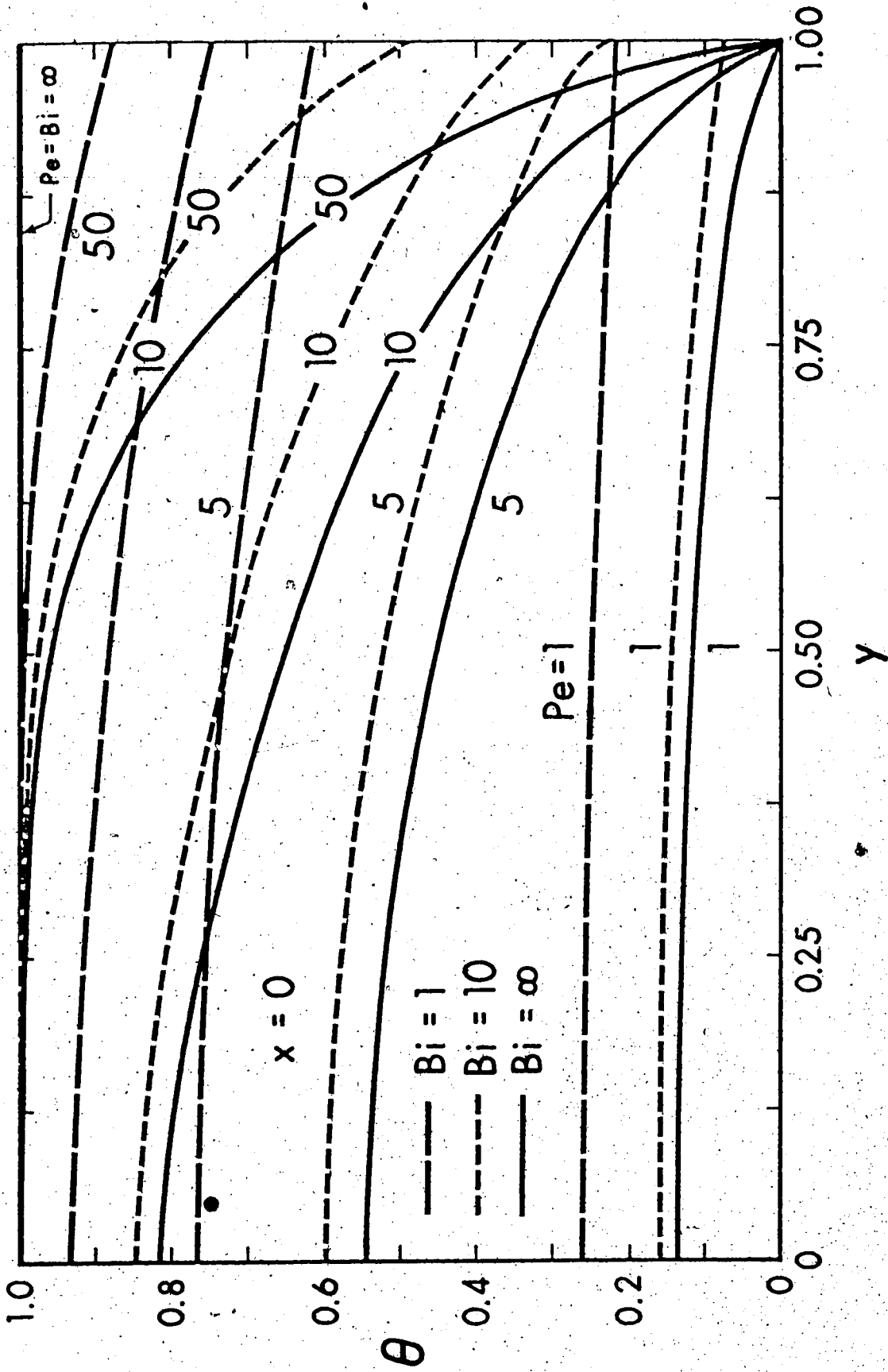
Figure 2. Temperature profiles at x=0 for Bi=1,10,∞ with Peclet number as parameter
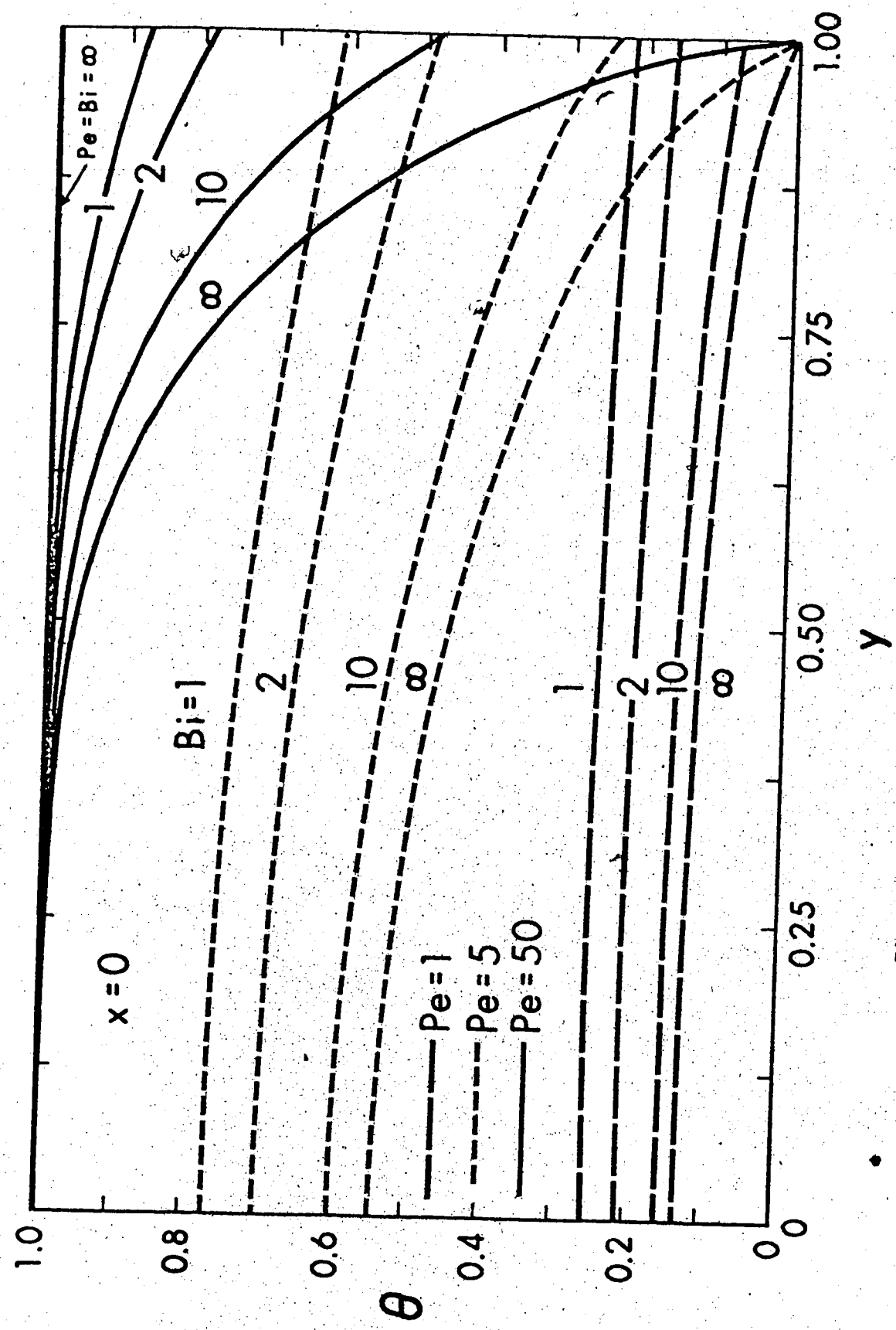
Figure 3. Temperature profiles at x=0 for Pe=1,5,50 with Biot number as parameter

114
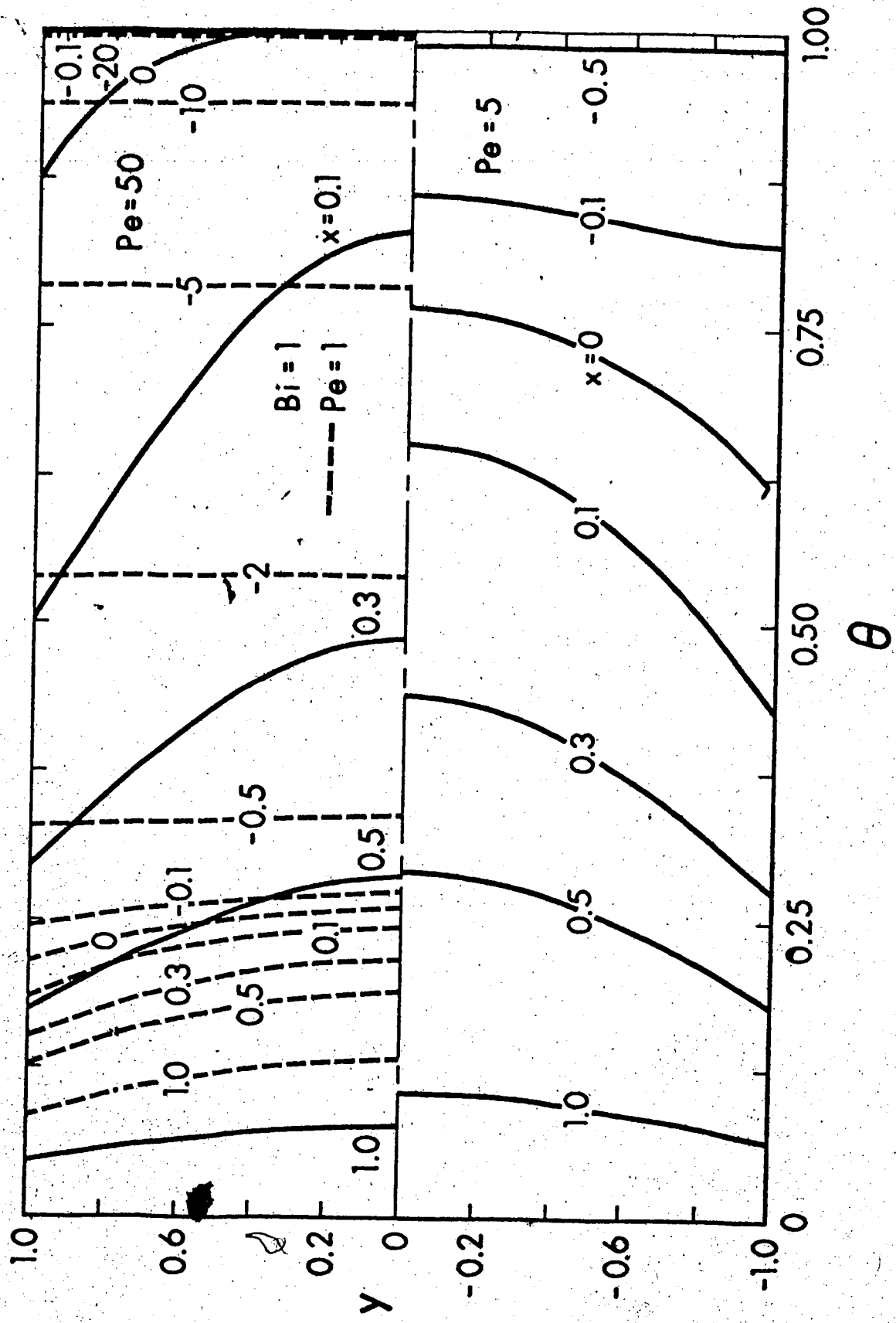
Figure 4. Developing temperature profiles for Bi=1 with Pe-1,5,50
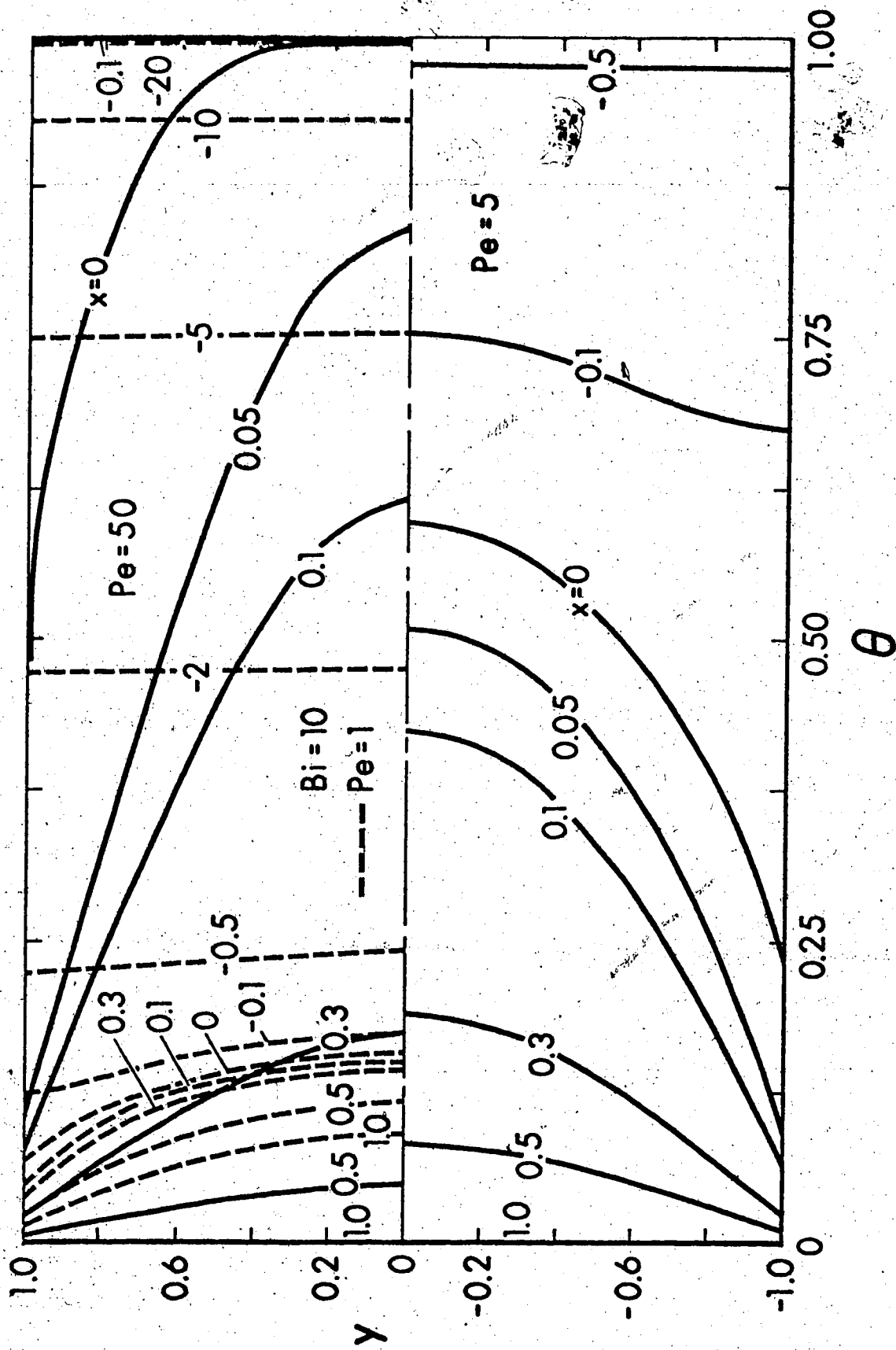
Figure 5. Developing temperature profiles for Bi=10 with Pe=1,5,50
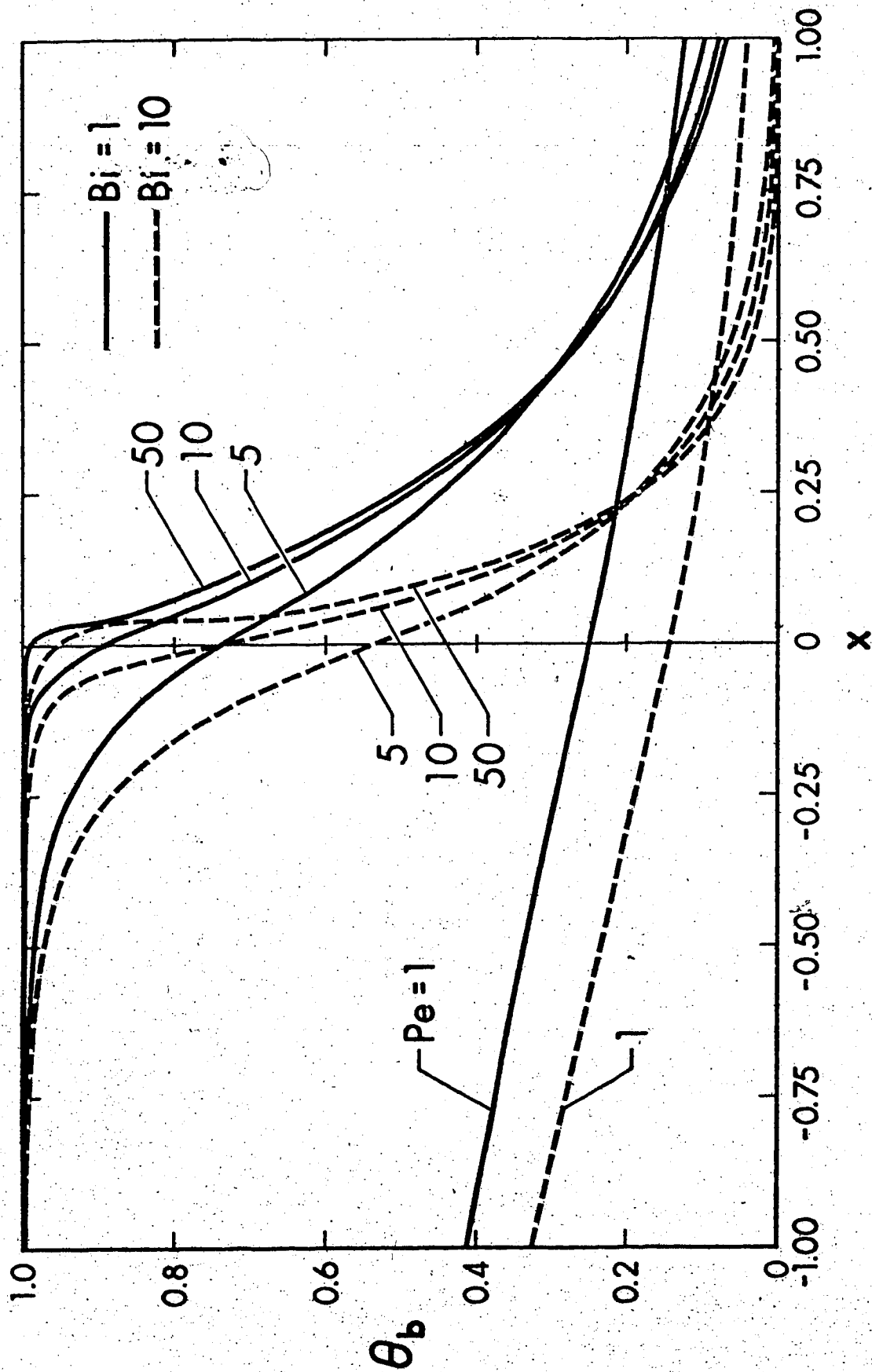
Figure 6. Axial bulk temperature distributions for Bi=1,10
with Peclet number as parameter
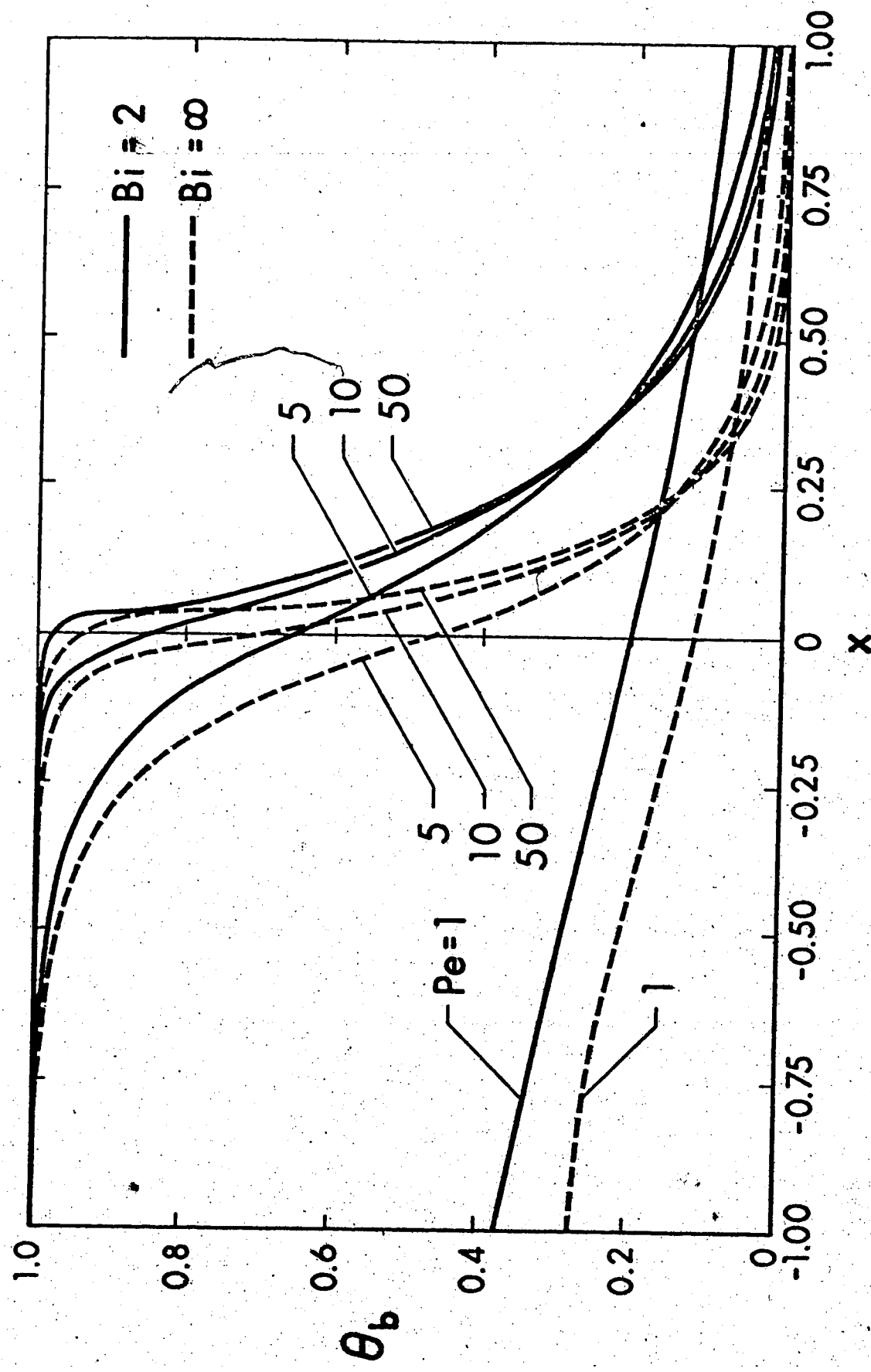
Figure 7. Axial bulk temperature distributions for Bi=2,∞ with Peclet number as parameter
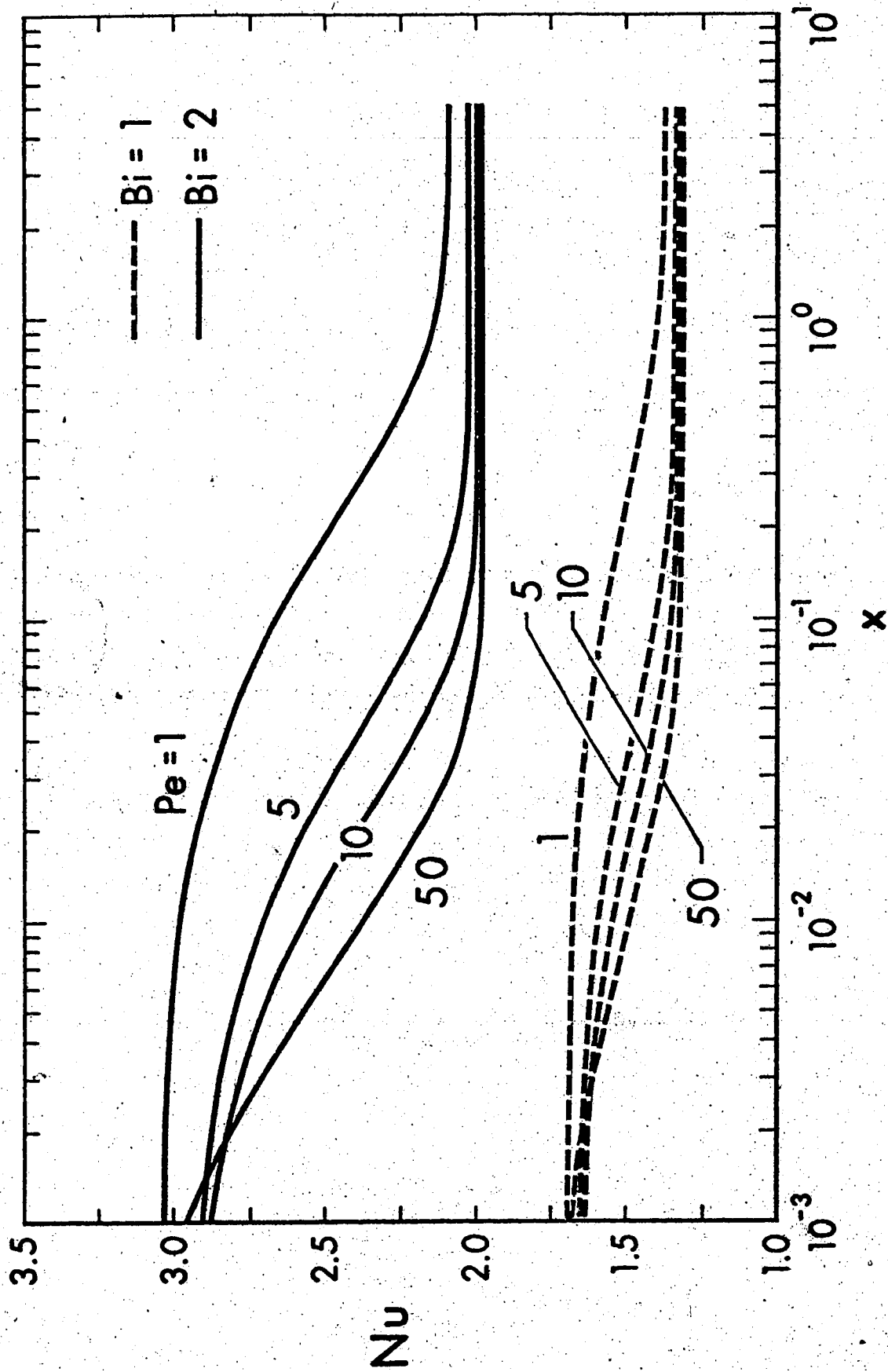
Figure 8.   Local Nusselt number results for Bi=1,2 with Pe=1,5,10,50
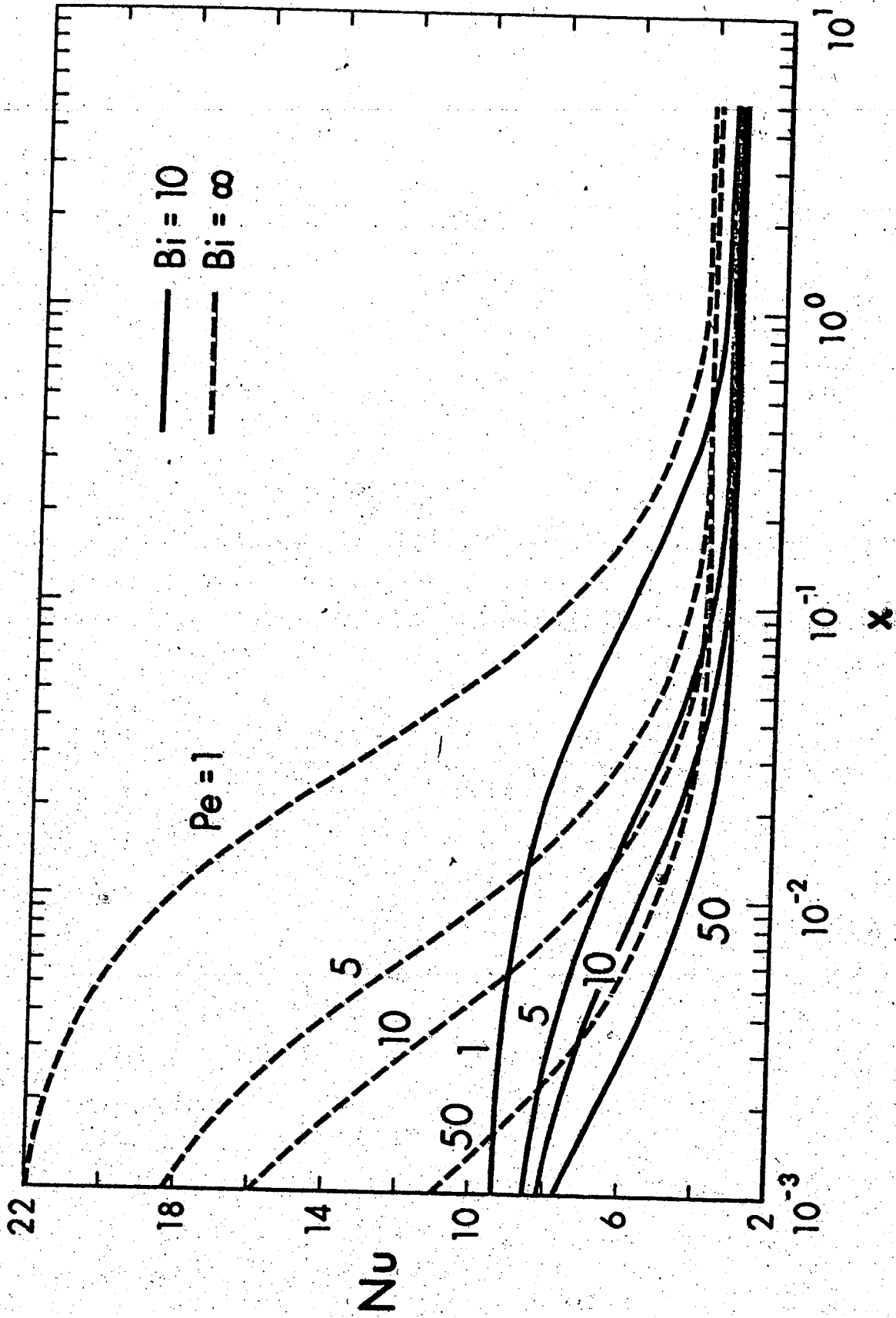
Figure 9. Local Nusselt number results for Bi=10,∞ with Pe=1,5,10,50
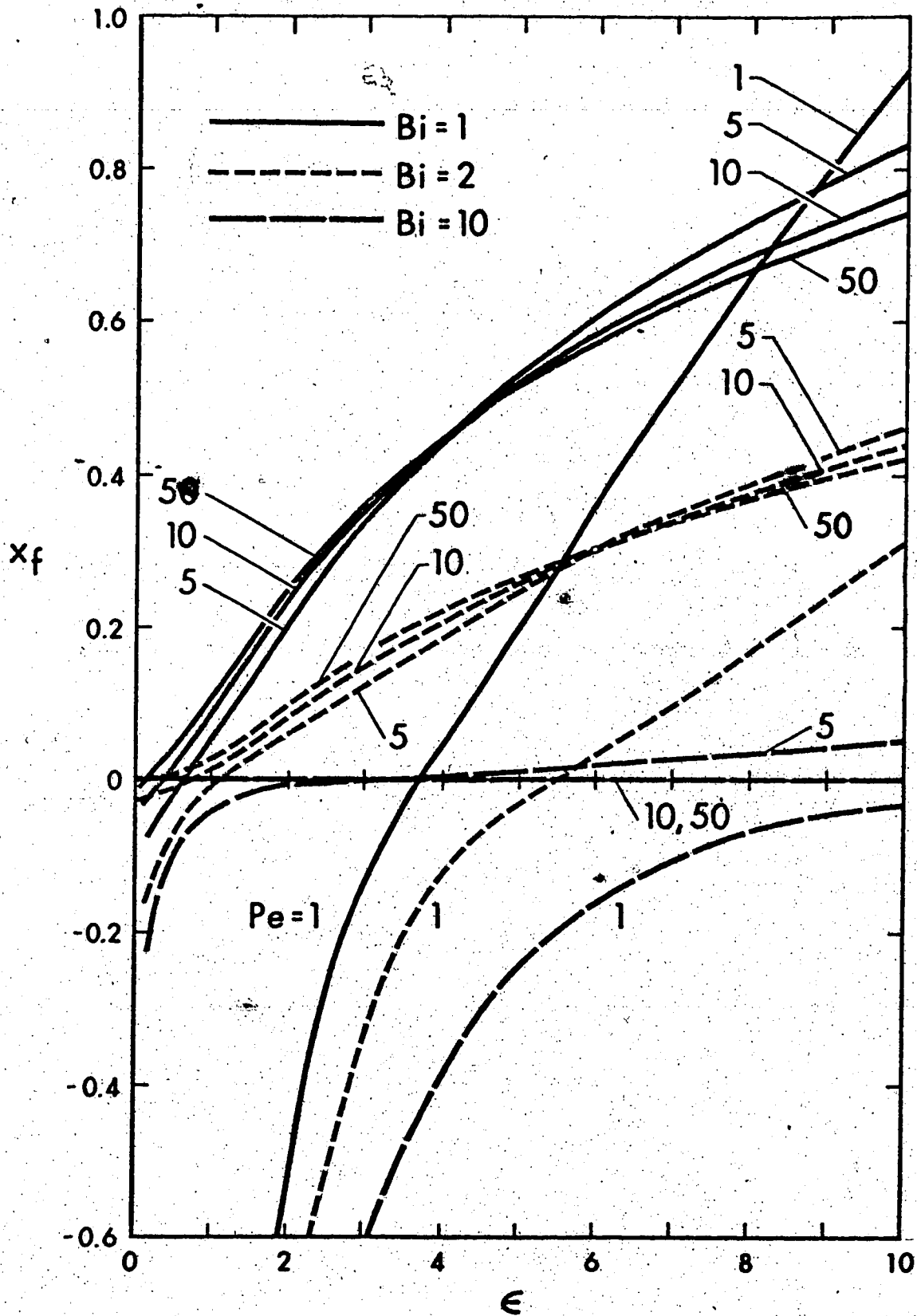
Figure 10. Liquid solidification-free length as a function of superheat ratio for Bi=1,2,10 with Pe=1,5,10,50

CHAPTER V

CONCLUSIONS

5.1 Scope of Results

The present investigation represents a generalization and further development of liquid solidification in a parallel-plate channel with a constant uniform wall temperature considered by Lee and Zerkle [1]. The problems considered in this study are more general and the work of Lee and Zerkle becomes a special case with $Bi = \infty$. With convective boundary conditions (Newton's law of cooling), one may assess the effect of thermal insulation and the results can be used to predict the insulation required to avoid "freeze shut" of a channel exposed to a cold environment. Recent theoretical analysis on liquid solidification in combined hydrodynamic and thermal entrance region of a circular tube with constant wall temperature and the related experimental results by Hwang and Sheu [2] confirm that the physical model used by Zerkle and Sunderland [3] leads to a good approximate analytical solution.

For both symmetric and unsymmetric liquid solidifications in parallel-plate channels with uniform convective boundary conditions (boundary condition of third kind), theoretical results are obtained for liquid solidification-free length, liquid-solid interface profile, pressure drop, bulk temperature, heat transfer rate and local Nusselt number for a range of values of Biot number and superheat ratio.

The Graetz problem with axial heat conduction effects in parallel-plate channels considering both the upstream and downstream

regions has been extended to the case of convective boundary condition. It is found that analytical solution in freezing zone cannot be obtained for low Peclet number flow regime and numerical solution must be sought.

5.2 Conclusions and Significance

The use of confluent hypergeometric function in finding the eigenvalues and eigenfunctions proves to be very efficient computationally and requires considerably less computing time than say the Runge-Kutta method. It is particularly effective when the boundary conditions at the upper and lower plates are unsymmetric and a large number of eigenvalues are required.

The Galerkin method of obtaining the series expansion coefficients involving the nonorthogonal eigenfunctions for Graetz problem with axial heat conduction effects is found to be simple, direct and considerably more efficient than the Gram-Schmidt orthonormalization procedure.

The effect of external thermal insulation on liquid solidification in parallel-plate channels has been investigated analytically for steady-state conditions. The Biot numbers, 0 and ∞, represent perfect insulation and constant wall temperature, respectively. Noting that the solution in freezing zone has been terminated at the dimensionless liquid-solid interface thickness $\delta = 10^{-3}$, one may estimate the conditions for "freeze shut" using the pressure drop and heat transfer results presented.

The liquid solidification-free length depends on superheat ratio and Biot number. On the other hand, the solid layer thickness in the freezing zone depends on thermal conductivity ratio k_{ℓ}/k_s and

Prandtl number additionally.

The symmetrical solidification problem in parallel-plate channels with convective boundary conditions arises in plate coolers or liquid-liquid heat exchangers in which the coolant is at a temperature below the freezing point of the warm liquid. The unsymmetrical solidification problem in parallel-plate channels with convective boundary conditions such as perfect insulation at lower plate and uniform convective cooling at upper plate arises in important applications such as freezing of rivers and continuous casting of metals. However, it should be pointed out that the physical models considered in this study are considerably simplified ones.

5.3 Some Suggestions for Future Work

It is desirable to verify the theoretical results reported in this thesis by experimental investigation. It is believed that the experimental investigation for unsymmetrical solidification with perfect insulation at one plate and convective cooling at other plate may serve as a good starting point in understanding the freezing of river. For the analysis on liquid solidification in parallel-plate channels with axial heat conduction effects (low Peclet number flow), one must use numerical method.

Future investigations on freezing of liquids in tubes or channels may include the case of turbulent flow. In some applications it may be desirable to promote freezing such as the use of a portable refrigeration device as a temporary shut-off value for a hydraulic line. This possibility may have future application in nuclear reactor field since the leakage of flowing liquid such as heavy water may be dangerous.

REFERENCES

1. Lee, D.G. and Zerkle, R.D., "The effect of liquid solidification in a parallel plate channel upon laminar-flow heat transfer and pressure drop", J. Heat Transfer 91C, 1969, pp. 583-585.

2. Hwang, G.J. and Sheu, J.P., "Liquid solidification in combined hydrodynamic and thermal entrance region of a circular tube", Can. J. Chem. Eng. 54, 1976, pp. 67-71.

3. Zerkle, R.D. and Sunderland, J.E., "The effect of liquid solidification in a tube upon laminar-flow heat transfer and pressure drop", J. Heat Transfer 90C, 1968, pp. 183-190.

An Order of Magnitude Analysis of the Governing Equations

The channel is placed horizontally so that body force effect is negligible. For Cartesian co-ordinates assuming no heat sources, no pressure work and negligible viscous energy dissipation, the governing equations are

Continuity:
$$\frac{D\rho}{Dt} + \rho\left(\frac{\partial U}{\partial X} + \frac{\partial V}{\partial Y}\right) = 0 \tag{1}$$

Momentum:
$$\frac{\partial U}{\partial t} + U\frac{\partial U}{\partial X} + V\frac{\partial U}{\partial Y} = -\frac{1}{\rho}\frac{\partial P}{\partial X} + \nu\left(\frac{\partial^2 U}{\partial X^2} + \frac{\partial^2 U}{\partial Y^2}\right) \tag{2}$$

$$\frac{\partial V}{\partial t} + U\frac{\partial V}{\partial X} + V\frac{\partial V}{\partial Y} = -\frac{1}{\rho}\frac{\partial P}{\partial Y} + \nu\left(\frac{\partial^2 V}{\partial X^2} + \frac{\partial^2 V}{\partial Y^2}\right) \tag{3}$$

Energy:
$$\frac{\partial T}{\partial t} + U\frac{\partial T}{\partial X} + V\frac{\partial T}{\partial Y} = \alpha\left(\frac{\partial^2 T}{\partial X^2} + \frac{\partial^2 T}{\partial Y^2}\right) \tag{4}$$

First, consider the energy equation. Using the following normalized variables, $x = X/X_c$, $y = Y/Y_c$, $u = U/U_c$, $v = V/V_c$, $\tau = t/t_c$, $\rho' = \rho/\rho_c$, $p = P/P_c$, $\phi = \theta/\theta_c$ where $\theta = T - T_w$, Equation (4) can be written as

$$\left(\frac{\theta_c}{t_c}\right)\frac{\partial\phi}{\partial\tau} + \left(\frac{U_c\theta_c}{X_c}\right)u\frac{\partial\phi}{\partial x} + \left(\frac{V_c\theta_c}{Y_c}\right)v\frac{\partial\phi}{\partial y} = \alpha\left(\frac{\theta_c}{X_c^2}\frac{\partial^2\phi}{\partial x^2} + \frac{\theta_c}{Y_c^2}\frac{\partial^2\phi}{\partial y^2}\right)$$

Multiplying the above equation by $Y_c^2/\theta_c\alpha$, one obtains

$$\left(\frac{Y_c^2}{\alpha t_c}\right)\frac{\partial\phi}{\partial\tau} + \left(\frac{U_c Y_c^2}{\alpha X_c}\right)\left[u\frac{\partial\phi}{\partial x} + \left(\frac{V_c X_c}{U_c Y_c}\right)v\frac{\partial\phi}{\partial y}\right] = \left(\frac{Y_c}{X_c}\right)^2\frac{\partial^2\phi}{\partial x^2} + \frac{\partial^2\phi}{\partial y^2}$$

If $\alpha t_c/Y_c^2 \gg 1$, then the unsteady term is insignificant. Therefore,

$$\left(\frac{U_c Y_c^2}{\alpha X_c}\right)\left[u\frac{\partial\phi}{\partial x} + \left(\frac{V_c X_c}{U_c Y_c}\right)v\frac{\partial\phi}{\partial y}\right] = \left(\frac{Y_c}{X_c}\right)^2\frac{\partial^2\phi}{\partial x^2} + \frac{\partial^2\phi}{\partial y^2}$$

Assuming the convection terms to be of the same order of magnitude as the conduction terms by setting

$$\frac{U_c Y_c^2}{\alpha X_c} = 1,$$

then the energy equation can be simplified to

$$u\frac{\partial\phi}{\partial x} + \left(\frac{V_c X_c}{U_c Y_c}\right)v\frac{\partial\phi}{\partial y} = \left(\frac{Y_c}{X_c}\right)^2\frac{\partial^2\phi}{\partial x^2} + \frac{\partial^2\phi}{\partial y^2} \tag{5}$$

Next, consider the continuity equation rewritten in the following form,

$$\frac{\partial\rho}{\partial t} + U\frac{\partial\rho}{\partial X} + V\frac{\partial\rho}{\partial Y} + \rho\frac{\partial U}{\partial X} + \rho\frac{\partial V}{\partial Y} = 0$$

After normalizing, one obtains

$$\left(\frac{\rho_c}{t_c}\right)\frac{\partial\rho'}{\partial\tau} + \left(\frac{\rho_c U_c}{X_c}\right)u\frac{\partial\rho'}{\partial x} + \left(\frac{\rho_c V_c}{Y_c}\right)v\frac{\partial\rho'}{\partial y} + \left(\frac{\rho_c U_c}{X_c}\right)\rho'\frac{\partial u}{\partial x}$$

$$+ \left(\frac{\rho_c V_c}{Y_c}\right)\rho'\frac{\partial v}{\partial y} = 0$$

But if $\nabla\rho = \left(\dfrac{d\rho}{d\theta}\right)_p \nabla\theta = -\beta\rho\nabla\theta$, one obtains

$$\frac{\partial\rho}{\partial X}\, \bar{e}_X + \frac{\partial\rho}{\partial Y}\, \bar{e}_Y = -\beta\rho\, \left(\frac{\partial\theta}{\partial X}\, \bar{e}_X + \frac{\partial\theta}{\partial Y}\, \bar{e}_Y\right)$$

One notices that

$$\frac{\partial\rho}{\partial X} = -\beta\rho\, \frac{\partial\theta}{\partial X} \quad \text{and} \quad \frac{\partial\rho}{\partial Y} = -\beta\rho\, \frac{\partial\theta}{\partial Y}$$

or, in dimensionless form,

$$\frac{\partial\rho'}{\partial x} = -\beta\rho'\theta_c\, \frac{\partial\phi}{\partial x} \quad \text{and} \quad \frac{\partial\rho'}{\partial y} = -\beta\rho'\theta_c\, \frac{\partial\phi}{\partial y}$$

where β is the coefficient of thermal expansion.

Using these relationships in the continuity equation, one obtains

$$\left(\frac{\rho_c}{t_c}\right) \frac{\partial\rho'}{\partial\tau} - \left(\frac{\rho_c U_c}{X_c}\right) u\beta\rho'\theta_c\, \frac{\partial\phi}{\partial x} - \left(\frac{\rho_c V_c}{Y_c}\right) v\beta\rho'\theta_c\, \frac{\partial\phi}{\partial y}$$

$$+ \left(\frac{\rho_c U_c}{X_c}\right) \rho'\, \frac{\partial u}{\partial x} + \left(\frac{\rho_c V_c}{Y_c}\right) \rho'\, \frac{\partial v}{\partial y} = 0$$

Multiplying the above equation by $X_c/\rho_c U_c$ yields

$$\left(\frac{X_c}{U_c t_c}\right) \frac{\partial\rho'}{\partial\tau} + \rho'\, \frac{\partial u}{\partial x} + \left(\frac{V_c X_c}{U_c Y_c}\right) \rho'\, \frac{\partial v}{\partial y} = \beta\theta_c\rho' \left[u\, \frac{\partial\phi}{\partial x} + \left(\frac{V_c X_c}{U_c Y_c}\right) v\, \frac{\partial\phi}{\partial y}\right] \qquad (6)$$

The coefficient for the unsteady term can be written as

$$\left(\frac{X_c}{U_c t_c}\right) = \frac{Y_c^2 U_c/\alpha}{U_c t_c} = \frac{Y_c^2}{\alpha t_c}$$

One notes that the coefficient is exactly the same as that in the energy equation. Therefore, if the unsteady term is insignificant in the energy equation, it can also be neglected in the continuity equation.

For water under atmospheric pressure, one has $\beta\theta_{c\ max} \ll 1$. Thus, the right-hand side of equation (6) can be suppressed, since

$$[u \frac{\partial\phi}{\partial x} + (\frac{V_c X_c}{U_c Y_c}) v \frac{\partial\phi}{\partial y}] \text{ is of order one.}$$

It is also seen that

$$(\frac{V_c X_c}{U_c Y_c}) = 0(1).$$

The continuity equation now becomes

$$\frac{\partial u}{\partial x} + \frac{\partial v}{\partial y} = 0 \tag{7}$$

The x and y - momentum equations in normalized form are given by

$$(\frac{U_c}{t_c}) \frac{\partial u}{\partial \tau} + (\frac{U_c^2}{X_c}) u \frac{\partial u}{\partial x} + (\frac{U_c V_c}{Y_c}) v \frac{\partial u}{\partial y} = - (\frac{P_c}{\rho X_c}) \frac{\partial p}{\partial x}$$

$$+ \nu [\frac{U_c}{X_c^2} \frac{\partial^2 u}{\partial x^2} + \frac{U_c}{Y_c^2} \frac{\partial^2 u}{\partial y^2}]$$

$$(\frac{V_c}{t_c}) \frac{\partial v}{\partial \tau} + (\frac{U_c V_c}{X_c}) u \frac{\partial v}{\partial x} + (\frac{V_c^2}{Y_c}) v \frac{\partial v}{\partial y} = - (\frac{P_c}{\rho Y_c}) \frac{\partial p}{\partial y}$$

$$+ \nu [\frac{V_c}{X_c^2} \frac{\partial^2 v}{\partial x^2} + \frac{V_c}{Y_c^2} \frac{\partial^2 v}{\partial y^2}]$$

Multiplying the first equation by $Y_c^2/\nu U_c$ and the second equation by $Y_c^2/\nu V_c$, one obtains

$$(\frac{Y_c^2}{\nu t_c}) \frac{\partial u}{\partial \tau} + (\frac{U_c Y_c^2}{\nu X_c}) [u \frac{\partial u}{\partial x} + (\frac{V_c X_c}{U_c Y_c}) v \frac{\partial u}{\partial y}]$$

$$= - (\frac{P_c Y_c^2}{\mu U_c X_c}) \frac{\partial p}{\partial x} + (\frac{Y_c}{X_c})^2 \frac{\partial^2 u}{\partial x^2} + \frac{\partial^2 u}{\partial y^2}$$

$$(\frac{Y_c^2}{\nu t_c}) \frac{\partial v}{\partial \tau} + (\frac{U_c Y_c^2}{\nu X_c}) [u \frac{\partial v}{\partial x} + (\frac{V_c X_c}{U_c Y_c}) v \frac{\partial v}{\partial y}]$$

$$= - (\frac{P_c Y_c}{\mu V_c}) \frac{\partial p}{\partial y} + (\frac{Y_c}{X_c})^2 \frac{\partial^2 v}{\partial x^2} + \frac{\partial^2 v}{\partial y^2}$$

Assuming the pressure term to be of the same order of magnitude as the viscous term, then one has $P_c Y_c^2/\mu U_c X_c = O(1)$ or $P_c = \mu U_c X_c/Y_c^2$. One notices that the coefficients in the momentum equations can be expressed in alternate form as,

$$\frac{Y_c^2}{\nu t_c} = (\frac{Y_c^2}{\alpha t_c})(\frac{\alpha}{\nu}) = (\frac{Y_c^2}{\alpha t_c}) \frac{1}{Pr}$$

$$\frac{U_c Y_c^2}{\alpha X_c} = (\frac{U_c Y_c^2}{\alpha X_c})(\frac{\alpha}{\nu}) = \frac{1}{Pr}$$

$$\frac{P_c Y_c}{\mu V_c} = (\mu \frac{U_c X_c}{Y_c^2}) \frac{Y_c}{\mu V_c} = (\frac{X_c}{Y_c})^2$$

$$\frac{Y_c}{X_c} = (\frac{Y_c}{Y_c^2 U_c/\alpha}) = \frac{1}{Re_{Y_c} Pr} = \frac{1}{Pe}$$

Again, if one assumes that $\alpha t_c / Y_c^2 \gg 1$ and $Pr > 1$, the unsteady terms in the momentum equations can also be neglected. Thus, the x and y - momentum equations now become

$$\frac{1}{Pr} \left[u \frac{\partial u}{\partial x} + v \frac{\partial u}{\partial y} \right] = - \frac{\partial p}{\partial x} + \frac{1}{Pe^2} \frac{\partial^2 u}{\partial x^2} + \frac{\partial^2 u}{\partial y^2} \tag{8}$$

$$\frac{1}{Pr} \left[u \frac{\partial v}{\partial x} + v \frac{\partial v}{\partial y} \right] = - Pe^2 \frac{\partial p}{\partial y} + \frac{1}{Pe^2} \frac{\partial^2 v}{\partial x^2} + \frac{\partial^2 v}{\partial y^2} \tag{9}$$

In summary, the governing equations are:

$$\frac{\partial u}{\partial x} + \frac{\partial v}{\partial y} = 0 \tag{10}$$

$$\frac{1}{Pr} \left[u \frac{\partial u}{\partial x} + v \frac{\partial u}{\partial y} \right] = - \frac{\partial p}{\partial x} + \frac{1}{Pe^2} \frac{\partial^2 u}{\partial x^2} + \frac{\partial^2 u}{\partial y^2} \tag{11}$$

$$\frac{1}{PrPe^2} \left[u \frac{\partial v}{\partial x} + v \frac{\partial v}{\partial y} \right] = - \frac{\partial p}{\partial y} + \frac{1}{Pe^4} \frac{\partial^2 v}{\partial x^2} + \frac{1}{Pe^2} \frac{\partial^2 v}{\partial y^2} \tag{12}$$

$$u \frac{\partial \phi}{\partial x} + v \frac{\partial \phi}{\partial y} = \frac{1}{Pe^2} \frac{\partial^2 \phi}{\partial x^2} + \frac{\partial^2 \phi}{\partial y^2} \tag{13}$$

where the following relationships are used

$$\frac{U_c Y_c^2}{\alpha X_c} = 1 \quad , \quad \frac{V_c X_c}{U_c Y_c} = 1 \quad , \quad \frac{P_c Y_c^2}{\mu U_c X_c} = 1 \quad ,$$

$$\frac{Y_c^2}{\alpha t_c} \gg 1 \quad , \quad \beta \theta_{c_{max}} \ll 1$$

The above equations will now be applied to the solidification-free zone

and the freezing zone.

A. Solidification-Free Zone

The flow is hydrodynamically fully developed in this region, thus, continuity equation becomes

$$\partial v/\partial y = 0 \quad \text{or} \quad v = 0$$

If the flowing liquid under consideration is water ($Pr = 7.88$ for water at $60^\circ F$ and 13.35 for ice at $32^\circ F$), then the axial heat conduction effect can be neglected if the Reynolds number is of order (10) or larger. The momentum and energy equations are then given by

$$\partial p/\partial x = \partial^2 u/\partial y^2 \tag{14}$$

$$\partial p/\partial y = 0 \tag{15}$$

$$u\partial\phi/\partial x = \partial^2\phi/\partial y^2 \tag{16}$$

For this analysis, if one takes $Y_c = L$ and U_c as the average velocity, the other reference quantities can be found accordingly. The results are

$$X_c = \frac{Y_c^2 U_c}{\alpha} = Re_{Y_c} PrL$$

$$V_c = \frac{U_c Y_c}{X_c} = \frac{F}{2Re_{Y_c} PrL}$$

$$\text{and } P_c = \frac{\mu U_c X_c}{Y_c^2} = \frac{\mu F Re_{Y_c} Pr}{2L^2}$$

Where F is the flow rate per unit depth of the infinite plate,

$F = 2LU_c$ and Re_{Y_c} is a Reynolds number based on Y_c. However, in the text, an equivalent hydraulic diameter is used.

B. Freezing Zone

The freezing zone can be subdivided into two parts, the liquid phase and the solid phase.

1. Liquid Phase

Because of the formation of frozen layer along the channel, the reduction of flow area causes the flow in this region to accelerate. Energy equation is thus given by

$$u \frac{\partial \phi_\ell}{\partial x} + v \frac{\partial \phi_\ell}{\partial y} = \frac{1}{Pe^2} \frac{\partial^2 \phi_\ell}{\partial x^2} + \frac{\partial^2 \phi_\ell}{\partial y^2}$$

The rate of solid layer growth is governed by the following energy balance at the liquid-solid interface.

$$- k_\ell \left[\frac{\partial T_\ell}{\partial Y}\right]_{Y=\delta} - \rho_s L_s \frac{d\delta}{dt} = - k_s \left[\frac{\partial T_s}{\partial Y}\right]_{Y=\delta}$$

where the subscripts ℓ and s denote properties in liquid and solid phases, respecitvely,

δ is the distance measured from centre line to the liquid-solid inter-

face, and

L_s is the latent heat of fusion.

Normalization gives

$$\left(\frac{k_\ell}{k_s}\ \epsilon\right)\left[\frac{\partial\phi_\ell}{\partial y}\right]_{y=\bar\delta} + \left(\frac{\rho_s L_s Y_c^2}{t_c k_s \theta_{cs}}\right)\frac{d\bar\delta}{d\tau} = \left[\frac{\partial\phi_s}{\partial y}\right]_{y=\bar\delta} \tag{17}$$

where the dimensionless variables are defined by

$$\bar\delta = \delta/Y_c \qquad , \qquad y = Y/Y_c \qquad , \qquad \tau = t/t_c$$

$$\phi_\ell = \frac{T_\ell - T_w}{\theta_{c\ell}} \qquad , \qquad \phi_s = \frac{T_s - T_w}{\theta_{cs}} \quad \text{and} \quad \epsilon = \frac{\theta_{c\ell}}{\theta_{cs}} = \text{superheat ratio.}$$

When the solid layer is growing, the coefficient of the middle term of equation (17) cannot be suppressed. Therefore, one obtains

$$\frac{\rho_s L_s Y_c^2}{t_c k_s \theta_{cs}} \sim 0\ (1)$$

or $\quad t_c = \dfrac{\rho_s L_s Y_c^2}{k_s \theta_{cs}}$

Now the heat balance at the interface reduces to

$$\left(\frac{k_\ell}{k_s}\ \epsilon\right)\left[\frac{\partial\phi_\ell}{\partial y}\right]_{y=\bar\delta} + \frac{d\bar\delta}{d\tau} = \left[\frac{\partial\phi_s}{\partial y}\right]_{y=\bar\delta} \tag{18}$$

If $1/Pe \ll 1$, then the axial heat conduction effect is negligible. Thus, the energy equation becomes

$$u\frac{\partial\phi_\ell}{\partial x} + v\frac{\partial\phi_\ell}{\partial y} = \frac{\partial^2\phi_\ell}{\partial y^2} \tag{19}$$

2. Solid Phase

   The energy equation is

$$\frac{\partial \theta_s}{\partial t} = \alpha \left(\frac{\partial^2 \theta s}{\partial X^2} + \frac{\partial^2 \theta s}{\partial Y^2} \right)$$

Normalization yields

$$\left(\frac{Y_c^2}{\alpha t_c} \right) \frac{\partial \phi_s}{\partial \tau} = \left(\frac{Y_c}{X_c} \right)^2 \frac{\partial^2 \phi s}{\partial x^2} + \frac{\partial^2 \phi s}{\partial y^2}$$

If one takes $Y_c = L$ and $X_c = Re_{Y_c} PrL$, one notices that $Y_c/X_c = 1/Pe$. Thus, if $1/Pe < 1$, axial conduction can be neglected in the solid region too. The coefficient in the unsteady term is

$$\frac{Y_c^2}{\alpha t_c} = \frac{Y_c^2}{\alpha \rho_s L_s Y_c^2 / k_s \theta_{cs}} = \frac{Cp_s \theta_{cs}}{L_s} = Ste$$

For $Ste \ll 1$, the problem is quasi-steady. If the liquid-solid interface reaches a steady-state, then

$$\frac{\partial \phi_s}{\partial \tau} = 0 \qquad \text{and} \qquad \frac{d\delta}{d\tau} = 0.$$

Therefore, the energy equation for the solid phase reduces to a Laplace equation as

$$\frac{\partial \phi_s}{\partial x^2} + \frac{\partial \phi_s}{\partial y^2} = 0 \quad \text{or} \quad \frac{\partial \phi_s}{\partial y^2} = 0 \qquad \text{without axial heat conduction.} \qquad (20)$$

The interface heat balance equation simplifies to

$$\left(\frac{k_\ell}{k_s} \epsilon \right) \left[\frac{\partial \phi_\ell}{\partial y} \right]_{y=\delta} = \left[\frac{\partial \phi_s}{\partial y} \right]_{y=\delta} \qquad (21)$$

APPENDIX 2

Derivation of the Expression for K_j in Chapter II

The determination of the eigenconstants K_j from Eq. (31) in Chapter II resolves to evaluation of the following integrals.

$$I_1 = \int_0^1 (1-\eta^2) N_j(\eta) d\eta$$

$$I_2 = \int_0^1 (1-\eta^2) Y_i(\eta) N_j(\eta) d\eta$$

$$I_3 = \int_0^1 (1-\eta^2) N_j^2(\eta) d\eta$$

Using Eq. (26) and integrating, the first integral becomes

$$I_1 = \left[-\frac{1}{\beta_j^2} \frac{dN_j}{d\eta} \right]_{\eta=0}^1 = -\frac{1}{\beta_j^2} \frac{dN_j}{d\eta} \quad (1)$$

Next consider the second integral. After some manipulations using Eqs. (4) and (26), the integral I_2 can be shown to be

$$I_2 = \left[\frac{-(N_j \frac{dY_i}{d\eta} - Y_i \frac{dN_j}{d\eta})}{(\alpha_i^2 - \beta_j^2)} \right]_{\eta=0}^1 = \frac{Y_i(1)}{(\alpha_i^2 - \beta_j^2)} \frac{dN_j}{d\eta} \quad (1)$$

where the following boundary conditions are used.

$$N_j(1) = 0 \quad , \quad \frac{dN_j}{d\eta}(0) = 0 \quad \text{and} \quad \frac{dY_i}{d\eta}(0) = 0$$

Following the same procedure, I_3 can be found and is given by

136

$$I_3 = \frac{1}{2\beta_j} \left[\frac{\partial N_j}{\partial \beta_j} \frac{dN_j}{d\eta} - N_j \frac{d}{d\eta} \left(\frac{\partial N_j}{\partial \beta_j} \right) \right]^1_{\eta = 0} = \frac{1}{2\beta_j} \frac{\partial N_j}{\partial \beta_j} (1) \frac{dN_j}{d\eta} (1)$$

Upon substitution of I_1, I_2 and I_3 into Eq. (31), the expression for K_j becomes

$$K_j = \frac{[(1+\epsilon)/\epsilon]2\beta_j \sum_{i=1}^{20} E_i Y_i (1)\exp(-8\alpha_i^2 X_f/3)}{(\alpha_i^2 - \beta_j^2)\partial N_j (1)/\partial \beta_j} + \frac{(2/\epsilon)}{\beta_j \partial N_j (1)/\partial \beta_j}$$

APPENDIX 3

Determination of Fully Developed Temperature
in Thermal Entry Region

From physical consideration of the problem, one expects the fully developed temperature profile to be independent of x and is of the following form

$$\theta_{fd} = \psi(y) \tag{1}$$

Eq. (1) must also satisfy the energy equation,

$$\frac{3}{8} (1-y^2) \frac{\partial \theta}{\partial x} = \frac{\partial^2 \theta}{\partial y^2} + \frac{1}{Pe^2} \frac{\partial^2 \theta}{\partial x^2} \tag{2}$$

and the boundary conditions

$$\partial \theta(x,0)/\partial y = 0 \tag{3}$$

$$\partial \theta(x,1)/\partial y = - Bi\theta(x,1) \tag{4}$$

Substituting Eq. (1) into Eq. (2), one obtains

$$\frac{d^2 \psi}{dy^2} = 0$$

or $\qquad \psi = C_1 y + C_2$ \hfill (5)

From Eq. (3), it is found that $C_1 = 0$. Thus, substituting $\psi = C_2$ into Eq. (4) yields

$$\theta_{fd} = \psi = 0 \tag{6}$$

In order to gain a better understanding of the problem, a heat balance from $X = -\infty$ in the adiabatic region to $X = X$ is performed as follows.

$$\rho C_p U_m L T_0 = -\int_0^X k_\ell \frac{\partial T_2}{\partial Y} (X,L) \, dX - k_\ell \int_0^L \frac{\partial T_{fd}}{\partial X} (X,Y) \, dY$$

$$+ \rho C_p U_m \int_0^L \frac{3}{2} [1 - (\frac{Y}{L})^2] T_{fd} dY \tag{7}$$

The term on the left-hand side is the energy input entering the channel at $X = -\infty$. The first term on the right-hand side is a heat loss through convection to the surrounding, while the second and third terms represent the axial heat conduction and energy leaving the channel at X, respectively.

Letting $\theta_2 = (T_2 - T_\infty)/(T_0 - T_\infty)$, $y = Y/L$, $x = X/LPe$ where $Pe = 4\rho C_p U_m L/k_\ell$, Eq. (7) can be transformed to

$$\frac{\rho C_p U_m L}{k_\ell Pe} \int_0^1 \frac{3}{2} (1-y^2) \frac{T_0 - T_{fd}}{T_0 - T_\infty} = -\int_0^x \frac{\partial \theta_2}{\partial y} (X,1) \, dx - \frac{1}{Pe^2} \int_0^1 \frac{\partial \theta_{fd}}{\partial x} dy \tag{8}$$

where one notes that $T_0 = \int_0^1 \frac{3}{2} (1-y^2) T_0 dy$.

Noting that

$$\frac{\rho C_p U_m L}{k_\ell Pe} = \frac{1}{4} \quad \text{and} \quad \frac{T_0 - T_{fd}}{T_0 - T_\infty} = 1 - \theta_{fd}, \text{ Eq. (8) becomes}$$

$$\frac{3}{2} \int_0^1 (1-y^2)(1-\theta_{fd}) \, dy = -4 \int_0^x \frac{\partial \theta_2}{\partial y} (x,1) \, dx + \frac{4}{Pe^2} \int_0^1 \frac{\partial \theta_{fd}}{\partial x} dy \tag{9}$$

With $\theta_{fd} = 0$, one obtains simply

$$1 = -4 \int_0^x \frac{\partial \theta_2}{\partial y} (x,1) \, dx \tag{10}$$

It can be concluded that all the energy entering the channel will eventually be transfered out through convection to the surrounding.

Analysis for Solidification with Axial Heat Conduction
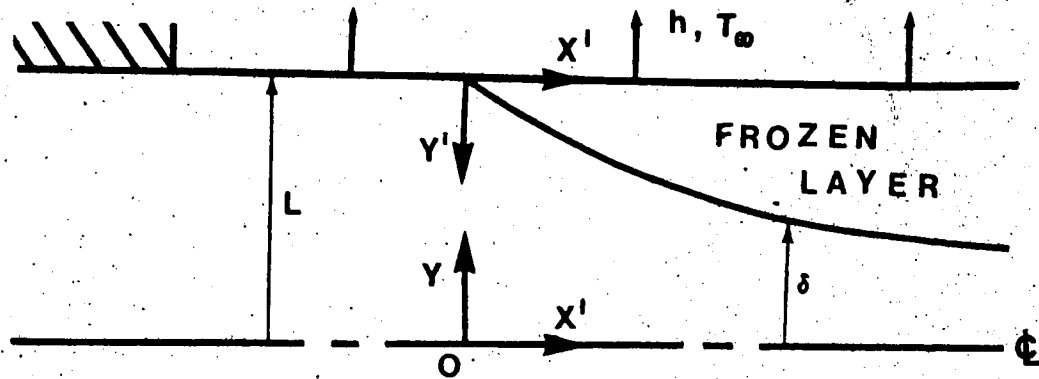
Fig. A1 Configuration and Co-ordinate System for
Solidification Region with Axial Conduction

The solidification region is subdivided into two systems; the liquid and the solid. The two systems are coupled through the heat balance condition at the interface. This coupling together with the fact that the solidification boundary cannot be found in advance, makes the present solidification problem very difficult to solve. With the axial heat conduction effect, the incipient point of solidification may occur in the adiabatic region. However, in this analysis, only cases where solidification occurs in the convective cooling region (downstream region) are considered.

1. Liquid System

As solid layers are being formed along the upper and lower walls of the channel, the fluid accelerates in the axial direction due to the constriction of flow area. The axial and transverse velocities which satisfy the mass flow rate criteria and also the no-slip boun-

dary conditions are given by

$$U(X',Y) = \frac{3}{2} \frac{LU_m}{\delta} [1 - (\frac{Y}{\delta})^2] \tag{1}$$

$$V(X',Y) = \frac{3}{2} \frac{LU_m Y}{\delta^2} [1 - (\frac{Y}{\delta})^2] \frac{d\delta}{dX'} \tag{2}$$

Substituting Eqs. (1) and (2) into the energy equation,

$$U\partial T_\ell/\partial X' + V\partial T_\ell/\partial Y = \alpha(\partial^2 T_\ell/\partial X'^2 + \partial^2 T_\ell/\partial Y^2),$$

one obtains

$$\frac{3}{2} \frac{LU_m}{\delta} [1 - (\frac{Y}{\delta})^2] \frac{\partial T_\ell}{\partial X'} + \frac{3}{2} \frac{LU_m}{\delta^2} Y \frac{d\delta}{dX'} [1 - (\frac{Y}{\delta})^2] \frac{\partial T_\ell}{\partial Y}$$

$$= \alpha [\frac{\partial^2 T_\ell}{\partial X'^2} + \frac{\partial^2 T_\ell}{\partial Y^2}].$$

Introducing the following dimensionless variables, $\bar{x} = X'/LPe$, $\bar{y} = Y/L$, $\bar{\delta} = \delta/L$, $\phi_\ell = (T_\ell - T_f)/(T_0 - T_f)$, the energy equation can now be written as

$$\frac{3}{8} \frac{1}{\bar{\delta}} [1 - (\frac{\bar{y}}{\bar{\delta}})^2] \frac{\partial \phi_\ell}{\partial \bar{x}} + \frac{3}{8} \frac{\bar{y}}{\bar{\delta}^2} \frac{d\bar{\delta}}{d\bar{x}} [1 - (\frac{\bar{y}}{\bar{\delta}})^2] \frac{\partial \phi_\ell}{\bar{\delta}\bar{y}} = \frac{1}{Pe^2} \frac{\partial^2 \phi_\ell}{\partial \bar{x}^2} + \frac{\partial^2 \phi_\ell}{\partial \bar{y}^2} \tag{3}$$

With boundary conditions

$$\frac{\partial \phi_\ell}{\partial \bar{y}} (\bar{x},0) = 0 \tag{4}$$

$$\phi_\ell(\bar{x},\bar{\delta}) = 0 \tag{5}$$

$$\phi_\ell(0,\bar{y}) = \frac{1+\varepsilon}{\varepsilon} \theta (x_f,y) - \frac{1}{\varepsilon} \qquad (6)$$

where ε is the superheat ratio.

The boundary conditions (5) and (6) show that the temperature at the liquid-solid interface remains constant at its freezing temperature T_f and the initial condition prescribed at $X' = 0$ is, in fact, the temperature solution of the solidification-free zone at $x = x_f$. Thus, one has

$$\theta(x_f,y) = \sum_{n=1}^{\infty} C_n R_n(y) \exp(-8\beta_n^2 x_f/3)$$

It can be seen that the unknown solid thickness δ appears in Eq. (5). In order to eliminate δ from the boundary condition, variable transformation as described in Chapters II and III may be used. One defines

$$\eta = \bar{y}/\delta = Y/\delta \qquad (7)$$

The purpose here is to transform $\theta(\bar{x},\bar{y})$ to $\theta(\bar{x},\eta)$ so that η changes from 0 to 1 when measured from the centre-line of the channel to the liquid-solid boundary.

Eq. (3) now becomes

$$\frac{3}{8}\frac{1}{\delta}(1-\eta^2)\frac{\partial\phi_\ell}{\partial\bar{x}} = \frac{1}{Pe^2}\left[\frac{\partial^2\phi_\ell}{\partial\bar{x}^2} + \frac{2\bar{y}}{\delta^3}(\frac{d\delta}{d\bar{x}})^2\frac{\partial\phi_\ell}{\partial\eta} - \frac{\bar{y}}{\delta^2}\frac{d^2\delta}{d\bar{x}^2}\frac{\partial\phi_\ell}{\partial\eta}\right.$$

$$\left. + (\frac{\bar{y}}{\delta^2}\frac{d\delta}{d\bar{x}})^2\frac{\partial^2\phi_\ell}{\partial\eta^2} - \frac{2\bar{y}}{\delta^2}\frac{d\delta}{d\bar{x}}\frac{\partial^2\phi_\ell}{\partial\eta\partial\bar{x}}\right] + \frac{1}{\delta^2}\frac{\partial^2\phi_\ell}{\partial\eta^2}$$

Assuming that the axial solid-thickness variation is gradual, one has

$\dfrac{d^2\bar{\delta}}{d\bar{x}^2}$ and $(\dfrac{d\bar{\delta}}{d\bar{x}})^2$ $<< 1$. The energy equation then reduces to

$$\frac{3}{8}\frac{1}{\bar{\delta}}(1-\eta^2)\frac{\partial\phi_\ell}{\partial\bar{x}} = \frac{1}{Pe^2}[\frac{\partial^2\phi_\ell}{\partial\bar{x}^2} - \frac{2\bar{y}}{\bar{\delta}^2}\frac{d\bar{\delta}}{d\bar{x}}\frac{\partial^2\phi_\ell}{\partial\eta\partial\bar{x}}] + \frac{1}{\bar{\delta}^2}\frac{\partial^2\phi_\ell}{\partial\eta^2} \tag{8}$$

with the boundary conditions

$$\partial\phi_\ell(\bar{x},0)/\partial\eta = 1 \tag{9}$$

$$\phi_\ell(\bar{x},1) = 0 \tag{10}$$

$$\phi_\ell(0,\eta) = (1+\epsilon)\theta(x_f,\eta)/\epsilon - 1/\epsilon \tag{11}$$

It should be noted that if the axial heat conduction effect is negligible, the energy equation reduces to that given in Chapter II.

2. Solid System

For the solid region, it is convenient to shift the co-ordinate origin to the upper plate of the channel as shown in Fig. A1. Thus, the steady-state energy equation for pure conduction is simply a Laplace Equation:

$$\frac{\partial^2 T_s}{\partial X'^2} + \frac{\partial^2 T_s}{\partial Y'^2} = 0 \tag{12}$$

The boundary conditions are

$$T_s(X', L-\delta) = T_f \tag{13}$$

$$k_s \frac{\partial T_s}{\partial Y'} (X',0) = - h_0 [T_s(X',0) - T_\infty] \tag{14}$$

$$T_s = \text{finite as } X' \to \infty \tag{15}$$

The interface condition which represents the coupling between the liquid and solid systems is given by

$$k_\ell [\frac{\partial T_\ell}{\partial Y}]_{Y=\delta} = k_s [\frac{\partial T_s}{\partial Y'}]_{Y'=L-\delta} \tag{16}$$

Eq. (12) can be written in dimensionless form as

$$\frac{1}{Pe^2} \frac{\partial^2 \phi_s}{\partial \bar{x}'^2} + \frac{\partial^2 \phi_s}{\partial \bar{y}'^2} = 0 \tag{17}$$

where the dimensionless variables, $\phi_s = (T_s - T_\infty)/(T_0 - T_f)$, $\bar{x}' = X'/LPe$, $\bar{y}' = Y'/L$ and $\bar{\delta} = \delta/L$ are used.

In order to eliminate $\bar{\delta}$ from the boundary condition, a variable transformation of the following form may be used.

$$\xi = \bar{y}'/(1 - \bar{\delta})$$

After transformation, Eq. (17) becomes

$$\frac{1}{Pe^2} \{\frac{\partial^2 \phi_s}{\partial \bar{x}'^2} + 2\frac{\bar{y}'}{(1-\bar{\delta})^2} \frac{d\bar{\delta}}{d\bar{x}'} \frac{\partial^2 \phi_s}{\partial \bar{x}'\partial \xi} + \frac{2\bar{y}'}{(1-\bar{\delta})^3} (\frac{d\bar{\delta}}{d\bar{x}'})^2 \frac{\partial \phi_s}{\partial \xi}$$

$$\frac{\bar{y}'}{(1-\bar{\delta})^2} \frac{d^2\bar{\delta}}{d\bar{x}'^2} \frac{\partial \phi_s}{\partial \xi} + [\frac{\bar{y}'}{(1-\bar{\delta})^2} \frac{d\bar{\delta}}{d\bar{x}'}]^2 \frac{\partial^2 \phi_s}{\partial \xi^2}\} + \frac{1}{(1-\bar{\delta})^2} \frac{\partial^2 \phi_s}{\partial \xi^2} = 0.$$

With $\dfrac{d^2\bar{\delta}}{d\bar{x}'^2}$ and $(\dfrac{d\bar{\delta}}{d\bar{x}'})^2 \ll 1$,

the energy equation becomes

$$\frac{1}{Pe^2} [\frac{\partial^2 \phi_s}{\partial \bar{x}'^2} + 2 \frac{\bar{y}'}{(1-\bar{\delta})^2} \frac{d\bar{\delta}}{d\bar{x}'} \frac{\partial^2 \phi_s}{\partial \bar{x}' \partial \xi}] + \frac{1}{(1-\bar{\delta})^2} \frac{\partial^2 \phi_s}{\partial \xi^2} = 0 \qquad (18)$$

with the boundary conditions

$$\phi_s (\bar{x}', 1) = 0 \qquad (19)$$

$$\frac{\partial \phi_s}{\partial \xi} (\bar{x}', 0) = - \frac{h_0 L}{k_s} [\phi_s(\bar{x}', 0) + \frac{1}{\epsilon}] \qquad (20)$$

$$\phi_s = \text{finite} \qquad\qquad \text{as } \bar{x}' \to \infty \qquad (21)$$

$$\text{and } k_\ell [\frac{\partial \phi_\ell}{\partial \bar{y}}]_{\bar{y}=\bar{\delta}} = k_s [\frac{\partial \phi_s}{\partial \bar{y}'}]_{\bar{y}'=1-\bar{\delta}} \qquad (22)$$

From physical consideration, as $\bar{x}' \to \infty$, one expects that the temperature distribution in the solid region is developed and is a function of $\bar{y}'$ only.

The main difficulty in solving this system of equations, Eqs. (8) to (11) and Eqs. (18) to (22) is the coupling condition given by Eq. (22) since it requires that the temperature solution in the liquid phase must also be known. When the axial heat conduction term is retained, the energy equation changes from a parabolic-type to an elliptic-type. As terms with $\bar{\delta}$ and $d\bar{\delta}/d\bar{x}'$ are present in the differential equation, one notices that the separation of variable tech-

nique employed in Chapters II and III is not applicable for the present problem. Thus, with the inclusion of the axial heat conduction term, it becomes extremely difficult to seek an analytical solution. One notices that the system of equations obtained after the foregoing transformation is no more easier to solve than the original set of equations. For the present problem, numerical methods such as finite difference method or finite element method are apparently preferred.

Mathematical Formulation for Poiseuille Pipe Flow

For the corresponding problem in circular pipes, the governing energy equation can be written as

$$2U_m[1 - (r/r_0)^2] \frac{\partial T_i}{\partial x} = \alpha [\frac{\partial^2 T_i}{\partial r^2} + \frac{1}{r} \frac{\partial T_i}{\partial r} + \frac{\partial^2 T_i}{\partial x^2}], \quad (i = 1, 2) \tag{1}$$

where r_0 is the radius of the pipe, U_m the mean velocity and $i = 1$, and 2 refer to the regions $- \infty < x \leq 0$ (upstream) and $0 \leq x < \infty$ (downstream), respectively. The appropriate boundary conditions to be satisfied are,

For $- \infty < x \leq 0$,

$$\frac{\partial T_1}{\partial r} (x,0) = \frac{\partial T_1}{\partial r} (x,r_0) = 0$$

$$T_1(-\infty,r) = T_0 \tag{2}$$

For $0 \leq x < \infty$

$$\frac{\partial T_2}{\partial r} (x,0) = 0$$

$$- k \frac{\partial T_2}{\partial r} (x,r_0) = h_0 [T_2(x,r_0) - T_\infty] \tag{3}$$

$$T_2 = T_{fd} \qquad \text{as} \qquad x \to \infty$$

At $x = 0$

$$T_1(0,r) = T_2(0,r)$$

$$\frac{\partial T_1}{\partial x}(0,r) = \frac{\partial T_2}{\partial x}(0,r) \tag{4}$$

Introducing the following dimensionless variables,

$$\theta_i = \frac{T_i - T_\infty}{T_0 - T_\infty} \; (i=1,2) \quad , \quad \xi = \frac{r}{r_0} \quad , \quad \eta = \frac{x}{r_0 Pe} \quad , \quad Bi = \frac{h_0 r_0}{k} \; ,$$

Eqs. (1) through (4) can be transformed to

$$(1-\xi^2)\frac{\partial \theta_i}{\partial \eta} = [\frac{\partial^2 \theta_i}{\partial \xi^2} + \frac{1}{\xi}\frac{\partial \theta_i}{\partial \xi} + \frac{1}{Pe^2}\frac{\partial^2 \theta_i}{\partial \eta^2}], \; (i = 1, 2) \tag{5}$$

For $-\infty < \eta \leq 0$

$$\frac{\partial \theta_1}{\partial \xi}(\eta,0) = \frac{\partial \theta_1}{\partial \xi}(\eta,1) = 0 \tag{6}$$

$$\theta_1(-\infty,\xi) = 1$$

For $0 \leq \eta < \infty$

$$\frac{\partial \theta_2}{\partial \xi}(\eta,0) = 0 \tag{7a}$$

$$\frac{\partial \theta_2}{\partial \xi}(\eta,1) = -Bi\theta_2(\eta,1) \tag{7b}$$

$$\theta_2 = \theta_{fd} \quad \text{as} \quad \eta \to \infty \tag{7c}$$

At $\eta = 0$

$$\theta_1(0,\xi) = \theta_2(0,\xi)$$

$$\frac{\partial\theta_1}{\partial\eta}(0,\xi) = \frac{\partial\theta_2}{\partial\eta}(0,\xi) \tag{8}$$

Using the same procedure as for the parallel-plate channels, the fully developed temperature is found to be

$$\theta_{fd} = 0 \tag{9}$$

The temperature solutions θ_1 and θ_2 are now sought in the following forms.

$$\theta_1 = 1 + \sum_{n=1}^{\infty} B_n Y_n(\xi) e^{\alpha_n^2 \eta} \qquad x < 0 \tag{10a}$$

$$\theta_2 = \sum_{n=1}^{\infty} C_n R_n(\xi) e^{-\alpha_n^2 \eta} \qquad x \geq 0 \tag{10b}$$

On substituting Eq. (10a) into Eqs. (5) and (6), the following characteristic equation is obtained,

$$\frac{d^2 Y_n}{d\xi^2} + \frac{1}{\xi}\frac{dY_n}{d\xi} + \alpha_n^2 \left[\frac{\alpha_n^2}{Pe^2} - (1-\xi^2)\right] Y_n = 0 \tag{11}$$

with the boundary conditions,

$$\frac{dY_n}{d\xi} = 0 \text{ at } \xi = 0 \text{ and } \xi = 1 \tag{12}$$

Similarly, substituting Eq. (10b) into Eqs. (5) and (7) yields the

following characteristic equation

$$\frac{d^2 R_n}{d\xi^2} + \frac{1}{\xi}\frac{dR_n}{d\xi} + \beta_n^2[\frac{\beta_n^2}{Pe^2} + (1-\xi^2)]\ R_n = 0 \tag{13}$$

with the boundary conditions,

$$\frac{dR_n}{d\xi} = 0 \qquad at \qquad \xi = 0 \tag{14a}$$

$$\frac{dR_n}{d\xi} = -B_i R_n \quad at \tag{14b}$$

Eq. (11) for the upstream region with boundary condition (12) has been solved by Hsu [10]. For the downstream region, Kummer's transform can again be employed. Thus, one has

$$z = \beta_n\xi^2 \quad and \quad W(z) = e^{\beta_n\xi^2/2}\ R_n(\xi)$$

$$or\ R_n(\xi) = e^{-\beta_n\xi^2/2}\ W(z) \tag{15}$$

$$dR_n/d\xi = -\beta_n\xi\ e^{-\beta_n\xi^2/2}\ W(z) + e^{-\beta_n\xi^2/2}\ W'(z)\beta_n(2\xi)$$

$$= e^{-\beta_n\xi^2/2}\ \beta_n\xi[-W(z) + 2\ W'(z)]$$

$$d^2R_n/d\xi^2 = e^{-\beta_n\xi^2/2}\ \{4\beta_n^2\xi^2 W''(z)+(2\beta_n-4\beta_n^2\xi^2)W'(z)+(\beta_n^2\xi^2-\beta_n)W(z)\}$$

Putting the foregoing two derivatives into Eq. (13), one obtains

$$z \frac{d^2W(z)}{dz^2} + (1-z) \frac{dW(z)}{dz} - \frac{1}{4} [2 - \beta_n(\frac{\beta_n^2}{Pe^2} + 1)] W(z) = 0 \qquad (16)$$

which is seen to be Kummer's equation with

$$a = \frac{1}{4} [2 - \beta_n(\frac{\beta_n^2}{Pe^2} + 1)] \text{ and } b = 1.$$

With the symmetric boundary condition $dR_n(0)/d\xi = 0$, the eigenfunctions, then, are given by

$$R_n(\xi) = e^{-\beta_n\xi^2/2} M(\frac{2-\beta_n(1+\beta_n^2/Pe^2)}{4}, 1, \beta_n\xi^2) \qquad (17)$$

Differentiating Eq. (17) with respect to ξ yields

$$dR_n/d\xi = e^{-\beta_n\xi^2/2} \{- \beta_n\xi \, M(\frac{2-\beta_n(1+\beta_n^2/Pe^2)}{4}, 1, \beta_n\xi^2)$$

$$+ \beta_n\xi [\frac{2-\beta_n(1+\beta_n^2/Pe^2)}{2}]M(\frac{6-\beta_n(1+\beta_n^2/Pe^2)}{4}, 2, \beta_n\xi^2)\} \qquad (18)$$

The eigenvalues are then obtained as roots of the following equation

$$\beta_n [\frac{2-\beta_n(1+\beta_n^2/Pe^2)}{2}]M(\frac{6-\beta_n(1+\beta_n^2/Pe^2)}{4}, 2, \beta_n)$$

$$+ (B_i - \beta_n)M(\frac{2-\beta_n(1+\beta_n^2/Pe^2)}{4}, 1, \beta_n) = 0 \qquad (19)$$

It should be noted that the above analysis can also be applied to the case without axial conduction and with different boundary conditions.

APPENDIX 6

COMPUTER PROGRAMS

153

```
CC
CC       DECK FOR COMPUTING EIGENVALUES AND EIGENCONSTANTS
CC                 IN SOLIDIFICATION FREE ZONE
CC
         IMPLICIT REAL*8 (A-H,O-Z)
         DIMENSION F(3)
         DO 100 II=1,5
         READ (5,901) BI
         WRITE (6,1001) BI
         N1=150
CC
CC 20 EIGENVALUES
CC
         DO 100 JJ=1,20
         READ (5,902) XL
         READ (5,902) XR
CC
CC SECANT METHOD
CC
         CALL FUNCT (BI,XL,N1,FL,F,R,N2)
         CALL FUNCT (BI,XR,N1,FR,F,R,N2)
CC
CC 30  ITERATIONS
CC
         DO 20 KK=1,30
         XM=(XR*FL-XL*FR)/(FL-FR)
         CALL FUNCT (BI,XM,N1,FM,F,R,N2)
         WRITE (6,1004) KK,FM,XM
         IF (DABS(FM).LT.1.D-7) GO TO 21
         XL=XR
         FL=FR
         XR=XM
         FR=FM
         IF (DABS(FL-FR).LT.1.D-10) GO TO 21
20       CONTINUE
21       WRITE (6,1005) II,XM,N2
         WRITE (6,1002) R
         B=XM
CC
CC COMPUTE EIGENCONSTANTS
CC
         N=1
         Y=RMULT(B,N)
         REF1=Y
         DO 30 N=2,200
         Y=Y+RMULT(B,N)
```

```
          IF (DABS(Y-REF1).LT.0.1D-7) GO TO 31
30        REF1=Y
          WRITE (6,444)
31        Y=(1.D0+Y)/DEXP(E/2.D0)
          IF (E.EQ.1.D0) GO TO 55
          N=1
          Y1=RMULT(E,N)*(-0.5D0+1.D0/E-SS(E,N))
          Y2=RMULT(E,N)*(-3.D0+E/2.D0+2.D0/E-SS(E,N)*(2.D0-E))
          REF2=Y1
          REF3=Y2
          DO 40 N=2,200
          Y1=Y1+RMULT(E,N)*(-0.5D0+N/E-SS(E,N))
          IF (DABS(Y1-REF2).LT.0.1D-7) GO TO 41
40        REF2=Y1
          WRITE (6,444)
41        Y1=(-0.5D0+Y1)/DEXP(E/2.D0)
          DO 50 N=2,200
          Y2=Y2+RMULT(E,N)*(-1.D0+E/2.D0-2.D0*N+2.D0*N*N/E
         X-SS(E,N)*(2.D0*N-E)
          IF (DABS(Y2-REF3).LT.0.1D-7) GO TO 51
50        REF3=Y2
          WRITE (6,444)
51        Y2=(-1.D0+E/2.D0+Y2)/DEXP(E/2.D0)
          GO TO 71
CC
55        Y1=0.5D0
          Y2=0.5D0
          T1=0.5D0
          REF=Y2
          DO 60 NN=2,200
          N=2*NN
          T1=4.D0*(NN-1)*T1/(N*(N-1))
          Y1=Y1+T1
          Y2=Y2+T1*(N-1)
          IF (DABS(Y2-REF).LT.0.1D-7) GO TO 61
60        REF=Y2
          WRITE (6,444)
61        Y1=(-0.5D0-Y1)/DEXP(E/2.D0)
          Y2=(-0.5D0-Y2)/DEXP(0.5D0)
CC
71        EC=-2.D0/(E*(Y1+Y2/BI))
          EK=EC*Y
          WRITE (6,222) JJ,EK,EC,Y1,Y2,Y,E
          WRITE (8,555) E,EC,Y,Y1,Y2
100       CONTINUE
222       FORMAT ('0','EK',I2,'=',F12.6,10X,'EC=',F12.6,5X,
```

```
      X'DY=',F12.6,5X,'DDY=',F12.6,5X,'Y=',F12.6,5X,'E=',
      XF12.6)
444   FORMAT (' NEED MORE THAN 200 TERMS')
555   FORMAT (5D15.8)
901   FORMAT (D15.8)
902   FORMAT (D8.4)
903   FORMAT (D20.10,D20.10)
1001  FORMAT ('1',15X,'BIOT NO. =',D10.3)
1002  FORMAT ('0',85X,'B(N) =',D15.8)
1004  FORMAT (' ',I2,5X,'BO =',D15.8,10X,'E =',D15.8)
1005  FORMAT ('0',80X,'EIGENVALUE ',I2,'=',F14.8,10X,
      X'N2=',I3)
      STOP
      END
CC
CC
      SUBROUTINE FUNCT (BI,E,N1,FU,F,R,N2)
      IMPLICIT REAL*8 (A-H,O-Z)
      DIMENSION F(3)
      A=1.D0
      A1=(1.D0-A*E)/4.D0
      NA1=A1
14    CALL FCN (BI,A1,E,N1,FN,FU,N2)
      R=FN/DEXP(E/2.D0)
      DO 60 J=1,3
      F(J)=0.D0
60    CONTINUE
61    RETURN
      END
CC
CC
      SUBROUTINE FCN (BI,T,E,N1,FN,FU,N2)
      IMPLICIT REAL*8 (A-H,O-Z)
      DIMENSION RN1(400)
      FU=0.D0
      N2=N1
9     AN=4.D0*T
      RN1(1)=AN*E/2.D0
      FN=1.D0+RN1(1)
      FCT=2.D0
      DO 10 L=1,N2
      FCT=FCT+2.D0
      AN=AN+4.D0
      N=L+1
      RN1(N)=AN*RN1(L)*E/(FCT*(FCT-1.D0))
      FN=FN+RN1(N)
```

```
10      CONTINUE
        IF ((DABS(RH1(N2+1))+DABS(RH1(N2))).LT.1.D-12)
       XGO TO 12
        N2=N2+50
        IF (N2.GE.400) GO TO 11
        GO TO 9
11      WRITE (6,1003)
        STOP
12      FU=BI-E
        DO 30 K=1,N2
        FU=FU+RH1(K)*(BI-E+2.D0*K)
30      CONTINUE
1003    FORMAT ('NEED MORE THAN 400 TERMS')
31      RETURN
        END
CC
CC

        REAL FUNCTION RMULT*8 (E,N)
        IMPLICIT REAL*8 (A-H,O-Z)
        RMULT=1.D0
        DO 37 L=1,N
        M=2*L
37      RMULT=(4.D0*L-3.D0-E)*E*RMULT/(M*(M-1))
        RETURN
        END
CC
CC

        REAL FUNCTION SS*8 (E,N)
        IMPLICIT REAL*8 (A-H,O-Z)
        SS=0.D0
        DO 80 J=1,N
80      SS=SS+1.D0/(4.D0*J-3.D0-E)
        RETURN
        END
```

```
CC
CC    CALCULATE 'DE', AND 'DNN'
CC
      IMPLICIT REAL*8 (A-H,O-Z)
      DO 100 J=1,20
      READ (5,111) E
      N=1
      C=RMULT(E,N)
      DE=C*(-0.5D0+1.D0/E-SS(E,N))
      DNN=C*(2.D0-E)
      REF1=DE
      REF2=DN
      DO 80 N=2,150
      DE=DE+RMULT(E,N)*(-0.5D0+N/E-SS(E,N))
      IF (DABS(DE-REF1).LT.0.1D-6) GO TO 81
80    REF1=DE
      WRITE (6,555)
81    DE=(-0.5D0+DE)/DEXP(E/2.D0)
      DO 70 N=2,150
      DNN=DNN+RMULT(E,N)*(2.D0*N-E)
      IF (DABS(DNN-REF2).LT.0.1D-6) GO TO 71
70    REF2=DNN
      WRITE (6,555)
71    DNN=(-E+DNN)/DEXP(E/2.D0)
      WRITE (6,222) J,E,DE,DNN
100   CONTINUE
111   FORMAT (F10.6)
222   FORMAT ('0',5X,'J=',I2,10X,'E=',F10.6,10X,'DE=',
     XF10.6,10X,'DNN=',F10.6)
555   FORMAT (' NEED MORE THAN 150 TERMS ')
      STOP
      END
```

```
CC
CC
CC          DECK FOR COMPUTING EIGENCONSTANTS, ICE PROFILE,
CC              PRESSURE DROP, HEAT TRANSFER RATE, BULK
CC              TEMP., LOCAL NUSSELT NO. IN FREEZING ZONE
CC
CC

           IMPLICIT REAL*8 (A-H,O-Z)
           DIMENSION ESQ(20),SQ(20),EK1(20),E2(20),EK(20)
           DIMENSION DELTA(15),DE(20),DNN(20)
           DO 3 I=1,15
3          READ (5,333) DELTA(I)
           DO 49 I=1,20
49         READ (5,444) DE(I),DNN(I)
CC
CC         EIGENVALUES FOR FREEZING ZONE CAN BE DETERMINED
CC         AS IN SOLIDIFICATION FREE ZONE
CC

           DO 52 I=1,20
           READ (5,333) E2(I)
52         CONTINUE
           READ (5,111) BI,XX,TS
           READ (5,904) QXF
           WRITE (6,222) BI,XX,TS
           DO 50 I=1,20
           READ (8,902) E1,EC1,Y,DY,DDY
           EK1(I)=EC1*Y
50         ESQ(I)=E1*E1
902        FORMAT (5D15.8)
           DO 100 J=1,20
           SQ(J)=E2(J)*E2(J)
           SUM=0.D0
           DO 55 K=1,20
           V=8.D0*ESQ(K)*XX/3.D0
           S1=EK1(K)/(DEXP(V)*(ESQ(K)-SQ(J)))
           IF (DABS(S1).LT.0.1D-6) GO TO 56
           SUM=SUM+S1
55         CONTINUE
56         WRITE (6,666) K,SUM
           SS=(1.D0*TS)*E2(J)*SUM
           EC2=(2.D0/(DE(J)*TS))*(1.D0/E2(J)+SS)
           EK(J)=EC2*DNN(J)
           WRITE (6,555) J,EK(J),EQ,DE(J),DNN(J)
904        FORMAT (D15.8)
100        CONTINUE
111        FORMAT (F9.6,F9.6,F9.6)
```

```
222     FORMAT ('0','BIOT NO. =',F9.6,5X,'X=',F8.6,5X,
       X'TS=',F8.6)
333     FORMAT (F10.6)
444     FORMAT (F8.6,F12.6)
555     FORMAT ('0',10X,'J=',I2,10X,'EIGENCONSTANT=',F10.6,
       X10X,'BC=',E15.6,5X,'DB=',F10.6,5X,'DNN=',F10.6)
666     FORMAT ('0',2X,'K=',I2,5X,'SUM=',F10.6)
CC
CC
CC      K FOR ICE = 1.28BTU/(HR-FT-F)
CC      K FOR WATER = 0.332 BTU/(HR-FT-F)
CC      KL/KS APPROX. 0.25
CC
CC
21      READ (5,901) XMAX,PR
777     FORMAT (F8.6,F10.6)
        IF (XMAX.EQ.-0.D0) GO TO 300
        BIS=BI/4.D0
        TE=4.D0/T
        WRITE (6,888) TE,PR
888     FORMAT ('1',10X,'TW=',F10.6,10X,'PR. NO. =',F10.6)
        I=0
        J=1
        K=1
        IP=0
        ISTT=-1
        DEL=1.D0
        DEL1=1.D0
        DEL2=1.D0
        A=0.D0
        B=0.D0
        X=0.D0
        XX=DELTA(1)
        PFNN=2.4D1*PR*XX
        PV1=0.D0
        QT=0.D0
4       I=I+1
        IF (I-10) 5,5,6
6       J=J+1
        IF (DELTA(J)) 21,21,51
51      I=1
5       IF (IP) 7,7,8
7       D=DELTA(J)*((1.D0/DEL1)+(1.D0/DEL))/2.D0
        IP=1
        GO TO 8
8       D=DELTA(J)*((1.D0/DEL2)+(4.D0/DEL1)+(1.D0/DEL))
```

```
      X/3.D0
        IP=0
9       BN=A+D
        SUMI=0.D0
        SUMJ=0.D0
        DO 10 M=1,20
        ARG=-8.D0*SQ(M)*BN/3.D0
        IF (8.D1+ARG) 25,25,22
22      C=BK(M)*DEXP(ARG)
        SUMI=SUMI+C
        SUMJ=SUMJ+(C/SQ(M))
10      CONTINUE
        GO TO 23
25      WRITE(6,26)
26      FORMAT (5X,'ARG. EXCEEDS 80.0')
23      DN=SUMI*(1.D0+BIS)/(BIS*(SUMI-TE))
        IF (DN.LT.1.D-4) GO TO 21
        IF (DN-DEL+0.1D-3) 11,12,13
13      IF (DN-DEL-0.1D-3) 12,12,11
11      DEL=DN
        K=K+1
        IF (K-15) 14,14,15
15      WRITE(6,16)
16      FORMAT (1X,'NOT CONVERGING')
        GO TO 21
14      IF (IP) 8,8,7
12      WRITE (6,1000) SUMI,SUMJ
1000    FORMAT (' ',30X,E14.6,5X,E14.6)
        QINT=SUMI/DN
        IF (ISTT) 200,200,201
200     QINT1=QINT
        ISTT=1
201     QT=QT-2.D0*DELTA(J)*(QINT1+QINT)
        DEL1T=DEL1*DEL1*DEL1
        DNT=DN*DN*DN
        IF (IP) 28,28,29
29      S=DELTA(J)*((1.D0/DEL1T)+(1.D0/DNT))/2.D0
        GO TO 31
28      S=DELTA(J)*((1.D0/DEL2T)+(4.D0/DEL1T)+(1.D0/DNT))
      X/3.D0
31      PV=2.4D1*PR*(B+S)
        X2=X1
        X1=X
        X=X+DELTA(J)
        K=1
        DDEL=(DN-DEL2)/(X-X2)
```

```
      D2DEL=(( DN-DEL1 )/( X-X1 )-( DEL1-DEL2 )/( X1-X2 ))/( X-X2 )
      PM=6.D0*( 1.D0-DEL1*DEL1 )/( 5.D0*DEL1*DEL1 )
      P=PM+PV1
      IF ( IP ) 34,34,27
34    WRITE (6,18) X1,DEL1,DDEL,D2DEL,BN
18    FORMAT ('0',2X,F9.6,4( 2X,E14.6 ))
      TB=TS*( 1.D0/TS-3.D0*SUMJ/2.D0 )/( 1.D0+TS )
      TT=1.D0/TS-TB*( 1.D0+TS )/TS
      RN=2.D0*SUMI/( DEL1*TT )
      WRITE (6,32) P,PM,PV1,QT1,TB,RN,X
32    FORMAT (7(2X,F12.5)
      AX=X+XX
      PP=P+PFREE
      QQQ=QT1+QXF
      WRITE (9,905) X,AX,DEL1,PP,QQQ,TB,RN
905   FORMAT (' ',E10.3,E10.3,5F10.3)
27    DEL2=DEL1
      DEL1=DEL
      DEL=DN
      DEL2T=DEL1T
      PV1=PV
      QINT1=QINT
      QT1=QT
      IF ( IP ) 20 ,20,19
20    A=BN
      B=B+S
19    IF (X-XMAX) 4,4,21
300   CONTINUE
      STOP
      END
```

```
CC
CC
CC                  LIQUID SOLIDIFICATION
CC          WITH BOTTOM PLATE INSULATED BI1 = 0
CC
CC          PROGRAMS FOR SOLIDIFICATION FREE ZONE
CC
CC          1. EIGENVALUES
CC
CC

      IMPLICIT REAL*8 (A-H,O-Z)
      DIMENSION X(20),F(20)
      BI1=0.D0
CC
CC BI2 = 1 , 2 , 10 , 100
CC
      DO 200 I=1,4
      READ (5,901) BI2
      WRITE (6,902) BI1,BI2
CC
CC 10 EIGENVALUES
CC
      DO 100 J=1,10
      READ (5,901) X(1)
      READ (5,901) X(2)
CC
CC SECANT METHOD
CC
      CALL FCN (BI1,BI2,X(1),F(1),PHI1,PHI2,R1,R2)
      DO 5 KK=1,20
      II=KK+1
      JJ=KK+2
      CALL FCN (BI1,BI2,X(II),F(II),PHI1,PHI2,R1,R2)
      X(JJ)=(X(II)*F(KK)-X(KK)*F(II))/(F(KK)-F(II))
      DD=X(JJ)-X(II)
      WRITE (6,904) KK,DD,X(JJ)
      IF (DABS(DD).LT.0.1D-7) GO TO 6
5     CONTINUE
6     CALL FCN (BI1,BI2,X(JJ),FU,PHI1,PHI2,R1,R2)
      C1=(-BI1+BI2)*(1.D0+R2)*DSQRT(X(JJ))/(PHI1*2.D0)
      WRITE (6,905) J,X(JJ),FU
      WRITE (6,906) C1
100   CONTINUE
200   CONTINUE
901   FORMAT (F10.6)
```

```
902   FORMAT ('1','BOTTOM PLATE BIOT NO. =',F10.6,5X,'UPPER
     XPLATE BIOT NO. =',F10.6)
904   FORMAT ('0','NO. =',I2,5X,'DIFFERENCE =',F10.6,10X,
     X'X =',F10.6)
905   FORMAT ('0',60X,'EIGENVALUE ( ',I2,' ) =',F10.6,10X,
     X'PU =',F12.7)
906   FORMAT ('0',60X,'C =',F10.6)
      STOP
      END
CC
      SUBROUTINE PCN (BI1,BI2,EE,PU,PHI1,PHI2,R1,R2)
      IMPLICIT REAL*8 (A-H,O-Z)
      DIMENSION RM1(200),RM2(200)
      E=EE/4.D0
      RM1(1)=(1.D0-E)*E/2.D0
      RM2(1)=(3.D0-E)*E/6.D0
      R1=RM1(1)
      R2=RM2(1)
      DO 10 N=2,150
      PCT=2.D0*N
      M=N-1
      RM1(N)=(4.D0*N-3.D0-E)*RM1(M)*E/(PCT*(PCT-1.D0))
      RM2(N)=(4.D0*N-1.D0-E)*RM2(M)*E/(PCT*(PCT+1.D0))
      R1=R1+RM1(N)
      R2=R2+RM2(N)
10    CONTINUE
      IF (DABS(RM1(150)-RM1(149)).GT.0.1D-7) WRITE (6,903)
      S1=0.D0
      S2=0.D0
      DO 20 I1=1,150
      S1=S1+RM1(I1)*(EE-8.D0*I1-(BI1+BI2))
20    CONTINUE
      DO 30 I2=1,150
      S2=S2+RM2(I2)*((BI1+BI2)/4.D0-E+2.D0*I2+1.D0)
30    CONTINUE
      PHI1=EE-(BI1+BI2)+S1
      PHI2=(BI1+BI2)/4.D0-E+1.D0+S2
      B=(BI1-BI2)*(BI1-BI2)/4.D0
      PU=PHI1*PHI2+B*(1.D0+R1)*(1.D0+R2)
903   FORMAT ('NEED MORE THAN 150 TERMS')
      RETURN
      END
CC
CC
CC    2. EIGENCONSTANTS AND ICE-FREE LENGEH
CC
```

```
CC
      IMPLICIT REAL*8 (A-H,O-Z)
      DIMENSION EG(10),ESQ(10),Y1(10),F1(201),F2(201)
     X Z1(201),Z2(201)
      BI1=0.D0
      DO 200 I=1,4
      READ (5,901) BI2
      WRITE (6,902) BI1,BI2
      DO 100 J=1,10
      READ (5,901) EE
      ESQ(J)=EE*EE
      E=EE/4.D0
      READ (5,901) C
      NDIM=201
      DO 90 MM=1,NDIM
      K=MM-1
      Y=0.05D-1*K
      CALL PM (Y,E,EE,C,W,W1,W2)
      F1(MM)=W1
      F2(MM)=W2
90    CONTINUE
      Y1(J)=W
      SP=0.05D-1
      CALL DQSF (SP,F1,Z1,NDIM)
      CALL DQSF (SP,F2,Z2,NDIM)
      EG(J)=Z1(201)/Z2(201)
      WRITE (6,904) J,EE,EG(J),Y1(J)
100   CONTINUE
CC
CC ICE FREE LENGTH
CC
      WRITE (6,905)
      X=0.D0
      DO 60 I1=1,50
      X=X+0.1D-1
      T=0.D0
      DO 50 I2=1,10
      DOM=ESQ(I2)*X
      IF (DOM.GT.8.D1) GO TO 51
      T=T+EG(I2)*Y1(I2)/DEXP(DOM)
50    CONTINUE
51    TS=(1.D0-T)/T
      WRITE (6,906) X,TS
60    CONTINUE
200   CONTINUE
901   FORMAT (F10.6)
```

```
902      FORMAT ('1','BOTTOM PLATE BIOT NO. =',F10.6,5X,'UPPER
        XPLATE BICT NO. =',F10.6)
904      FORMAT ('0','J =',I2,10X,'EIGENVALUE =',F10.6,10X,
        X'EIGENCONSTANT =',F10.6,10X,'Y1 =',F12.6)
905      FORMAT ('1',' ICE FREE LENGTH')
906      FORMAT ('0',5X,'X =',F10.6,10X,'TEMP. OF SUPERHEAT ='
        X,F10.6)
         STOP
         END
CC

         SUBROUTINE PN (Y,E,EE,C,W,W1,W2)
         IMPLICIT REAL*8 (A-H,O-Z)
         DIMENSION RM1(200),RM2(200)
         YY=Y-1.D0/2.D0
         RM1(1)=(1.D0-E)*EE*YY*YY/2.D0
         RM2(1)=(3.D0-E)*EE*YY*YY/6.D0
         R1=RM1(1)
         R2=RM2(1)
         DO 10 N=2,150
         FCT=2.D0*N
         M=N-1
         RM1(N)=(4.D0*N-3.D0-E)*RM1(M)*EE*YY*YY/(FCT*(FCT-1.D0))
         RM2(N)=(4.D0*N-1.D0-E)*RM2(M)*EE*YY*YY/(FCT*(FCT+1.D0))
         R1=R1+RM1(N)
         R2=R2+RM2(N)
10       CONTINUE
         IF (DABS(RM1(150)-RM1(149)).LT.0.1D-7) GO TO 11
         IF (DABS(RM2(150)-RM2(149)).LT.0.1D-7) GO TO 11
         WRITE (6,903)
         STOP
11       W=(C*(1.D0+R1)+DSQRT(EE)*YY*(1.D0+R2))
        X/DEXP(EE*YY*YY/2.D0)
         W1=Y*(1.D0-Y)*W
         W2=W1*W
903      FORMAT ('NEED MORE THAN 150 TERMS')
         RETURN
         END
CC
CC
CC
CC     PROGRAMS FOR FREEZING ZONE
CC
CC     1. EIGENVALUES
CC
CC

         IMPLICIT REAL*8 (A-H,O-Z)
         DIMENSION X(20),F(20)
```

```
        WRITE (6,901)
        DO 100 J=1,10
        READ (5,902) X(1),X(2)
CC
CC SECANT METHOD
CC
        CALL FF (X(1),F(1),R1,R2)
        DO 5 KK=1,20
        II=KK+1
        JJ=KK+2
        CALL FF (X(II),F(II),R1,R2)
        X(JJ)=(X(II)*F(KK)-X(KK)*F(II))/(F(KK)-F(II))
        DD=X(JJ)-X(II)
        WRITE (6,904) KK,DD,X(JJ)
        IF (DABS(DD).LT.0.1D-7) GO TO 6
5       CONTINUE
6       CALL FF (X(JJ),FU,R1,R2)
        WRITE (6,905) J,X(JJ),FU
        C=-DSQRT(X(JJ))*(1.D0+R2)/(2.D0*(1.D0+R1))
        WRITE (6,906) C
100     CONTINUE
901     FORMAT ('1','FREEZING ZONE')
902     FORMAT (F10.6,F10.6)
904     FORMAT ('0','NO. =',I2,5X,'DIFFERENCE =',F10.6,10X,
       X'X =',F10.6)
905     FORMAT ('0',60X,'EIGENVALUE (',I2,') =',F10.6,16X,
       X'FU =',F10.6)
906     FORMAT ('0',60X,'C =',F10.6)
        STOP
        END
CC
        SUBROUTINE FF (EE,FU,R1,R2)
        IMPLICIT REAL*8 (A-H,O-Z)
        DIMENSION RH1(200),RH2(200)
        E=EE/4.D0
        RH1(1)=(1.D0-E)*E/2.D0
        RH2(1)=(3.D0-E)*E/6.D0
        R1=RH1(1)
        R2=RH2(1)
        DO 10 N=2,150
        FCT=2.D0*N
        M=N-1
        RH1(N)=(4.D0*N-3.D0-E)*RH1(M)*E/(FCT*(FCT-1.D0))
        RH2(N)=(4.D0*N-1.D0-E)*RH2(M)*E/(FCT*(FCT+1.D0))
        R1=R1+RH1(N)
        R2=R2+RH2(N)
```

```
10      CONTINUE
        IF (DABS(RM1(150)-RM1(149)).LT.0.1D-7) GO TO 11
        IF (DABS(RM2(150)-RM2(149)).LT.0.1D-7) GO TO 11
        WRITE (6,903)
        STOP
11      S1=2.D0*E
        S2=E-1.D0
        DO 20 J=1,150
        S1=S1+RM1(J)*(2.D0*E-4.D0*J)
        S2=S2-RM2(J)*(-E+2.D0*J+1.D0)
20      CONTINUE
        FU=S1*(1.D0+R2)+2.D0*(1.D0+R1)*S2
903     FORMAT ('NEED MORE THAN 150 TERMS')
        RETURN
        END
CC
CC
CC        2. EIGENCONSTANTS, ICE THICKNESS PROFILE,
CC             PRESSURE DROP, BULK TEMP., HEAT
CC             TRANSFER RATE, LOCAL NUSSELT NO.
CC
CC
        IMPLICIT REAL*8 (A-H,O-Z)
        DIMENSION E1(10),EK1(10),E2(10),EK2(10),C1(10),
       XC2(10),DNN(10),F1(101),F2(101),Z1(101),Z2(101),
       XEK(10),SQ(10),DELTA(15)
        READ (5,901) BI1,BI2
        WRITE (6,904) BI2,BI1
        DO 50 I=1,10
        READ (5,902) E1(I),EK1(I),C1(I)
        READ (5,901) E2(I),C2(I)
        SQ(I)=E2(I)*E2(I)
50      CONTINUE
        DO 52 I=1,10
52      READ (5,222) DNN(I)
        DO 3 I=1,15
3       READ (5,222) DELTA(I)
        DO 300 NN=1,3
        READ (5,901) T,XE
        READ (5,222) QXF
        WRITE (6,906) T,XE
        DO 900 J=1,10
        NDIM=101
        DO 100 NN=1,NDIM
        K=NN-1
        Y=0.1D-1*K
```

```
        S=0.D0
        DO 90 L=1,10
        CALL FF (Y,E1(L),C1(L),W1)
        S1=E1(L)*E1(L)*XE
        IF (S1.GT.8.D1) GO TO 91
        S=S+EK1(L)*W1/DEXP(S1)
90      CONTINUE
91      SUM=(1.D0+T)*S/T-1.D0/T
        CALL FF (Y,E2(J),C2(J),W2)
        F=Y*(1.D0-Y)*W2
        P1(MM)=F*SUM
        P2(MM)=F*W2
100     CONTINUE
CC
CC NUMERICAL INTEGRATION
CC
        SP=0.1D-1
        CALL DQSF (SP,P1,Z1,NDIM)
        CALL DQSF (SP,P2,Z2,NDIM)
        EK2(J)=Z1(101)/Z2(101)
        EK(J)=DNN(J)*EK2(J)
        WRITE (6,903) J,E2(J),EK2(J),DNN(J),EK(J)
        WRITE (6,905) Z1(101),Z2(101)
900     CONTINUE
Z22     FORMAT (F10.6)
901     FORMAT (F10.6,F10.6)
902     FORMAT (F10.6,F10.6,F10.6)
903     FORMAT ('0',I2,5X,'E =',F10.6,5X,'EK2 =',F10.6,5X,
       X'DN/DN(1) =',F10.6,5X,'EK2*DN =',F10.6)
904     FORMAT ('1','UPPER PLATE BIOT NO. =',F10.6,10X,
       X'BOTTOM PLATE BIOT NO. =',F10.6)
905     FORMAT ('0',80X,E10.5,5X,E10.4)
906     FORMAT ('0',5X,'SUPERHEAT RATIO =',F10.6,10X,
       X'ICE FREE LENGTH =',F10.6)
CC
CC
CC      K FOR ICE = 1.28BTU/(HR-FT-F)
CC      K FOR WATER = 0.332 BTU/(HR-FT-F)
CC      KL/KS APPROX. 0.25
CC
CC
21      READ (5,901) XMAX,PR
        IF (XMAX.EQ.-0.D0) GO TO 300
        BIS=BI2/4.D0
        TE=4.D0/T
        WRITE (6,888) TE,PR
```

```
888      FORMAT ('1',10X,'TW=',F10.6,10X,'PR. NO. =',F10.6)
         I=0
         J=1
         K=1
         IP=0
         ISTT=-2
         DEL=1
         DEL1=1.D0
         DEL2=1.D0
         A=0.D0
         B=0.D0
         X=0.D0
         X1=DELTA(1)
         PXF=1.44D2*PR*XE
         PV1=0.D0
         QT=0.D0
4        I=I+1
         IF (I-10) 5,5,6
6        J=J+1
         IF (DELTA(J)) 21,21,51
51       I=1
5        IF (IP) 7,7,8
7        D=DELTA(J)*((1.D0/DEL1)+(1.D0/DEL))/2.D0
         IP=1
         GO TO 9
8        D=DELTA(J)*((1.D0/DEL2)+(4.D0/DEL1)+(1.D0/DEL))
         X/3.D0
         IP=0
9        BN=A+D
         SUMI=0.D0
         SUMJ=0.D0
         DO 10 N=1,40
         ARG=-SQ(N)*BN
         IF (8.D1+ARG) 25,25,22
22       C=BK(N)*DEXP(ARG)
         SUMI=SUMI+C
         SUMJ=SUMJ-(6.D0*C)/SQ(N)
10       CONTINUE
         GO TO 23
25       WRITE(6,26)
26       FORMAT (5X,'ARG. EXCEEDS 80.0')
23       DN=SUMI*(1.D0+BIS)/(BIS*(SUMI-TE))
         IF (DN.LT.1.D-4) GO TO 21
         IF (DN-DEL+0.1D-3) 11,12,13
13       IF (DN-DEL-0.1D-3) 12,12,11
11       DEL=DN
```

```
      K=K+1
      IF (K-15) 14,14,15
15    WRITE (6,16)
16    FORMAT (1X,'NOT CONVERGING')
      GO TO 21
14    IF (IP) 8,8,7
12    WRITE (6,1000) SUMI,SUMJ
1000  FORMAT (' ',30X,E14.6,5X,E14.6)
      QINT=SUMI/DN
      RNU=-QINT/SUMJ
      RNUU=-QINT/(SUMJ+1.DO/T)
      IF (ISTT) 200,200,201
200   QINT1=QINT
      ISTT=1
201   QT=QT-3.DO*DELTA(J)*(QT
      DEL1T=DEL1*DEL1*DEL1
      DNT=DN*DN*DN
      IF (IP) 28,28,29
29    S=DELTA(J)*((1.DO/DEL1T)+(1.DO/DNT))/2.DO
      GO TO 31
28    S=DELTA(J)*((1.DO/DEL2T)+(4.DO/DEL1T)+(1.DO/DNT))
     //3.DO
31    PV=1.44D2*PR*(B+S)
      X2=X1
      X1=X
      X=X+DELTA(J)
      K=1
      DDEL=(DN-DEL2)/(X-X2)
      D2DEL=((DN-DEL1)/(X-X1)-(DEL1-DEL2)/(X1-X2))/(X-X2)
      PR=6.DO*(1.DO-DEL1*DEL1)/(5.DO*DEL1*DEL1)
      P=PR+B*1
      IF (IP) 34,34,27
34    WRITE (6,18) X1,DEL1,DDEL,D2DEL,BR
18    FORMAT ('0',2X,F9.6,4(2X,E14.6))
      TB=T*(1.DO/T+SUMJ)/(1.DO+T)
      WRITE (6,32) P,PR,PV1,QT1,TB,RNU
32    FORMAT (' ',4(2X,F14.5),20X,F14.5,2X,F14.5)
      XX=X1+XE
      PT=P+PXP
      QQQ=QT1+QXP
      WRITE (8,1111) X1,XX,DEL1,PT,QQQ,TB,RNU,RNUU
1111  FORMAT (' ',E10.3,E10.3,6(F10.3))
27    DEL2=DEL1
      DEL1=DEL
      DEL=DN
      DEL2T=DEL1T
```

```
        PV1=PV
        QINT1=QINT
        QT1=QT
        IF (IP) 20 ,20,19
20      A=
        B=B+S
19      IF (X-XMAX) 4,4,21
300     CONTINUE
        STOP
        END
CC
        SUBROUTINE PP (Y,EE,C,W)
        IMPLICIT REAL*8 (A-H,O-Z)
        DIMENSION RM1(200),RM2(200)
        E=EE/4.D0
        YY=Y-1.D0/2.D0
        RM1(1)=(1.D0-E)*EE*YY*YY/2.D0
        RM2(1)=(3.D0-E)*EE*YY*YY/6.D0
        R1=RM1(1)
        R2=RM2(1)
        DO 10 N=2,150
        FCT=2.D0*N
        M=N-1
        RM1(N)=(4.D0*N-3.D0-E)*RM1(M)*EE*YY*YY/(FCT*(FCT-1.D0))
        RM2(N)=(4.D0*N-1.D0-E)*RM2(M)*EE*YY*YY/(FCT*(FCT+1.D0))
        R1=R1+RM1(N)
        R2=R2+RM2(N)
10      CONTINUE
        IF (DABS(RM1(150)-RM1(149)).LT.0.1D-7) GO TO 11
        IF (DABS(RM2(150)-RM2(149)).LT.0.1D-7) GO TO 11
        WRITE (6,903)
        STOP
11      W=(C*(1.D0+R1)+DSQRT(EE)*YY*(1.D0+R2))
     X  /DEXP(EE*YY*YY/2.D0)
903     FORMAT ('NEED MORE THAN 150 TERMS')
        RETURN
        END
```

```
CC
CC
CC      PROGRAMS FOR SOLIDIFICATION FREE ZONE
CC          INCLUDING AXIAL HEAT CONDUCTION
CC
CC      1. EIGENVALUES
CC
CC
        IMPLICIT REAL*8 (A-H,O-Z)
        DIMENSION F(3)
        DO 100 II=1,12
        READ (5,901) BI,PE
        N1=150
        WRITE (6,1001) BI,PE
CC
CC 20 EIGENVALUES
CC
        DO 100 I=1,20
        READ (5,902) XL
        READ (5,902) XR
CC
CC FALSE POSITION
CC
        CALL HYPFN (PE,XR,N1,FR,F,R,N2)
        CALL HYPFN (PE,XL,N1,FL,F,R,N2)
CC
CC 30 ITERATIONS
CC
        DO 20 KK=1,30
        XH=XL-(XR-XL)*FL/(FR-FL)
        CALL HYPFN (PE,XH,N1,FH,F,R,N2)
        WRITE (6,1004) KK,FH,XH
        IF (DABS(FH).LT.1.D-8) GO TO 21
        IF (FL*FH) 1,21,3
1       XR=XH
        FR=FH
        GO TO 20
3       XL=XH
        FL=FH
20      CONTINUE
21      WRITE (6,1005) I,XH,N2
        WRITE (6,1002) R
        WRITE (7,903) XH,R
100     CONTINUE
901     FORMAT (D15.8,D15.8)
902     FORMAT (D8.4)
```

```
903    FORMAT (D20.10,D20.10)
1000   FORMAT ('1',10X,'BIOT NO. =',F10.5,15X,
      X'PECLET NO. =',F10.5)
1002   FORMAT ('0',85X,'R(1) =',D15.8)
1004   FORMAT (' ',I2,5X,'FO =',D15.8,10X,'B =',D15.8)
1005   FORMAT ('0',80X,'EIGENVALUE ',I2,' =',F14.8,
      X10X,'N2 =',I3)
       STOP
       END
CC
CC
CC     2. EIGENCONSTANTS
CC
CC

       IMPLICIT REAL*8 (A-H,O-Z)
       REAL*4 EPS
       DIMENSION AL(20),BE(20),YN(20,201),RN(20,201)
       DIMENSION A(40,40),B(40),W1(201),W2(201)
       DIMENSION W(201),Z(201),D(20,20),AA(1600)
       READ (5,902) (AL(I),I=1,20)
       READ (5,903) ((YN(N,K),K=1,201),N=1,20)
CC
CC BI = 1 , 2 , 10 , INFINITY
CC

       DO 950 IC=1,4
       READ (5,901) BI,PE
       IF (BI.LT.1.D10) GO TO 1
       WRITE (6,1009) PE
       GO TO 2
1      WRITE (6,1001) BI,PE
2      WRITE (6,1002)
       WRITE (6,1003) (AL(I),I=1,20)
       N1=150
       DO 10 J=1,20
       READ (5,904) BE(J)
       E=BE(J)
       A=1.D0+(6.4D1*E*E)/(9.D0*PE*PE)
       A1=(1.D0-A*E)/4.D0
       Y=-0.5D-2
       DO 10 K=1,201
       Y=Y+0.5D-2
       CALL FUNY (PE,E,A1,Y,N1,BR,N2)
       RN(J,K)=BR
10     CONTINUE
       WRITE (6,1004)
       WRITE (6,1003) (BE(I),I=1,20)
```

```
      NDIM=201
      H=0.5D-2
      DO 200 L=1,20
      DO 200 M=1,20
      DO 100 N=1,201
      W(N)=BW(N,N)*YN(L,N)
100   CONTINUE
      CALL DCSP (H,W,Z,NDIM)
      A(L,M)=Z(201)
      LL=20+L
      MM=20+M
      A(MM,LL)=AL(LL)*AL(L)*A(L,M)
200   CONTINUE
      WRITE (6,1011)
      WRITE (6,1008) ((A(I,J),J=1,20),I=1,20)
      WRITE (6,1012)
      WRITE (6,1008) ((A(I,J),J=21,40),I=21,40)
      CALL SYMX (H,NDIM,YN,D)
      DO 300 I=1,20
      JJ=20
      DO 300 J=1,20
      JJ=JJ+1
      A(I,JJ)=-D(I,J)
300   CONTINUE
      WRITE (6,1012)
      WRITE (6,1008) ((A(I,J),J=21,40),I=1,20)
      CALL SYMX (H,NDIM,BW,D)
      DO 400 J=1,20
      II=20
      DO 400 I=1,20
      II=II+1
      A(II,J)=D(I,J)*BE(J)*BE(J)
400   CONTINUE
      WRITE (6,1012)
      WRITE (6,1008) ((A(I,J),J=1,20),I=21,40)
      DO 600 I=1,20
      DO 500 J=1,201
      W(J)=YN(I,J)
500   CONTINUE
      CALL DCSP (H,W,Z,NDIM)
      B(I)=Z(201)
600   CONTINUE
      DO 700 K=21,40
      B(K)=0.D0
700   CONTINUE
      WRITE (6,1013)
```

```
      WRITE (6,1008) (B(I),I=1,40)
      DO 750 J=1,40
      DO 750 I=1,40
      IJ=(J-1)*40+I
      AA(IJ)=A(I,J)
750   CONTINUE
      M=40
      N=1
      EPS=1.E-14
CC
CC SOLVE SYSTEM OF EQUATIONS 40*40
CC         A*X=B
CC
      CALL DGELG (B,A,M,N,EPS,IER)
      WRITE (6,1005) IER
      WRITE (6,1006) (B(I),I=1,40)
      WRITE (7,903) (B(I),I=1,40)
      DO 900 I=1,201,10
      T1=1.D0
      T2=0.D0
      DO 800 J=1,20
      JJ=20+J
      T1=T1+B(JJ)*YN(
      T2=T2+B(J)*BN(
      WRITE (6,1010)
800   CONTINUE
      WRITE (6,1007) I,T1,T2
      WRITE (7,1015) T2
900   CONTINUE
CC
CC CHECK BULK TEMP. AT X=0
CC
      Y=0.D0
      DO 920 I=1,201
      S1=0.D0
      S2=0.D0
      JJ=20
      DO 910 J=1,20
      JJ=JJ+1
      S1=S1+B(JJ)*YN(J,I)
      S2=S2+B(J)*BN(J,I)
910   CONTINUE
      W1(I)=(1.D0-Y*Y)*S1
      W2(I)=(1.D0-Y*Y)*S2
      Y=Y+H
920   CONTINUE
```

```
        CALL DQSF (H,W1,Z,NDIM)
        T1M=1.D0+1.5D0*Z(201)
        CALL DQSF (H,W2,Z,NDIM)
        T2M=0.15D1*Z(201)
        WRITE (6,1014) T1M,T2M
950     CONTINUE
901     FORMAT (D15.8,D15.8)
902     FORMAT (D16.9)
903     FORMAT (5D16.9)
904     FORMAT (D20.10)
1001    FORMAT ('1',20X,'BIOT NO. =',F12.4,15X,'PECLET NO.
        X,F12.4)
1002    FORMAT ('0','ALPHA :')
1003    FORMAT ('0',5X,5D16.9)
1004    FORMAT ('0','BETA :')
1005    FORMAT ('0','EIGENCONSTANTS :',50X,'IER =',I2)
1006    FORMAT ('0',10X,5D16.9)
1007    FORMAT ('0',20X,I3,5X,'T1 =',D16.9,10X,'T2 =',D16.9)
1008    FORMAT (' ',5D16.9)
1009    FORMAT ('1',15X,'BIOT NO.= INFINITY',15X,'PECLET NO.
        X=',F12.4)
1010    FORMAT (' ',5X,D16.9,5X,D16.9)
1011    FORMAT ('0',' : MATRIX A : ')
1012    FORMAT ('0',5X,' : ',10X,' : ',10X,' : ',10X,' : ')
1013    FORMAT ('0',' : MATRIX B : ')
1014    FORMAT ('0',5X,'X=0',19X,'T1M =',D16.9,9X,'T2M ='
        X,D16.9)
1015    FORMAT (F7.4)
        STOP
        END
CC
CC
CC
CC
CC
CC
C
C     3. BULK TEMP. AND LOCAL NUSSELT NO.
C         DOWNSTREAM AND UPSTREAM
C
C
        IMPLICIT REAL*8 (A-H,O-Z)
        DIMENSION AL(20),BB(20),WN(20,201),RN(20,201),B(20)
        DIMENSION C(20),X(35),W(101),Z(101),D(101),DR(20)
        H=0.1D-1
        NDIM=101
        N1=150
        READ (5,901) (X(I),I=1,35)
        READ (5,902) BI,PE
        WRITE (6,1001) BI,PE
        READ (5,905) (AL(I),I=1,20)
```

```
      READ  (5,903) . (BE(I),I=1,20)
      READ  (5,904)  (C(I),I=1,20)
      READ  (5,904)  (B(I),I=1,20)
      READ  (5,904)  ((YN(I,J),J=1,201),I=1,20)
      DO 200 I=1,20
      Y=-H
      DO 200 J=1,NDIM
    . Y=Y+H
      A=1.D0+(6.4D1*BE(I)*BE(I))/(9.D0*PE*PE)
      A1=(1.D0-A*BE(I))/4.D0
      CALL PONY (PE,BE(I),A1,Y,N1,RR,N2)
      RN(I,J)=RR
200   CONTINUE
      Y=1.D0
      DO 150 I=1,20
      A=1.D0+(6.4D1*BE(I)*BE(I))/(9.D0*PE*PE)
      A1=(1.D0-A*BE(I))/4.D0
      A2=A1+1.D0
      CALL PONY (PE,BE(I),A1,Y,N1,P1,N2)
      CALL PONY (PE,BE(I),A2,Y,N1,P2,N2)
      DR(I)=((-BE(I)-2.D0*A1)*P1+2.D0*A1*P2)
150   CONTINUE
      WRITE (6,906)
      WRITE (6,1005) (A   I=1,20)
      WRITE (6,1005) (B     1,20)
      WRITE (6,906)
      WRITE (6,1005) (BE(I),I=1,20)
      WRITE (6,1005) (C(I),I=1,20)
      WRITE (6,1004) YN(10,201),YN(20,201)
      WRITE (6,1007) RN(10,101),RN(20,101)
      WRITE (6,906)
      WRITE (6,1005) (DR(I),I=1,20)
      WRITE (6,906)
      DO 100 K=1,10
      Y=-H
      IF (X(K).LT.0.D0) GO TO 51
      DO 90 KK=1,101
      Y=Y+H
      SUM1=0.D0
      DO 80 L=1,20
      S=BE(L)*BE(L)
      Q1=8.D0*S*X(K)/3.D0
      IF (Q1.GT.8.D1) GO TO 81
      SUM1=SUM1+C(L)*RN(L,KK)/DEXP(Q1)
80    CONTINUE
81    D(KK)=SUM1
```

```
         W(KK)=SUM1*(1.D0-Y*Y)
90       CONTINUE
         CALL DCSP (H,W,Z,NDIM)
         TM=1.5D0*Z(101)
         SUM2=0.D0
         DO 95 I=1,20
         U=BE(I)*BE(I)
         Q2=8.D0*U*X(K)/3.D0
         IF (Q2.GT.7.D1) GO TO 96
         SUM2=SUM2+C(I)*DR(I)/DEXP(Q2)
95       CONTINUE
96       BNU=-2.D0*SUM2/TM
         WRITE (6,1002) X(K),TM,BNU
         WRITE (6,1006) (D(I),I=1,101,10)
         GO TO 100
CC
CC UPSTREAM SOLUTION
CC
51       DO 40 M=1,201,2
         Y=Y+H
         SUM3=1.D0
         DO 30 N=1,20
         Q3=8.D0*AL(N)*AL(N)*X(K)/3.D0
         IF (Q3.GT.7.D1) GO TO 31
         SUM3=SUM3+B(N)*TM(N,M)*DEXP(Q3)
30       CONTINUE
31       NN=(M+1)/2
         W(NN)=SUM3*(1.D0-Y*Y)
         D(NN)=SUM3
40       CONTINUE
         CALL DCSP (H,W,Z,NDIM)
         TM=1.5D0*Z(101)
         WRITE (6,1003) X(K),TM
         WRITE (6,1006) (D(I),I=1,101,10)
100      CONTINUE
901      FORMAT (5D10.4)
902      FORMAT (D10.4,D10.4)
903      FORMAT (D20.10)
904      FORMAT (5D16.9)
905      FORMAT (D16.9)
906      FORMAT ('0',/)
1001     FORMAT ('1',15X,'BIOT NO. =',F10.4,10X,'PECLET NO. ='
        X,F10.4)
1002     FORMAT ('0',5X,'X =',F8.4,5X,'BULK TEMP. =',F10.4,
        X10X,'NU NO. =',F15.4)
1003     FORMAT ('0',5X,'X =',F8.4,5X,'BULK TEMP. =',F10.4)
```

```
1004   FORMAT ('0',5X,'YN(10,201)=',D16.9,10X,'YN(20,201)='
      X,D16.9)
1005   FORMAT (5X,5D16.9)
1006   FORMAT (' ',80X,F10.4)
1007   FORMAT ('0',5X,'RN(10,101)=',D16.9,10X,'RN(20,101)='
      X,D16.9)
       STOP
       END
CC
CC
       SUBROUTINE HYPFN (PE,E,N1,FU,F,R,N2)
       IMPLICIT REAL*8 (A-H,O-Z)
       DIMENSION F(3)
       A=1.D0+(6.4D1*E*E)/(9.D0*PE*PE)
       A1=(1.D0-A*E)/4.D0
       NA1=A1
       IF (A1.GE.-2.D0) GO TO 14
CC
CC        *** F(1)= M (AJ+2 , 1/2 , E ) ***
CC        *** F(2)= M (AJ+1 , 1/2 , E ) ***
CC
       T1=A1-NA1
       T2=T1+1.D0
       CALL FCN (PE,T2,E,N1,F(1),DUMP,N2)
       CALL FCN (PE,T1,E,N1,F(2),DUMP,N2)
CC
CC        *** GENERATE F(3)= M (AJ , 1/2 , E ) ***
CC
       N1=-NA1
       DO 50 I=1,N1
       T1=T1-1.D0
       F(3)=-((T1+1.D0)*F(1)-(2.D0*T1+E+1.5D0)*F(2)
      X/(T1+0.5D0)
       F(1)=F(2)
       F(2)=F(3)
50     CONTINUE
       FU=(E1-E-2.D0*A1)*F(2)+2.D0*A1*F(1)
       R=F(2)/DEXP(E/2.D0)
       GO TO 61
14     CALL FCN (PE,A1,E,N1,FN,FU,N2)
       R=FN/DEXP(E/2.D0)
       DO 60 J=1,3
       F(J)=0.D0
60     CONTINUE
61     RETURN
       END
```

```
      SUBROUTINE FCN (PE,T,E,N1,FN,FU,N2)
CC
CC        ***WHEN T.LT.-2 THIS SUBROUTINE GENERATES
CC            FN = M (T , 1/2 , E )
CC
      IMPLICIT REAL*8 (A-H,O-Z)
      DIMENSION RM1(400)
      FU=0.D0
      N2=N1
9     AM=4.D0*T
      RM1(1)=AM*E/2.D0
      FN=1.D0+RM1(1)
      FCT=2.D0
      DO 10 I=1,N2
      FCT=FCT+2.D0
      AM=AM+4.D0
      M=L+1
      RM1(M)=AM*RM1(L)*E/(FCT*(FCT-1.D0))
      FN=FN+RM1(M)
10    CONTINUE
      IF ((DABS(RM1(N2+1))+DABS(RM1(N2))).LT.1.D-12 )
     XGO TO 12
      N2=N2+50
      IF (N2.GE.400) GO TO 11
      GO TO 9
11    WRITE (6,1003)
      STOP
12    IF (T.LT.-2.D0) GO TO 31
      FU=BI-E
      DO 30 K=1,N2
      FU=FU+RM1(K)*(BI-E+2.D0*K)
30    CONTINUE
1003  FORMAT ('NEED MORE THAN 400 TERMS')
31    RETURN
      END
CC
      SUBROUTINE FUNY (PE,E,A1,Y,N1,R,N2)
      IMPLICIT REAL*8 (A-H,O-Z)
      DIMENSION F(3)
      NA1=A1
      IF (A1.GE.-2.D0) GO TO 14
      T1=A1-NA1
      T2=T1+1.D0
      CALL FNY (PE,T2,E,Y,N1,F(1),N2)
      CALL FNY (PE,T1,E,Y,N1,F(2),N2)
      N1=-NA1
```

```
            DO 50 I=1,N1
            T1=T1-1.D0
            F(3)=-((T1+1.D0)*F(1)-(2.D0*T1+E*Y*Y+1.5D0)*F(2))
           X/(T1+0.5D0)
            F(1)=F(2)
            F(2)=F(3)
   50       CONTINUE
            B=F(2)/DEXP(E*Y*Y/2.D0)
            GO TO 61
   14       CALL FNY (PE,A1,E,Y,N1,FN,N2)
            B=FN/DEXP(E*Y*Y/2.D0)
   61       RETURN
            END
CC
            SUBROUTINE FNY (PE,T,E,Y,N1,FN,N2)
            IMPLICIT REAL*8 (A-H,O-Z)
            DIMENSION RM1(400)
            N2=N1
    9       AM=4.D0*T
            RM1(1)=AM*E*Y*Y/2.D0
            FN=1.D0+RM1(1)
            FCT=2.D0
            DO 10 L=1,N2
            FCT=FCT+2.D0
            AM=AM+4.D0
            M=L+1
            RM1(M)=AM*RM1(L)*E*Y*Y/(FCT*(FCT+1.D0))
            FN=FN+RM1(M)
   10       CONTINUE
            IF ((DABS(RM1(N2+1))+DABS(RM1(N2))).LT.1.D-12)
           XGO TO 12
            N2=N2+50
            IF (N2.GE.400) GO TO 11
            GO TO 9
   11       WRITE (6,1003)
            STOP
   12       CONTINUE
 1003       FORMAT ('NEED MORE THAN 400 TERMS')
            RETURN
            END
CC
            SUBROUTINE SYMX (H,NDIM,PM,D)
            IMPLICIT REAL*8 (A-H,O-Z)
            DIMENSION PM(20,20),D(20,20),W(20),Z(20)
            K=0
            DO 2 I=1,20
```

```
      K=K+1
      DO 2 J=1,K
      DO 1 N=1,201
      W(N)=PN(I,N)*PN(J,N)
1     CONTINUE
      CALL DQSF (H,W,Z,NDIM)
      D(I,J)=Z(201)
      IF (I.EQ.J) GO TO 2
      D(J,I)=D(I,J)
2     CONTINUE
      RETURN
      END
```